

# Natural Polymers as Alternative Adsorbents and Treatment Agents for Water Remediation

Diego Gomez-Maldonado, Iris B. Vega Erramuspe, and Maria S. Peresin \*

This review examines the roles of different natural polymers, composites, and nanoengineered materials that have been studied in the last 10 years for their use in water treatment. As water quality is a global concern, the use of natural and sustainable materials is fundamental to obtain high value products that can remediate water systems without generating other pollution sources or require extra energy inputs or high side costs. Filtration systems often can provide an ideal alternative to conventional water treatment. Herein the attention is focused on polysaccharides, as these can be easily obtained from green processes and can be sourced from what nowadays are considered as agricultural waste. The inherent variety of functional groups that they have provides a better interaction with certain types of pollutants. Thus, biomaterials have been harnessed to generate filtration systems and other water treatment options.

*Keywords:* Biomaterials; Natural fibers; Polysaccharides; Composite materials; Water treatment; Filtration materials

*Contact information:* Forest Products Development Center, School of Forestry and Wildlife Science, Auburn University, 520 Devall Drive 36830, Auburn, Alabama, United States;

\* Corresponding author: soledad.peresin@auburn.edu

## INTRODUCTION

Access to drinking water is essential to human health and has been considered as an inherent human right since 2008 (World Health Organization 2014). Healthful drinking water constitutes a vital component of an effective policy for health protection, for national and regional development, and a matter of international concern, permeating all stages of wellbeing in a country. The lack of investment in water supply and sanitation has led to poor availability of high-quality sources of water; thus, about 2.2 billion people of the 7.6 billion worldwide are without access to safely managed drinking water services (Ware and Whitacre 2006; World Health Organization 2017). In addition, global warming has led to an increase in temperature of water, which has affected the normal lifecycles of bacteria and algae, mainly by increasing the duration of bloom seasons. As a result of these changes, concentrations of toxins generated as by-products from these organisms have increased, and this has had a high impact on human health (Paul 2008; Wilson 2017). Furthermore, the rise in industrial activities, especially those that use secondary compounds and high amounts of water in their processes, has increased the concentration in water sources of pollutants, such as metals, radioactive materials, halogenated compounds, persistent organic pollutants, and bioaccumulative and toxic chemicals, such as pesticides.

These discharged substances from industries contaminate waters, and the increase of normal concentrations of microorganism had raised concerns, leading to the generation of **regulations** that would enhance public health and improve water quality. The World Health Organization (WHO) has provided recommendations for the levels of each

contaminant, and these can be found in the Guidelines for Drinking-water Quality, 2011 (World Health Organization 2014). In this document 41 microorganisms and 85 components are identified as pollutants that need to be monitored and controlled, as they represent an important health risk.

Also, some local authorities have generated their own standards, such as the European Union's Directives on the Quality of Water intended for Human Consumption (The European Commission 2015), where they considered the WHO recommendations and some other ISO standards to set the parameters values that should be followed by all of their members for 5 microorganisms and 35 principal components. Similarly, the U.S. Environment Protection Agency has specified 88 contaminants that should be monitored and reported in their National Primary Drinking Water Regulation (U.S. Environmental Protection Agency 2017) plus 30 unregulated elements that present a health risk that were set for national monitoring at the Fourth Unregulated Contaminant Monitoring Rule (U.S. Environmental Protection Agency 2006). The main share points between these different regulations are the counting of microorganisms such as *Escherichia coli* and other coliform bacteria and *Pseudomonas aeruginosa*, as they represent the more harmful gram-negative bacteria. These regulations also include heavy metal ions used in industry such as copper (Cu(II)), chromium (Cr(VI)), mercury (Hg(II)), and lead (Pb(II)); soft ions, *e.g.* ammonium (NH<sub>4</sub><sup>+</sup>), chloride (Cl<sup>-</sup>), aluminum (Al(III)), manganese (Mg(II)), nitrate (NO<sub>3</sub><sup>-</sup>), and sodium (Na<sup>+</sup>); and organic molecules including benzene, 1,2-dichloroethane, acrylamide, epichlorohydrin, trihalomethanes, polycyclic aromatic hydrocarbons, and pesticides.

The main challenge that comes from the identification and monitoring of these risk factors is the need to treat water sources that exceed the safety values. The most common remediation treatments are precipitation, filtration, chlorination, and ozonation (Hitzfeld *et al.* 2000; Mahfoudhi and Boufi 2017). **Ozone treatment** was developed in 1886 and is based on the formation of ozone from molecular oxygen present in the air by an induced electric field. Ozone is a reactive form of oxygen that is able to oxidize minerals, eliminate color and turbidity from water, degrade organics, and inactivate microorganisms (Camel and Bermond 1998; Glaze *et al.* 1987; Langlais *et al.* 1991). This process was relegated after World War I, as chlorine was easier to obtain. In an analogous way, **chlorination** is able to disrupt cellular processes and structures due to the interactions with cell-membrane proteins, inactivating microorganisms, and generating a long-term resistance, as ions stay in the water for a longer period of time inhibiting the microorganisms' growth (Du *et al.* 2017; Rosenblum *et al.* 2017). The downside of these processes is that chlorination generates halogenated compounds and ozone can generate other organic compounds. Often these by-products present a higher risk than the original compounds (Mao *et al.* 2018).

The **precipitation and filtration** methods are linked processes, as a lot of the precipitated components should then be removed from the water source by filtration, especially when they remain suspended instead of sedimenting as sludge. Aside from being retained by size, some compounds can be adsorbed directly into the material base of the filters, making adsorption the most convenient water treatment method, as components can be directly removed and treated (Luo *et al.* 2013; Faisal *et al.* 2017; Mahfoudhi and Boufi 2017).

The principle of the precipitation method is the use of pH changes or increase in ionic strength, which turns the excess nutrients (*i.e.* nitrates or phosphates) or other heavy ions into salts or gelatinous precipitates that can easily be removed from water lines and treatment plants. Depending on the substance that needs to be removed, a combination of buffer salts can be added to improve the salting out of the pollutants; some examples are

the use of calcium salts for phosphate anions removal or sodium carbonate with iron trichloride for radioactive strontium removal (Tomson and Vignona 1984; Nyberg *et al.* 1994; Kim *et al.* 2009; Lemlikchi *et al.* 2012; Luo *et al.* 2013). With the precipitates formed and the newly added ions free in the water, the filtration and adsorption to the filter are key points for the improvement of the water quality. This last step involves the isolation of precipitate products and the removal of any by-product generated during the previous steps of the treatment. The process's capability of removal is influenced by the surface area, which shows the dominance of interfacial phenomena, the specificity of the surface of the materials, and the mechanical and structural integrity of the selected material (Ali and Gupta 2007; Zhou *et al.* 2011b; Mahfoudhi and Boufi 2017).

The materials used for treatment by filtration of the water flow can be roughly categorized into: inorganic, carbon-based, polymeric, and bio-based. Depending on the pollutant to be removed and the media conditions, the selection of the ideal material should be completed and then adjusted to make it as selective as needed. Apart from these common materials, new filtration systems have been developed with enhanced activity via the addition of nanoparticles and by composite generation (Shrivastava 2010; Trujillo-Reyes *et al.* 2014). The use of nanoparticles immobilized on the surface of a solid support seems to be a good alternative, as the system usually shows good mechanical stability and prevents the leaching of the nanoparticles into the water that is being purified, preventing contamination with metals or molecules that formed the nanoparticle (Tyagi *et al.* 2012). It is vital to understand that the nature of the scaffolds selected for the nanoparticles are going to have an impact on the reactivity of the particles, which can either enhance or eliminate the activity (Haruta 1997).

Even with all the regulations and newly developed technologies, the investment into environmental remediation generally has not been a priority for companies or industries, as it is a low profit activity with high operating costs. For this reason, the systems generated must have a minimum energy consumption, economic feasibility, and be environmental friendly to avoid further contamination (Haruta 1997; Shrivastava 2010; Tyagi *et al.* 2012). To accomplish this, bio-based materials are of primary interest, as they are renewable and low priced. They can be highly versatile, especially when biopolymers are used, as they have a wide range of systems that can be developed from them, such as nanoparticles, nanofibers, scaffolds, hydrogels, and more (Renard *et al.* 1997; Klemm *et al.* 2005; Nevárez *et al.* 2011).

The focus of this review is to provide an overview of how natural polymers have been employed in water remediation, with an emphasis on polysaccharides, and the different filtration systems that have been generated from them.

## **Natural Polymers**

Biological systems bio-synthesize three main polymer types: nucleic acids, proteins, and polysaccharides; these are the major macromolecules that constitute any organism or biosystem, as they sustain metabolic and structural functions, as well as energy storage, carrying and effecting genetic information, and synthesis of analogous molecules by the enzymes and complex that are formed from the interaction between them (Smith and Wood 1997). Other polymers present in biosystems include polyesters (*i.e.* PHAs), polyisoprene (rubber), polyethers (lignin), and other complex polyaromatics (melanin and suberin) (Meyers *et al.* 2008).

The use of natural polymers eliminates steps in industrial processing, as the need for industrial synthesis is avoided, and the purification can be completed using more

environmentally friendly solvents. As many of these polymers are already residues from other industrialized processes, they represent a major advantage relative to the generation of new materials, which may be needed to address day-to-day problems, lowering costs and emissions. From this wide variety of available polymers, polysaccharides are generally more abundant, cheap, and easy to extract, as they have less variation within than nucleic acids and proteins; therefore, polysaccharides are ideal materials with which to develop remediation target systems.

## Polysaccharides

As the name suggests, polysaccharides are polymers formed from sugar monomers (saccharides) linked by a glycoside bond with a general formula of  $[C_n(H_2O)_n]_m$ , where  $m$  is between 40 to 3,000 units (Chen *et al.* 2012; IUPAC 2014). Smaller chains are called oligosaccharides, which have their own diversity and helpfulness in environmental remediation, as they have higher reactivity and more conformational states. Between these, one can highlight cyclodextrins and derived surfactants, such as *N*-alkylmaltonamides (Zhang and Marchant 1996; del Valle 2004; Saeki *et al.* 2009).

Among polysaccharides, **cellulose** and **chitin** are the most abundant, being structural building blocks in plants and animals, respectively (Chen *et al.* 2012; Luo *et al.* 2016). Furthermore, chitin can be deacetylated to become chitosan, which maintains the characteristics that can be favorable for environmental and biomedical uses (*e.g.* biocompatibility, biodegradability, non-toxicity, among others); at the same time, it increases the reactivity of the molecule, as amino functional groups are now present in the structure and have been found to have antibacterial properties in acidic conditions, which is convenient for environmental applications (Rinaudo 2006; Pavinatto *et al.* 2010). Another highly used linear polysaccharide is **alginate**, which has a high water absorption capability due to the abundance of carboxyl groups; it also can be easily crosslinked to generate hydrogels and embed other active compounds in a matrix or as beads (Lee and Mooney 2012).

Branched polysaccharides provide different characteristics, as they contain a higher density of surface groups such as acetyls, hydroxyls, and carboxyls, which can be used for immobilization or for modification. However, the branches also give these polysaccharides a more challenging morphology. Of these, **hemicelluloses** and **amyloses** are the main alternatives, as they are highly abundant and have good water uptake and have a low extraction cost (Hult *et al.* 2002; Wittaya 2012).

### Cellulose

As previously mentioned, cellulose is the most abundant polymer worldwide, accounting for about 45% of dry weight of wood, around 33% of all plants, between 20 and 30% in green algae, and a byproduct of some bacteria and a few animals (Klemm *et al.* 2005; Xiang *et al.* 2016; Zhao *et al.* 2015b). Because of this abundance and the easiness to obtain, cellulose is a referent in the generation of systems for environmental remediation, especially because of the numerous modification options that the hydroxyl groups present, involving both chemical and physical phenomena. These groups can be exploited to generate selective and self-standing approaches (Mahfoudhi and Boufi 2017).

Cellulose is rarely found as a single molecule, as it tends to form networks or fibers that have intermolecular hydrogen bonding between the hydroxyl groups. The cellulose chains acquire a supra-structure that will further interact with the other cell components; because of this, different methods have been developed to extract and purify the fibers from

natural resources. When brought to the nanoscale, cellulose has shown desirable properties for water remediation, such as a low solubility in water, a tunable surface-volume ratio, and surface charge depending on the raw material and extraction method utilized. As surface area is maximized and interfacial phenomena can occur, the more reactive and energetic points are exposed (Zhou *et al.* 2011b). Thus, the use of nanocellulose is an attractive alternative that promises more efficient adsorbents with better binding affinities (Ali 2012; Carpenter *et al.* 2015).

Cellulose, without any further modification, is composed of anhydro-glucose units linked by a  $\beta$ -1-4 glycosidic bonds (Fig. 1). These result in a linear polymer that has 3 hydroxyl groups in the C2, C3, and C6 positions of each anhydroglucose unit. This polymer presents an isoelectric point between 2.5 and 3.7, depending on the literature source (Sookne and Harris 1941; Lee *et al.* 2011), and its hydroxyl groups present dissociation constant (pKa) values between 10 and 12 for the secondary hydroxyl groups and approximately 14 for the primary group (Feng *et al.* 2013). The described properties make cellulose negatively charged in most media and prone to interact with molecules and ions that are suspended or diluted at the same media (Stana-Kleinschek *et al.* 1999).

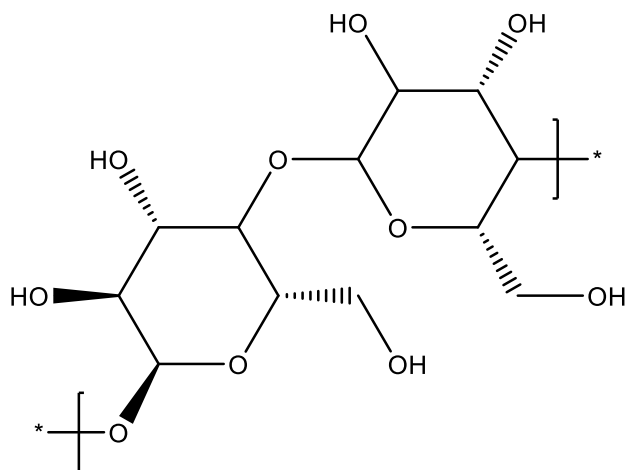


**Fig. 1.** Structure of cellulose monomer

The interaction mechanisms with cellulose-derived materials depend on the solute that is to be removed from the contaminated water. In the case of ions and cationic molecules, it has been characterized that adsorption affects the pores and surfaces; the mechanisms of ion exchange, chelation and complexation, and chemisorption by coordination bonding are understood as being the most likely (Hokkanen *et al.* 2013; Lawrance 2013; Olivera *et al.* 2016). Meanwhile, for anions or larger molecules, hydrogen bonding and electrostatic interactions with the hydroxyl groups seem to be the more likely processes (Jin *et al.* 2015; Olivera *et al.* 2016). Interestingly, it has also been studied that crystallinity has an effect on the adsorption capability of the fibers; organic molecules, such as benzophenone, tend to adsorb into amorphous regions on the fibers, but at low concentrations, these molecules are more prone to be adsorbed onto the crystalline region (Ilharco *et al.* 1997).

The negative nature of the cellulose has been exploited mainly for the removal of cations, as cellulose and especially nanocellulose fibers have been shown to be able to adsorb metals such as Cd(II), Pb(II), and Ni(II) in concentrations of 9.7, 9.42, and 8.55 mg/g, respectively; this was tested in metal solutions with initial concentrations of

25 mg/L. Regeneration was obtained with 0.5 M hydrochloric acid and nitric acid, this can be done for up to 3 cycles with similar adsorption outcomes (Kardam *et al.* 2014). Usually, this negative charge characteristics can be further enhanced by the addition of negative moieties, such as carboxylate, phosphates, and phosphoryl groups (Hokkanen *et al.* 2013; Liu *et al.* 2015; Olivera *et al.* 2016; Suopajarvi *et al.* 2015).

Carboxylation has proven to be one of the easiest and most used methods to raise the negative charge character of cellulosic surfaces, and by it, the adsorption of cations. Fibers that have been oxidized with 2,2,6,6-tetramethyl-1-piperidinyloxy (TEMPO) have demonstrated the capability to adsorb up to 67.2 mg/g of Cu(II) (*ca.* 43.6 mg/L), where the degree of substitution (DO) was 1.5 and the concentration was 200 mg/L (Liu *et al.* 2016). In fibers with a degree of oxidation (DO) of 0.34 at pH 6.2, the removal of Cu(II) was 135.5 mg/g, and the solution had the same initial ion concentration as the previous case (Sehaqui *et al.* 2014). The same type of fibers, but with a DO of 0.26, also presented adsorptions of 58 mg/g of Cr(III), 49 mg/g of Ni(II), and 66 mg/g of Zn(II) (Sehaqui *et al.* 2014). Similarly, fibers with a DO of 0.075 (1.4 mmol of carboxylic groups per gram) presented an adsorption capability of 167 mg/g of UO<sub>2</sub>(II), with the side effect that this ion gelled the fibers (Ma *et al.* 2012).

TEMPO oxidation is not the only path to obtaining carboxylated cellulose, as nanocellulose with low crystallinity (~ 35%) and DO of 0.062 (1.15 mmol of carboxyl /g) was obtained using nitric acid and sodium nitrite for 12 h at 50 °C (Sharma *et al.* 2017b). These fibers proved to be also effective to the removal of 1470 mg/g of UO<sub>2</sub>(II) (Sharma *et al.* 2017a), 2270 mg/g of Pb(II) (Sharma *et al.* 2018b), and 2550 mg/g of Cd(II) (Sharma *et al.* 2018a).

Other modifications with the same aim of increasing the negative charge density with carboxylic and carbonyl groups have also proved to be effective in the immobilization and removal of metallic ions. For example, a modification to mercerized nanocellulose fibers with succinic anhydride was able to successfully remove 231.8 mg/g of Cd(II), 120.7 mg/g of Cu(II), 105.3 mg/g of Zn(II), 78.8 mg/g of Co(II), and 43.7 mg/g of Ni(II) (Hokkanen *et al.* 2013). This was not as high as when only cellulose microfibers were used, which had the removal values of 153.8 mg/g for Cu(II), 249.8 mg/g for Cd(II), and 500.0 mg/g for Pb(II) (Gurgel *et al.* 2008). Even when the microfibrillar cellulose appears to have higher removal values, nanocellulose proved to be regenerated with high efficiency using nitric acid and sonication.

As previously mentioned, carboxylation is not the only modification available. Enzymatic phosphorylated nanocellulose adsorbed 120 mg/g of Ag(I), 114 mg/g of Cu(II), and 73 mg/g of Fe(III), this with an initial concentration of 62.5 mg/L using 0.2 g of the nanocellulose; this work also found that when used in a mixture, CNF adsorbed more Fe than Cu, with final concentrations of 109 and 59 mg/g, respectively, while Ag adsorption was kept constant (Liu *et al.* 2015). Sulfonated nanocellulose was used to eliminate Pb(II); these fibers had a DO of 0.024 (0.45 mmol sulfonic acid /g) and were able to remove efficiently 248.6 mg/g of Pb(II), which was 15x greater than CNF without the modification (Suopajarvi *et al.* 2015). Fibers modified with taurine also present a sulfonate group exposed at the surface; these fibers were found to be efficient for the recovery of suspended Au(III) with a capacity calculated with Langmuir isotherms of 34.5 mg/g, which can still be adsorbed even when other ions such as Ni(II), Cr(VI), Cd(II), Co(II), and As(V) are present (Dwivedi *et al.* 2014). Even though the main objective of the study was not for environmental purposes, the modification approach can be oriented to it, especially as metal desorption was achieved using acidic thiourea.

Aside from adding functional groups, whole molecules can be used as the modifier moieties. Exploiting the inherent reactivity of silanes to react with hydroxyl groups, cellulose microfibrils were modified with aminopropyltriethoxysilane (APS), which gave the surface of the fibers a surface positive charge, as amino groups were exposed; herein the maximum adsorption was of 160.5 mg/g for Ni(II), 200.2 mg/g for Cu(II), and 471.6 mg/g of Cd(II). These adsorption values were between 1 and 2 orders higher with the modification than with the raw microfibril, as the metals are able to coordinate with the exposed nitrogen of the amino group (Hokkanen *et al.* 2014). Other modifications explored for Cr(III) and Cr(VI) are with paraben and (2,3-epoxypropyl) trimethylammonium chloride, respectively. This work obtained a maximum sorption capacity of 23.9 mg of Cr(III) and 24.0 mg of Cr(VI) per g of sorbent (Jain *et al.* 2016). Both final modifications used an epoxy group to modify the surface hydroxyl groups, taking advantage of the non-directed reactivity of this group that can easily react with polysaccharides.

Besides epoxy groups, anhydrides can be used as reactive groups too; for instance, ethylenediaminetetraacetic acid (EDTA, PubChem CID: 6049) was used as a grafting molecule when transformed to its anhydride form in pyridine and then reacted in a cellulose paper filter to improve the capacity to remove metal ions from water solutions. In the study Ag(I), Pb(II), Cd(II), Ni(II), Zn(II), Sn(II), and Cu(II) were tested with removal efficiency between 90 and 95%. Among all of the tested cations, adsorption of Pb and Cd ions were modeled by Langmuir isotherms showing a maximum adsorption capacity of 227.3 mg/g and 102 mg/g respectively, and 5 cycles of recyclability for Pb(II) in 0.5 M HCl, with non-apparent loss of adsorption efficiency (D'Halluin *et al.* 2017).

The structure of the sorbent also has proved to be an important variable in the adsorption capability of the cellulose nanofibers, as surface area will be affected by the conformations that the systems can acquire. Thus, cellulose hydrogels with TEMPO-oxidized cellulose were also found to adsorb Cu(II) with a maximum of 268.2 mg/g, which after regeneration was also used with other ions combined such as Zn(II), Fe(III), Cd(II), and Cs(I) (Isobe *et al.* 2013). Likewise, a nanofiber network embedded with TEMPO-oxidized cellulose nanocrystals (CNC) was used to adsorb Ag(I), Cu(II), and Fe(III), presenting capabilities of 0.023, 33, and 55 mg/g, respectively (Karim *et al.* 2016); the results in these two studies indicate that further modification by incrementing the structural complexity has an impact in the area exposed to retain these metal ions and other organic molecules.

Moreover, the structural modification can also be achieved when nanocomposites are generated; the grafting of other polymers, the entrapping of nanoparticles, or the boosting of an interaction due to different layers are some of the main strategies used for the formation of these materials. Grafting from polymers to cellulose fibers can be done using two approaches, “grafting from” and “grafting to” (Hatton *et al.* 2015). The “grafting from” approach is when a surface group is used as an anchoring point from where the monomers will generate the branches as they polymerize and elongate the chains. On the other hand, the “grafting to” approach is when the polymer is already generated and is only going to be attached to the cellulose fibers.

A “grafted from” polyaniline on cellulose was used to adsorb two model dye molecules, methyl orange (C<sub>14</sub>H<sub>14</sub>N<sub>3</sub>NaO<sub>3</sub>S, PubChem CID:23673835) and eosin yellow (C<sub>20</sub>H<sub>6</sub>Br<sub>4</sub>Na<sub>2</sub>O<sub>5</sub>, PubChem CID: 11048); this system removed 20.9 and 58.1 mg/g, respectively, with maximum concentrations of 10 and 30 mg/L (Bhowmik *et al.* 2018). A similar method was used with poly (glycidyl methacrylate) (GMA) and copolymerized with acrylic acid, acrylamide, or acrylonitrile; these different modified celluloses were

characterized and used to remove Fe(II), Cu(II), and Cr(VI). To further understand the effects of the functional groups added to the cellulose, the polymers were partially hydrolyzed with 0.5 N NaOH for 48 h at room temperature. All systems were tested in a solution containing 0.1 g of polymer in 20 mL of solution containing 20 mg of metal salt per liter; the best performance for Cr(VI) before hydrolysis was of 24.6% removal from the cellulose grafted with glycidyl methacrylate and acrylamide and co-grafted with acrylonitrile, which after hydrolysis removed 16.4%. For Cu(II), the best uptake was by the co-grafted with acrylic acid, removing 22.8 and 68.9% before and after hydrolysis, respectively. Finally, for Fe(II) before hydrolysis the best one was the cellulose-g-poly (glycidyl methacrylate), which removed 51.9% of the metal content in the solution, but after hydrolysis, this underperformed, removing only 74.6%, while the co-grafted polymers with acrylamide and acrylic acid removed 100% (Chauhan *et al.* 2005).

Polymers also were synthesized on okra cellulose fibers; the system was an aminoxide version of poly(acrylonitrile-co-methacrylic acid) and was evaluated under different pH ranges, which influenced the adsorption capacity. The best performance for Cu(II) was at pH 5.5 with a maximum of 76.8 mg/g; at the same pH, this system removed 268.3 mg/g of Pb(II). For Cd(II) at pH 6, the adsorption was of 141.7 mg/g, and for Zn(II) the maximum was of 62.9 mg/g at pH 6.5 (Singha and Guleria 2014). Poly(methacrylic acid-co-maleic acid) fibers were grafted from a CNF aerogel using Fenton's reagent; these branches decreased the specific surface area from 85 to 65 m<sup>2</sup>/g but increased the carboxyl content from 0.54 to 7.5 mmol/g. All experiments were done at a constant pH of 5, which allowed for the study of only the effects of the COO<sup>-</sup> concentration. Therefore, this high negative surface charge was used to efficiently remove up to 95% of Pb(II), Cd(II), Zn(II), and Ni(II) when the solution had concentrations lower than 10 ppm (mg/L) and ranging from 90 to 60 % with higher concentrations, obtaining a maximum of 165.8, 134.9, 136.0, and 115.6 mg/g for Pb(II), Cd(II), Zn(II), and Ni(II), respectively. Regeneration of the material was possible with 1 mM EDTA solution pH 5 (Maatar and Boufi 2015). This last work also demonstrated that the initial ionic strength (KCl) of the media has an effect on the adsorption capability of the different metals; the higher the salt concentration, the lower the adsorption capacity of the aerogel to adsorb the metals through coordination with exposed oxygen atoms of the side chains.

As for the "grafted to," TEMPO-oxidized cotton nanofibers (TOCNF) were used to generate an aerogel with branched polyethyleneimine (bPEI) in a ratio 1:2; the resulting sponge was used to serve as an adsorbent for some organic pollutants (p-nitrophenol, 2,4,5-trichlorophenol, and amoxicillin) and some metals (Cu, Co, Ni, and Cd). When a Langmuir isotherm was evaluated, the adsorption capability observed for the organic pollutants in a solution with initial concentrations of ranging from 0.1 and 50 mM was determined to be 1630, 205 and 556 mg/g, for p-nitrophenol, 2,4,5-trichlorophenol, and amoxicillin, respectively. Meanwhile for metals, the maximum absorption with an initial concentration of 0.1M was of 89.0, 57.2, 155.1, and 64.6 mg/g for Cu(II), Co(II), Cd(II), and Ni(II). When the four metals were mixed together, the Cu(II) was the most compatible with the gel, as it removed around 69.9 mg/g and only 8.8, 36.0, and 8.8 mg/g of Co(II), Cd(II) and Ni(II), respectively (Melone *et al.* 2015). A similar system was also tested for Cu(II) and Pb(II), but herein the nanofibers were from bleached softwood, and a ratio of 1:1 was selected. With the Langmuir model of an initial concentration of 3 mM, it was found that the maximum adsorption was of 175.4 and 357.1 mg/g (Li *et al.* 2018). When compared, the 2:1 ratio adsorbed 89.0 mg/g of Cu(II), while the 1:1 captured 175.4 mg/g; this could be due to the difference of the origin of the CNF or from the concentrations of the initial

solution, even though, these systems showed a non-specific selection, which provides versatility in the application possibilities.

The versatility and efficiency of these grafting processes can provide highly engineered material, with exciting designs and high selectivity in its performance; for example, an electrospun polyacrylonitrile scaffold was infused with ultrafine cellulose fibers, which were TEMPO oxidized and crosslinked to the scaffold through a carbodiimide reaction. This membrane was able to retain bacteria including *E. coli* and even viruses (MS2), improving the applications in the water treatment field (Sato *et al.* 2011). Another engineered grafted system for water treatment was generated with polyhedral oligomeric silsesquioxanes bearing multi-*N*-methylol groups (R-POSS) grafted to cellulose using citric acid and  $\text{MgCl}_2$  as linker and catalyst, respectively (Xie *et al.* 2010). This system proved to be effective in the removal of the reactive dyes Yellow B-4RFN and Blue B-RN. The removal was dependent upon the temperature; the higher it was, the less dye was adsorbed. Maximum capture for both was at 293 K with 16.6 and 14.4 mg/g, respectively (Xie *et al.* 2011).

As cellulose in the nanoscale enhances the surface area and availability of negative moieties, other nanoparticles have catalytic activities or a strong affinity to molecules that can be used in parallel for water treatment (Shrivastava 2010; Tyagi *et al.* 2012; Adeleye *et al.* 2016); when these nanoparticles are used as a composite with cellulose, the specific properties of both materials can be used in an additive way to obtain a better performance than when used alone. For example, hydroxyapatite is known to have an affinity for fluoride, which is a WHO regulated compound; because of it, a cellulose nanocomposite was developed with cotton fibers where hydroxyapatite was grown at the surface. When the material was immersed in a solution with 10 mg of  $\text{F}^-$  /L, the removal capacity reached a Langmuir maximum capacity of 4.2 mg/g, which is higher than the nano-hydroxyapatite *per se* (1.457 and 0.489 mg/g) and did not show any decrease in adsorption when other anions ( $\text{NO}_3^-$ ,  $\text{SO}_4^{2-}$ , and  $\text{PO}_4^{3-}$ ) were present (Yu *et al.* 2013). A similar study was performed, but herein the fibers were from bleached birch, and the aim was the removal of Cr(VI); the adsorption at 25 °C was of 2.21 mg/g. Interestingly, this system appeared to have a buffering effect in the solutions, so there was no impact from the pH to the removal capacity, but temperature seemed to have a positive relationship; this means that at a higher temperature a higher adsorption was obtained (Hokkanen *et al.* 2016).

Metallic nanoparticles, such as titanium dioxide, also have been used to develop photocatalytic nanocomposites with cellulose nanofibers. In one study that explains this, *Eucalyptus* TEMPO oxidized nanofibers were decorated with titanium dioxide particles to degrade a model organic molecule solution (0.01 g/L of methylene blue,  $\text{C}_{16}\text{H}_{18}\text{ClN}_3\text{S}$ , PubChem CID: 6099); simultaneously, two films were also decorated with Au and Ag nanoparticles above the preexisting titanium ones. The base film was able to degrade 60% of the methylene blue in the solution, while both Au and Ag charged specimens degraded 75%. As reusability is desired, mechanical tests were performed after each cycle, where the Ag-TiO<sub>2</sub>-CNF composite outperformed the others (Snyder *et al.* 2013). Another study was done on carboxymethyl cellulose (CMC) coated with zero-valent iron particles for the removal of trichloroethylene; herein, from a 10 mg/L solution, this system was able to extract only 9.7%, which is not the best performance but demonstrated the concept that this modified cellulose could be used for composites with metallic particles (Han *et al.* 2016). CMC was also used with hydroxyethyl cellulose as a citrate cross-linked hydrogel carrying potassium copper hexacyanoferrate; this system was generated to selectively capture cesium in seawater. From a solution with 19.9 mg/L of  $\text{Cs}^+$ , 12.4 g/L of  $\text{Na}^+$ , 2.3 g/L of

Mg<sup>2+</sup>, 469.1 mg/L of K<sup>+</sup>, and 148.3 mg/L of Ca<sup>2+</sup>, the hydrogel was able to remove 90.1% of Cs (*ca.* 265.8 mg/g) in only 1 h (Kim *et al.* 2017).

The use of ceramic and metallic particles is non-exclusive, as demonstrated by the use of a cellulose composite with magnetite that entrapped acid activated bentonite for the removal of Pb(II). This composite was evaluated at a range of 60 to 160 mg/L and at 298, 303, and 313 K; the Langmuir maximum capacity of the material was 2.86 mg/g at 298 K (Luo *et al.* 2016). Herein, the purpose of each component was different, as bentonite was the one targeting Pb(II), cellulose was the matrix, and the function of magnetite was to allow the separation and recovery of the material. The use of these specific properties creates the possibility of solving different limitations that water remediation systems present nowadays.

As previously mentioned, non-reactive interactions between cellulose and other materials can also provide composites with valuable properties. For example, a diaminobutane base poly(propyleneimine) dendrimer carrying 16 thiol groups was embedded in cellulose and used to reduce the permeability of metals from a 1 mmol solution of Cd(II), Hg(II), and Pb(II) at about 20% for the Cd(II) and 45% for the two latter mentioned (Algarra *et al.* 2014). Furthermore, an already modified cellulose can be used to generate the composites; hence, complex systems are obtained. For instance, a cystine grafted nanocellulose was embedded in an electrospun polyacrylonitrile, where the large resulting area and high surface thiol groups of the cysteine (109 mg/g) were used to adsorb Cr(VI) and Pb(II) with a removal capacity of 87.5 and 137.7 mg/g, respectively (Yang *et al.* 2014).

The use of these complex structures when the conforming materials are from different chemical natures can generate composites that are not selective adsorbents, but which have a hierarchical structure that gives them the potential to perform phase separations, extraction of oils, or the adsorbance of organic molecules with low solubility and hydrophobic domains. For example, a designed layered double hydroxide (LDH) composite based on alumina modified cotton cellulose fibers (Zhang *et al.* 2014b) was used as a template for an auto-assembled superhydrophobic-superoleophilic membrane with steric acid being deposited to the surface; this system proved to have a separation efficiency above 95% with various oil/water mixtures regardless of the mass ratio and was reused for up to 10 cycles (Yue *et al.* 2017). The same aim was accomplished by drop-casting steric acid and graphite flakes onto a cellulose 3-D scaffold (stabilized with polyethylene and polypropylene); the drop-casted materials provided a non-selective cellulose with a hydrophobic nature that allowed the adsorption of oils and organic solvents without an intake of water. The adsorption capacity of these sponges was reduced to 60% at the third cycle; but this level of uptake was fairly constant for 11 more cycles, in all tested oils (Calcagnile *et al.* 2017).

The numerous systems mentioned above demonstrate the use of cellulose for generation systems with environmental targeted applications, such as organic molecule removal, or more general, such as oil/water separation. The main advantage of cellulose is its high availability and the wide range of specific properties to select from, such as degree of crystallinity, aspect ratio, surface charge, among others, which makes the design of the systems as broad as the imagination can get.

**Table 1.** Cellulose-derived Materials and Pollutants Adsorbed

Material	DS	Pollutant	Capacity [mg/g]	Regeneration	Reference
Nanocellulose fibrils		Cd (II)	9.7	0.5 M HCl/ 0.5 M HNO <sub>3</sub>	Kardam <i>et al.</i> 2014
		Pb (II)	9.42		
		Ni (II)	8.55		
TEMPO-oxidized fibers	1.5	Cu(II)	67.2		Liu <i>et al.</i> 2016
	0.34	Cu(II)	135.5		Sehaqui <i>et al.</i> 2014
	0.26	Cr(III)	58		
		Ni (II)	49		
		Zn(II)	66		
	0.075	UO <sub>2</sub> (II)	167		Ma <i>et al.</i> 2012
Carboxylated fibrils	0.062	UO <sub>2</sub> (II)	1470		Sharma <i>et al.</i> 2017a
		Pb (II)	2270		Sharma <i>et al.</i> 2018b
		Cd (II)	2550		Sharma <i>et al.</i> 2018a
Nanocellulose with succinic anhydride		Cd (II)	231.79		Hokkanen <i>et al.</i> 2013
		Cu (II)	120.73		
		Zn (II)	105.26		
		Co (II)	78.85		
		Ni (II)	43.67		
Cellulose microfibers with succinic anhydride		Cu (II)	153.84		Gurgel <i>et al.</i> 2008
		Cd (II)	249.77		
		Pb (II)	499.97		
Phosphorylated nanocellulose		Ag (I)	120		Liu <i>et al.</i> 2015
		Fe (III)	73		
		Cu (II)	114		
		Fe (III)/Cu (II)	109/59		
Sulfonated nanocellulose	0.024	Pb (II)	248.64		Suopajärvi <i>et al.</i> 2015
		Au (III)	34.5	Acidic thiourea	Dwivedi <i>et al.</i> 2014
APTS modified microfibers		Ni (II)	160.47		Hokkanen <i>et al.</i> 2014
		Cu (II)	200.17		
		Cd (II)	471.56		
(2,3-epoxypropyl) trimethylammonium modified fibers		Cr(III)	23.92		Jain <i>et al.</i> 2016
		Cr (VI)	23.99		
EDTA modified microfibers		Pb (II)	227.3	0.5 M HCl	D'Halluin <i>et al.</i> 2017
		Cd (II)	102		
TEMPO-oxidized nanocellulose hydrogel		Cu (II)	268.2		Isobe <i>et al.</i> 2013

Nanocellulose hydrogel with TEMPO-oxidized CNC	Ag (I)	0.023	Karim <i>et al.</i> 2016	
	Cu (II)	33		
	Fe (III)	55		
Cellulose-g-polyaniline	Methyl orange	20.87	Bhowmik <i>et al.</i> 2018	
	Eosin yellow	58.14		
Cellulose-g-poly(acrylonitrile-co-methacrylic acid)	Cu(II)	76.82	Singha <i>et al.</i> 2014	
	Pb (II)	268.32		
	Cd (II)	141.73		
	Zn (II)	62.89		
Cellulose nanofibrils-g-poly(methacrylic acid-co-maleic acid)	Pb (II)	165.76	1 mM EDTA solution pH 5	Maatar <i>et al.</i> 2015
	Cd (II)	134.89		
	Zn (II)	135.99		
	Ni (II)	115.62		
TEMPO oxidized cotton nanofibers with polyethyleneimine (1:2)	p-nitrophenol	1630	Melone <i>et al.</i> 2015	
	2,4,5-trichloropheno I	205		
	amoxicillin	556		
	Cu (II)	88.96		
	Co (II)	57.16		
	Cd (II)	155.13		
	Ni (II)	64.56		
	Cu(II)/Co(II)/Cd(II)/Ni(II)	69.90/8.84/35.97/8.8		
TEMPO oxidized bleach softwood nanofibers with polyethyleneimine (1:1)	Cu (II)	175.44	Li <i>et al.</i> 2018	
	Pb (II)	357.14		
R-POSS grafted to nanocellulose	Yellow B-4RFN	16.61	Xie <i>et al.</i> 2011	
	Blue B-RN	14.4		
Cotton fiber with hydroxyapatite	F-	4.2	Yu <i>et al.</i> 2013	
Cotton fiber with nanohydroxyapatite	F-	1.45		
Bleached birch fibers with hydroxyapatite	Cr (VI)	2.208	Hokkanen <i>et al.</i> 2016	
CMC/hydroxyethyl cellulose with potassium copper hexacyanoferrate	Ce (I)	265.8	Kim <i>et al.</i> 2017	

Cellulose with magnetite and bentonite		Pb (II)	2.86		Luo <i>et al.</i> 2016
Cysteine-g-nanocellulose embedded in electrospun polyacrylonitrile		Cr (VI)	87.5		Yang <i>et al.</i> 2014
		Pb (II)	137.7		

### Chitin

Chitin, as cellulose, is a linear polymer that is a widely available structural polymer and is considered the second most abundant natural polysaccharide on earth. Chitin is composed of  $\beta(1 \rightarrow 4)$  2-acetamido-2-deoxy- $\beta$ -D-glucose (Fig. 2); therefore, the structure is akin to that of cellulose, except that it has acetamide functional groups at the carbon 2 position (Kumar Dutta *et al.* 2004). Even though the backbone is structurally alike, properties of both differ importantly; chitin is highly hydrophobic and insoluble in water and most organic solvents, therefore stable at natural environment. Also chitin is prone to interact with calcium and proteins, which can also be easily removed when necessary for reuse (Syahmani *et al.* 2018).

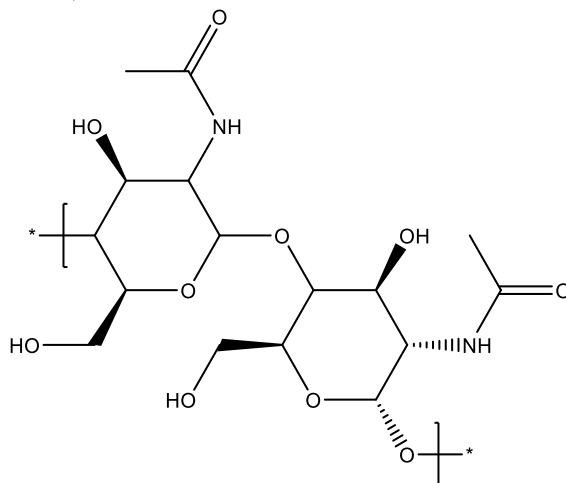


**Fig. 2.** Structure of chitin monomer

The acetyl amine groups allow the formation of hydrogen bonds and allows the chitin to serve as an excellent base material to design and develop water treatment systems. This capacity was shown when black water carrying Fe and Mn flowed through a column filled with newly extracted chitin from shrimp shell waste. The original water sample contained 10.34 and 0.20 mg/L, Fe and Mn, respectively, 210 mg/L of organic matter, and was dark brown colored with a pH of 3.88. After flowing through 25 cm of the column, 86.7% and 91.8% of the two metals, and 98.7% of the organic matter were removed from the solution, leaving a final stream with a pH 6.5 and a colorless flow (Syahmani *et al.* 2018). This simple experiment confirms the capacity of the chitin for entrapping metals and organic molecules, which also proved to be reversible in the case of metals when using a nitrite acid 0.5 M, providing the chance for reuse of the system. Moreover, chitin has proven to be even a better adsorbent than cellulose (cellulose I $\alpha$ , I $\beta$ , and cellulose triacetate) to eliminate insensitive munitions compounds such as 2,4-dinitroaniline (DNAN), 3-nitro-

1,2,4-triazol-5-one (NTO), nitroguanidine (NQ), and 1,1-diamono-2,2-dinitroethene (FOX7), due to the stronger interaction and lower energies required for the compounds to interact with the resulting composite surface (Todde *et al.* 2018).

Compared to the other polysaccharides, chitin presents facility to obtain derivatives with surface group modifications; the most common reaction for chitin is deacetylation to obtain chitosan, but this will be addressed in its own following section. Meanwhile, other modifications, such as the addition of new groups or oxidation of the acetlyamine (like carboxylic groups via TEMPO oxidation) can also be utilized to obtain functional materials. TEMPO oxidation demonstrated that, when performed before fibrillation, the surface area can be increased by about 25% compared with untreated chitosan nanofibrils (ChNF) and reduce the mean diameter of the fibers (Saito and Isogai 2004). When these two fibers were tested against CNF and TOCNF in Cu(II) adsorption at pH 6.2, TOCNF had the best performance with a removal of 135 mg/g; TOChNF removed 55 mg/g, ChNF 27 mg/g, and CNF 13 mg/g (Sehaqui *et al.* 2014). This last experiment showed how TEMPO-oxidation of the fibers enhances the adsorption capacity of both systems. The main difference is that the degree of oxidation of the TOChNF was not reported, while for TOCNF it was 0.34; this has an impact on the surface charge content (SCC) and, therefore, in the adsorption capacity. For example, CNF has a SCC of 0.1 mmol/g, and ChNF has 0.88 mmol/g, so a higher adsorption is expected of the ChNF. Another modification that was demonstrated was to thiol-functionalize (*ca.* 1.1 mmol/g) ChNF with cysteine via NHS/EDS coupling. From a range of 4 to 11 in pH and concentrations of 10 to 100 ppm of As(III), this system had the best capturing performance at a pH 7, having a calculated maximum adsorption of 149 mg/g (Yang *et al.* 2015).

As surface area is fundamental for adsorption capacity, methodologies to increase it have been developed; the most commonly reported are the mechanical treatments such as fibrillation by grinding (Liu *et al.* 2013; Oh *et al.* 2015), crystal generation (Fan *et al.* 2009; Jiang *et al.* 2018a), micro-structuration of particles (Gotoh *et al.* 2004; Wang *et al.* 2015a), and ultrasonication (Dotto *et al.* 2015).

The latter approach was shown to adsorb methylene blue when supported on a sand bed (5 g of ultrasonicated chitin and 180 g of sand); herein a MB solution with 50 mg/L flowed at a rate of 10 mL/min for 370 min through a column with 2.5 cm of internal diameter and 25 cm height. This system presented a maximum adsorption capacity of 51.8 mg/g, which represents 51.5% of removal and maintained this performance for up to 5 cycles after washings with 300 mM HCl solutions (Dotto *et al.* 2015).

When comparing chitin microparticles (ChMP) with nanofibers (ChNF) regarding their capacity to eliminate different metals such as Cd(II), Ni(II), Cu(II), Zn(II), Pb(II), and Cr(III), it was found that the nanomaterial was able to adsorb between 5 to 6 times more ions per gram of adsorbent and with less time to reach the saturation capacity (approximately 10 min for 80% of saturation). ChMP removed 59.4, 42.6, 23.4, 38.4, 198.2, and 6.4 mg/g respectively; while with ChNF, the maximum adsorption capacity was of 330.2, 134.7, 141.1, 134.0, 303.5, and 16.3 mg/g of Cd(II), Ni(II), Cu(II), Zn(II), Pb(II), and Cr(III), respectively (Liu *et al.* 2013).

Chitin microspheres were used as templates for immobilization of  $\alpha$ -amylase to generate catalytic composites with Au and magnetic composites modified with Reactive Black 5 (C<sub>26</sub>H<sub>21</sub>N<sub>5</sub>Na<sub>4</sub>O<sub>19</sub>S<sub>6</sub>, PubChem CID: 5360531) to adsorb methylene blue (Wang *et al.* 2015a). Herein, it was demonstrated that 2 g of the microspheres were able to eliminate all color in a 10 mg/L solution, and when the initial concentration was of 80 mg/L, the system presented a maximum adsorption capability of 46 mg/g. Similarly, a chitin

microsphere-clay composite was used to capture methylene blue, with a maximum capacity of 156.7 mg/g estimated with a Langmuir isotherm, when using an aqueous solution of 10 mg/mL in 20 min, with a small decrease in removal efficiency of 1% after 5 cycles with desorption through 1 M NaOH aqueous solutions (Xu *et al.* 2018).

A composite with bentonite was studied for Cr(VI) adsorption at varying pH to find the optimal conditions. The results showed that the maximum adsorption occurred at pH 4 and declined while pH increased, except that beyond pH 9 the Cr(VI) became insoluble, precluding the adsorption; herein it was also found that when concentrations of sorbent exceeded 1 g/ 100 mL of ion solution, the adsorption capacity decreased. After the Langmuir isotherm (from 5 to 1000 mg/L) was generated, the maximum adsorption capacity was found to be of 443.7 mg/g (Saravanan *et al.* 2013).

Chitin-derived structures can also be used for photocatalytic systems, to not only capture but also to degrade the organic pollutants in water sources. For example, Cu<sub>2</sub>O nanoparticles were synthesized on the surface of a regenerated chitin/graphene oxide film; this was tested for 3 h to degrade methyl orange. The best performance was when 4.5 g of chitin had 80 mg of graphene oxide and nanoparticles were obtained from a solution of 0.2 mol/L; this system was tested with concentrations of 10, 25, and 50 mg/L, reaching a removal of 92.1%, 72.3%, and 48.3%, respectively and degradation rates of 7.6, 15.6, and 20.1 mg/g h (Wang *et al.* 2015b). Another catalytic system was inspired by the tunicate tunichrome that selectively captures metals from water. To mimic it, ChNF that were homogenized by a high-performance grinder was used, and as a side effect of this treatment, fiber loss was approximately 11.2% of its surface acetyl groups. Then, the hydroxyl groups on the surface of these fibers were subjected to chemical reactions with maleic acid; the aim was to capture Au(III), and while doing so, to generate gold nanostructures on the surface of the fibers that were used as catalyst to degrade 4-nitrophenol. The maximum adsorption capacity of gold on the system was of 532.5 mg/g and with it, 0.5 mg/g\*h of the organic compound was degraded (Dwivedi *et al.* 2017).

Elsewhere, a polyurethane matrix was imbedded with chitin (*ca.* 99% and *ca.* 79% of acetylation), a polymeric amine as an additive, and two different catalysts, one being a hydroxyl substituted amine, while the second being a tertiary amine. All the combinations were used as an optimization platform for fluoride removal from a 15 mg/L solution for 72 h. The results showed that the best composition was 60% chitin (*ca.* 79%), 40% polymer, 2% of the catalyst with the tertiary amine, and no additive; this system was able to adsorb 0.29 mg/g at a pH of 5 (Davila-Rodriguez *et al.* 2009). A similar system, 53% chitin, 47% polymer, and 2% catalyst, was packed in columns and tested with natural waters containing carbonites, chloride, fluoride, sulfates, and organics for the same fluoride concentration of 5.1 mg/L. These tests resulted in an efficiency of about 85%, with 50 bed volumes treated in 20 min, and the system was regenerated with only 4 bed volumes of 0.1 M sodium hydroxide (Davila-Rodriguez *et al.* 2012).

Not only have chitin fibers been used by themselves, but also with nanocrystals (ChNC), which are usually referred to as nanowhiskers. ChNC have been used to develop composite fibers by electrospinning. One example is an electrospun membrane with polyvinylidene fluoride (PVDF) as a matrix carrying the ChNC, which was used to adsorb indigo carmine (C<sub>16</sub>H<sub>8</sub>N<sub>2</sub>Na<sub>2</sub>O<sub>8</sub>S<sub>2</sub>, PubChem CID: 5284351). This system had a maximum adsorption capability of 72.6 mg/g and a removal efficiency of 88.9% within 4 h of contact (Gopi *et al.* 2017). A less specific system was developed to separate oil-in-water emulsion by generating a super-hydrophilic membrane using ChNC in a matrix of N, N-isopropylacrylamide (NIPAAm) copolymerized with methylolacrylamide (NMA). The test

sample was made by adding 30 mL of toluene to 970 mL of deionized water with 10 mg of polysorbate 80 (Tween-80, C<sub>32</sub>H<sub>60</sub>O<sub>10</sub>, PubChem CID: 5281955) and flowed through the membrane with a driving pressure of 0.3 bar. Here, the fibers containing 10% of ChNC proved to be structurally stable under different pH conditions and salinity (2 M NaCl) with a removal of about 99% for up to 15 cycles in all of these treatments (Wu *et al.* 2018).

Therefore, the use of chitin in water treatment systems seems to be an easy approach for pollutant removal, as it also has low cost, is easy to obtain, and has the advantage of the characteristic moiety that allows for an easier modification approach. The system can be exploited to both main approaches, adsorption or to generate composites with higher specificity.

**Table 2.** Chitin-derived Materials and Pollutants Adsorbed

Material	Pollutant	Capacity [mg/g]	Regeneration	Reference
Chitin nanofibrils	Cu(II)	27		Sehaqui <i>et al.</i> 2014
TEMPO chitin nanofibrils		55		
Chitin nanofibrils with cystein	As(III)	149		Yang <i>et al.</i> 2015
Ultrasonicated chitin	Methylene Blue	51.8	300 mM HCl	Dotto <i>et al.</i> 2015
Chitin microparticles	Cd(II)	59.42		Liu <i>et al.</i> 2013
	Ni(II)	42.62		
	Cu(II)	23.45		
	Zn(II)	38.36		
	Pb(II)	198.19		
	Cr(III)	6.4		
Chitosan nanofibrils	Cd(II)	330.15		
	Ni(II)	134.72		
	Cu(II)	141.08		
	Zn(II)	134.03		
	Pb(II)	303.49		
	Cr(III)	16.28		
Chitin microspheres with Au, magnetic particles and Reactive Black 5	Methylene Blue	46		Wang <i>et al.</i> 2015a
Chitin/clay microsphere	Methylene Blue	156.7	1 M NaOH	Xu <i>et al.</i> 2018
Chitin-bentonite composite	Cr(VI)	443.71		Saravanan <i>et al.</i> 2013
Chitin nanofibrils with maleic acid	Au(III)	532.5		Dwivedi <i>et al.</i> 2017
Polyurethane/chitin and tertiary amine	F-	0.29		Davila-Rodriguez <i>et al.</i> 2009
polyvinylidene electrospun with chitin nanocrystals	Indigo carmine	72.6		Gopi <i>et al.</i> 2017

### Chitosan

Chitosan is the main derivative of chitin; it is obtained through the hydration of the amide moiety by concentrated NaOH and heat (40% at 120 °C for 1-3 h) or through enzymatic hydrolysis with chitin deacetylase (Shukla *et al.* 2013). This derivative is more often used in bio-applications than chitin due to its better solubility in water and in organic acids; this property is caused by the basic nature of this polysaccharide, which contrasts with the natural acidic nature of most other polysaccharides (Kumar Dutta *et al.* 2004).

Because of the deacetylation, chitosan is defined as a copolymer of  $\beta$ -(1 $\rightarrow$ 4) linked D-glucosamine and N-acetyl-D-glucosamine (Fig. 3). The main difference between chitin and chitosan lies in the number of glucosamine groups, or the degree of deacetylation (DD). The latter, as well as the molecular weight, purity and polymorphous structure are usually reported as important parameters that will define the properties of the consequent materials, such as viscosity, polyelectrolyte behavior, metal chelation, polyoxysalt formation, optical properties, and film formation (Struszczyk 2002; Kumar Dutta *et al.* 2004). Depending on the DD, the pK<sub>a</sub> also varies, but it is usually close to 7. When the DD is in a range of 70 to 80% the reported pK<sub>a</sub> value is approximately 6.5, which leads to a majority of deprotonated groups when the pH is above this value, challenging the interactions with other systems above this value (Orelma *et al.* 2012). Additionally, chitosan, as well as other polysaccharides with (1 $\rightarrow$ 4)- $\beta$ -D linked glucans, have been found to adhere irreversibly to cellulose and between them, being an useful property to generate composites with low energy consumption (Mishima *et al.* 1998; Orelma *et al.* 2011).

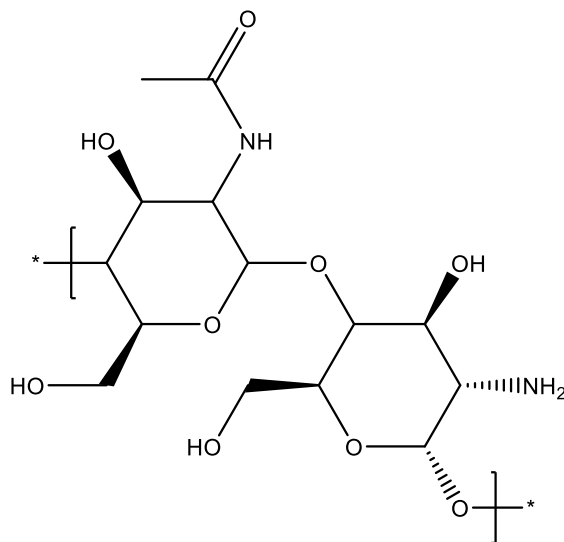


**Fig. 3.** Structure of chitosan monomers

The importance for water treatment of the molecular weight DD, and viscosity is clearly shown by the work from the group of Lopez Maldonado and coworkers (Meraz *et al.* 2016), where two different chitosan products were compared to flocculate organic compounds suspended in waste water from the maize industry (nejayote). The first chitosan had high molecular weight, 85% of DD and dynamic viscosity of 2.35 Pa/s, while the second one had low molecular weight, 95% of DD and a viscosity of 0.39 Pa/s. The sample wastewater was pretreated by centrifugation (3500 rpm for 5 min) in order to remove the non-colloidal particles. The final total organic carbon was 9836 mg/L, and the initial  $\zeta$  was

-6.62 mV. It was later mixed with 10, 15, 20, 25, 30, and 50 mg of the chitosan solutions (from a stock of 1% w/w using acetic acid 1% v/v), stirred for 1 min at 800 rpm, followed by 5 min at 200 rpm, and characterized by  $\zeta$ -potential measurements. Results showed a high dependency of pH, having the best performance at 5.5, with 80% of turbidity removal with only 2.35 g of chitosan of low molecular weight (MW) and 2.9 g of chitosan with high MW (Meraz *et al.* 2016). The paper shows how even the same material, without further modification can have an impact on the removal of contaminants and final applications and how easily chitosan can be used to adjust wastewater to meet regulations with simple measurement techniques.

Even though chitosan has been shown to be a good adsorbent material because of the surface charge provided by the acetyl amine and amine functional groups in the backbone, its interactions are not specific; for this, further modification can be done to add moieties or structures that add as selective attractors to the pollutants. For example, carboxymethyl groups were grafted to the surface of chitosan beads to make them selective to Cu(II) when a blend of Pb(II) and Mg(II) was also present; herein, the effects of pH, temperature, and adsorption equilibrium were studied. For the first part, the pH ranged from 1 to 5 with a constant concentration of 6 mmol/L; the best adsorption was found at a pH of 5. The temperature and equilibrium were therefore studied at this condition. The concentration for the equilibrium was varied from 40 to 450 mg/L, and the temperatures studied were 10, 21, 30, and 40 °C. The carboxylic groups had a higher preference for the Cu(II) ions over the other two metals and proved to be independent from the temperature. In all cases the maximum Langmuir adsorption calculated was of 130 mg/g for the modified chitosan, which was almost 2.5x greater than in pristine chitosan beads. When cycles of regeneration were performed using 0.1 M HCl, the system showed the same removal for 6 cycles without significant recovery lost; additionally, it was found that once the Cu(II) was adsorbed, the system was able to uptake 58 mg/g of phosphates, which would not happen without the metal (Yan *et al.* 2011).

A similar study was performed, but with a chitosan crosslinked covalently by epichlorohydrin and ionically by triphosphate (CTS-ECH-TPP) and adsorbing Cu(II), Cd(II) and Pb(II); it was also studied how many protons were titratable. The optimal adsorption pH was found to be of 5 for Pb(II), 6 for Cu(II), and 7 for Cd(II) with a maximum adsorption capability of 166.9, 130.7, and 83.8 mg/g, respectively, as calculated by Langmuir isotherms. In parallel fashion, 0.1 M nitric and hydrochloric acids proved to be the best eluents for the system for recycling the system with around 90% desorption (Laus *et al.* 2010).

This ionic crosslinking was also used to provide structure to chitosan microspheres that were later dried (80% of final porosity) and used for the separation of an oil/water solution in a packing column (7.8 mm \* 200 mm). This material was able to reduce by 90% (180 ppm) the average oil concentration with a flow of 3 mL/min and 7 mL/min, keeping its shape and with minimum porosity lost (final of 78%) after treating up to 50 L and 28 L for each flow, respectively (Grem *et al.* 2013).

As iron is the fourth most abundant material in the earth's crust and is non-toxic, cheap, easy to reduce and process, and has a redox potential of -0.44 V by which its reactivity with other metals is enhanced, it is widely proposed for composites that will be facilitating the removal of metals and other pollutants from water sources (Fu *et al.* 2014). When used in oxide form, the resulting nanoparticles also have a low toxicity, are easy to manipulate and modify, and especially, present super-paramagnetism, which can be used to recover and extract materials and sorbents from water solutions (Xu *et al.* 2012).

Because of this and its easy interaction with chitosan by the simple dipping process, iron in different forms has been widely used in composites with this material.

One example of the use of iron for water treatment is the comparison of chitosan iron coated flakes and iron-doped-glutaraldehyde-crosslinked chitosan granules for the removal of As(II) and As(V) from groundwater; experiments were performed using 0.1 g in 20 mL of solution pH 7 at 25 °C for 4 h, with As concentrations from 1 to 10 mg/L. Langmuir isotherms presented a maximum adsorption capacity of 2.32 and 2.24 mg/g of As(III) and As(V), respectively, for the granules, and 16.15 and 22.47 mg/g for the flakes. Both systems showed little interference from common anions (sulfate, phosphate, and silicates) present in the solutions, and they were able to be reused after regeneration with 0.1 M NaOH, for at least two cycles in a column reactor approach (Gupta *et al.* 2009).

Another type of iron used for As removal is a Fe-Mn binary oxide that was impregnated to chitosan beads; sorption isotherms were made using 1 g/L of the system at pH 7 and varying As concentrations from 5 to 60 mg/L with a contact time of 36 h on an orbital shaker at 180 rpm and 25°C. The pH influence was evaluated in the range of 5.5 to 11.5 with 50 mg of sorbent in a solution with 10 mg/L of As, while competitiveness of other ions ( $\text{SO}_4^{2-}$ ,  $\text{HCO}_3^-$ ,  $\text{SiO}_3^{2-}$ ,  $\text{HPO}_4^{2-}$ ,  $\text{Ca}^{2+}$ ,  $\text{Mg}^{2+}$ ) was tested in a 10 mg/L As concentration using 1 g/L of sorbent and a fixed pH of 7, all with the same contact time. The Langmuir maximum adsorption capacity was 39.1 mg/g for As(V) and 54.2 mg/g for As(III); adsorption efficiency decreased as the pH increased, but pH showed no significant impact from a range of 6 to 8 for As(V) and from 6 to 9 for As(III). For the ions competition,  $\text{SO}_4^{2-}$  did not present a significant effect, a slight inhibition was present with  $\text{HCO}_3^-$  and  $\text{SiO}_3^{2-}$ , and a significant decrease was consequent with the presence of  $\text{HPO}_4^{2-}$ . On the contrary, cations seemed to have a small enhancing effect on the adsorption. This system was also evaluated for reusability with 0.5 M NaOH; herein, efficiency dropped to 85 and 83% for As(III) and As(V), respectively, after the fourth regeneration; however, the system showed good mechanical stability with no apparent crushing or mass loss (Qi *et al.* 2015).

For magnetic iron nanoparticles, more work is allowed, as the magnetic properties provide an extra push, and a more convenient recovery can be performed. For example, a spun hollow chitosan fiber was used as a scaffold to generate magnetic iron oxide ( $\text{Fe}_3\text{O}_4$ ) nanoparticles (FeONP), which were then tested to adsorb Se(IV). In this work, to determine which variables were the more influential on the adsorption kinetics, a second order polynomial model was generated, and an Analysis of Variance (ANOVA) test was performed; the obtained results showed that only pH and sorbent concentration had a large effect on the experimental adsorption capacity of the Se(IV), which in optimum conditions (291.36  $\mu\text{g/L}$  of Se(IV) diluted, 92.97 mg/L of fibers, 3.67 pH, and 109.22 min of contact) was of 1.34 mg/g. When a Langmuir equilibrium model was generated, the maximum adsorption capacity was 15.6 mg/g. Finally, the presence of other recurring ions was tested at optimum conditions to see whether they have a negative effect on adsorption when concentrations of 1 to 10 mM were added to the solution; chloride and nitrates had no significant effect on the adsorption, but phosphate and bicarbonate did significantly reduce the capacity of the material for removal (Seyed Dorraji *et al.* 2017).

A more complex structure was obtained when using the chelating agents: ethylenediaminetetraacetic acid (EDTA) or diethylenetriaminepentaacetic acid (DTPA,  $\text{C}_{14}\text{H}_{19}\text{N}_3\text{O}_8$  PubChem CID: 100825), to crosslink and functionalize magnetic chitosan, and to then remove Cd(II), Pb(II), Co(II), and Ni(II) from wastewater with an adjusted pH of 3.5, using 2 g/L of the sorbents and a contact time of 16 h. Herein, the maximum adsorption capacity for the systems linked with EDTA was 168.5, 213.4, 72.8, and 81.0 mg/g,

respectively, and 175.5, 181.9, 66.0, and 69.7 mg/g for the beads crosslinked with DTPA. These systems were reused for 10 cycles using a 2 M HNO<sub>3</sub> solution for regeneration; the EDTA maintained an efficiency above 90% until the eight cycle, while the DTPA derivatives lost this threshold at the sixth cycle. The main advantage of both systems is the green chemistry employed for the synthesis and the easiness to recuperate them after use by the magnetic properties (Zhao *et al.* 2015a).

Composite systems have also been developed with this magnetic chitosan, and they have been found to benefit from the functional groups of other materials and the electrostatic and entropic interactions that come with them. For example, a covalently bonded composite of carboxymethyl chitosan was generated with the highly amine dense branched polyethyleneimine for Pb(II) removal. Here the Langmuir isotherm was not the best fit, as the R<sup>2</sup> was 0.9531, with a maximum adsorption capacity of 114.7 mg/g; the Langmuir-Freundlich isotherm had an R<sup>2</sup> fit of 0.9952 and a maximum of 124.0 mg/g. In this study, the optimal conditions were obtained using a contour plot with a fixed time of 3 h and a solution initial concentration of 50 mg/L; the optimum pH was 4.5 with a dosage of sorbent of 0.4 mg/L. Thermodynamic parameters were calculated, finding a negative  $\Delta G$  (~-9.5 kJ/mol) at the studied temperatures (303, 313, and 323 K) and an entropic gain of 21.80 J/mol K. Finally, recycling was tested using three different eluents with 0.1M concentration for all (EDTA, HCl, and NaOH). EDTA had the best performance, with 90% desorption efficiency; after 5 cycles this system still maintained about 85% removal efficiency, but some mass losses were observed (Wang *et al.* 2017).

This magnetic chitosan system has also been further composited with graphene oxide (GO) to adsorb different pollutants; for example, the adsorption of methylene blue was demonstrated in this system with a Langmuir isotherm calculation of the maximum adsorption capacity of 180.8 mg/g. The effect of pH was also studied in this experiment, and it was found that the optimal adsorption was obtained when the solution's pH was 10, and the system was recuperated without complication using a magnet, which made it an efficient adsorbent for dyes in water suspension (Fan *et al.* 2012). Another pollutant that was removed with this system was the drug ciprofloxacin, which presented a maximum adsorption capacity of 282.9 mg/g when a Langmuir isotherm was generated using 10 mg of sorbent in 30 mL of ciprofloxacin solution at pH 5. Subsequently, effects of ionic strength and pH were studied with a fixed concentration of 20 mg/L for ionic strength NaCl (20 and 200 mM) and CaCl<sub>2</sub> (1 and 10 mM). For the pH effect, it was shown that when the pH was below range for the species to be in its zwitterionic form (between 6.1 and 8.7), the adsorption was enhanced, which indicates that the electrostatic interaction is favored when is at the cationic state and was optimal at a pH of 5. With respect of the effects of the ions, both species decreased the interaction with the sorbent on 40.9 and 37.5%, respectively, probably due to the preferred interaction with these ions than to the drug and the interference with the  $\pi$ - $\pi$  interactions of the drug with the GO. Finally, regeneration was suitable for 3 cycles; the regenerated material presented a remaining 72% adsorption capacity when methanol (100%) was selected as eluent (Wang *et al.* 2016). For metal adsorption, the system was impregnated with an ionic liquid, specifically tetraoctylammonium bromide (C<sub>32</sub>H<sub>68</sub>BrN, PubChem CID: 2734117) in methanol (6.6%). This system was tested with Cr(VI) and described by a Langmuir isotherm to present a maximum adsorption capacity of 145.4 mg/g; the optimal pH was found to be in the range of 3 to 4 due to the protonated state of the hydroxyl and amino surface groups. Above this range the adsorption decreased around 20%. The system was evaluated for multiple cycles

using HCl for desorption, but after the third cycle, adsorption capacity started to drop drastically, retaining a capacity of 20 mg/g at the 10<sup>th</sup> cycle (Li *et al.* 2014).

Another composite generated with the ferromagnetic nanoparticles used them as seeds to grow a shell with ZrO<sub>2</sub> for a photocatalytic system with chitosan that can recover Cr(VI) and degrade 4-chlorophenol. Here, the nanoparticles with and without the chitosan matrix were tested using 50 mg of the sample in 100 mL of a solution with 70 mg/L of K<sub>2</sub>Cr<sub>2</sub>O<sub>7</sub> with pH of 2 at 30 ± 0.5 °C. For the chlorophenol, 0.01 g were added to 100 mg with 20 mg/L under natural sunlight for 3 h, and for the reuse, 6 continuous cycles were performed with a duration of 2 h for Cr(VI) and 3 h for the 4-chlorophenol. The NP by themselves presented a reduction of Cr of 71.2%, but when anchored to chitosan, this reduction increased to 84.7%; these results were improved by the addition of 0.2 mL of ethanol or isopropanol, to 92.4% and 98.5%, which was explained by a side reaction. The process also showed the influence of pH, as the performance decreased when pH become higher. Reductions of 84.7%, 61.2%, 40.5%, and 28.7 % were obtained with the pH of 2, 4, 6, and 8, respectively. For the 4-chlorophenol, degradation was of 66% with the nanoparticles alone, and of 88.6% when they were in with chitosan; the normal mechanism is the generation of –OH, which will attack and lead to dechlorination to produce 1,4-benzenediol or other alcohols with further nucleophilic reactions. Adsorption of the phenol was also measured in dark conditions to avoid the degradation; herein, it was 7.3% for the nanoparticles alone, while the chitosan adsorbed 22%, which facilitates the degradation and explains the better performance that this system has in the degradation. Finally, regarding reusability, for the Cr(VI), the photoreduction capability of the system with chitosan decreased after the 6 cycles from 87.1% to 85.1%, while for the 4-chlorophenol it changed from 71.2% to 67.3%. These results show that the systems with chitosan and magnetic nanoparticles are not only effective and easy to recuperate, but also are versatile in the systems that can degrade and adsorb, eliminating them from water sources and waste streams (Kumar *et al.* 2016).

Hydrous zirconium oxide (HZO) was also used in chitosan beads crosslinked with triphosphate for the removal of F<sup>-</sup> and Pb(II). Here, studies to find the best ratio of HZO and chitosan were performed; the conditions for the study were 2.5 g/L of the adsorbents, a pH of 5 for 160 h, and initial concentrations of 10.2 and 46.1 mg/L of F<sup>-</sup> and Pb(II), respectively. The best ratio was found to be 2:2.5 chitosan:HZO. However, such combinations were observed to have bad stability, so the ratio 2:2 was selected for the adsorption experimentation. The Langmuir isotherm presented a maximum adsorption capacity of 22.1 mg/g for fluoride and 222.2 mg/g for Pb(II); interestingly, the pH influence was inverse for the elements, as fluoride adsorption peaked at pH 3 and Pb(II) at pH 7, demonstrating that it is possible to select the element needs to be preferentially removed with the same system (Cho *et al.* 2016).

Zirconium (IV)-chitosan coordinated composites have also been of interest lately, as they prove to have a good ion exchange mechanism, which was used to remove Cr(VI) and V(V) from water (Zhang *et al.* 2013a, 2014a). For Cr(VI), the Langmuir modeling showed a maximum adsorption capacity of 175 mg/g in a solution with pH 5 and 30 °C; this pH makes the interactions occur via electrostatic forces and ligand-exchange mechanism, because when pH decreases or increases, the efficiency plummets. Also, when ions (Cl<sup>-</sup>, NO<sup>-3</sup>, and SO<sub>4</sub><sup>2-</sup>) are present in the solution, the adsorption capability is decreased by more than 60% as a result of the competition of the ions for the active spaces (Zhang *et al.* 2013a). For V(V), the Langmuir isotherm model maximum adsorption capacity is 208 mg/g at 30 °C, but in this case the optimum pH was found to be 4; this is a

consequence of the other vanadium oxidation states that are formed a higher pH, which affects the composite's adsorption capacity. Regarding the ions' competitiveness, chloride and nitrite had little effect, but the sulfite ion reduced the effectiveness when tested in a solution with 500 mg/L of  $\text{SO}_4^{2-}$  and 30 mg/L of V(V) (Zhang *et al.* 2014a). Both systems were evaluated for regeneration by 0.01 M NaOH solutions, which maintained 89% of the initial capacity after 5 cycles, and with a 0.05 M NaOH, for which the effectiveness was of 90% after 3 cycles for the Cr(VI) tests.

Zinc oxide (ZnO), as with the other oxide and metallic nanoparticles considered, has shown good efficiency for the removal of metals from water (Trujillo-Reyes *et al.* 2014); the generation of composites with natural polymers can then enhance these existing properties to maximize the removal performance. For example, ZnO nanoparticles coated with chitosan were tested to eliminate Pb(II), Cd(II), and Cu(II) and to study the viability of the reuse of this system. Langmuir isotherm modeling presented a maximum adsorption capacity of 476.1, 135.1, and 117.6 mg/g, respectively, with optimum pH at 6, 6.5, and 4. These values are close to the pKa of chitosan, which helps the adsorption add less competition between protons and the ions is present. As previously mentioned, the system was tested for reusability; for this, 0.01 M of EDTA was used as a regeneration solution. Herein, after 4 cycles, the system preserved > 90% of the removal capacity for all ions. Finally, three wastewater samples were used to analyze the viability in an uncontrolled environment; the results were satisfactory, as all metals were removed with efficiencies of more than 90%, with the decrease in uptake being linked to the concentrations of calcium, sodium, and potassium ions in the sample (Saad *et al.* 2018).

Metal-chitosan composites can be employed in many versatile ways to purify water; for example, an aluminum oxyhydroxide-chitosan was shown to be a good base system to modify with iron-zero valent,  $\text{MnO}_2$  nanoparticles, or silver nanoparticles, all to use as a filter for different purposes. The first was established for As(V) and Fe(II) removal, the second modification for Pb(II) removal, and the silver composite was used for the controlled release of Ag ions, exploiting the bactericidal properties of the ion. The system was tested first in a batch mode for the antimicrobial activity, using 2 g of the silver carrying system; it was shown that after 500 batches, only 29% of the silver nanoparticles were released, maintaining always below the safety threshold concentrations, and *E. coli* growth was eliminated completely. After this, all the systems were tested with a flow of 50 mL/min in a filter, where 1500 L of solution was passed with concentrations of  $1.5 \times 10^5$  CFU, 5 mg/g of Fe(II), and 150 mg/g of Pb(II). 400 mL of a 1 mg/L solution of As(V) was also tested. All solutions were purified with final concentrations below the permitted regulations, presenting evidence of the feasibility of the systems to be cheap and useful in low income houses (Sankar *et al.* 2013).

A non-metal oxide that has also been used for water treatment is  $\text{SiO}_2$ . Herein, like the last case, the oxide-chitosan (silicagel/chitosan) composite was used to adsorb another compound; in this case, La(III) was used, as it generates a better interaction with the fluoride ion that needs to be removed. When tested for adsorption in a solution with 10 mg/L and an initial dosage of 0.1 g of the materials at 303 K and pH 7, the system with La(III) removed 4.9 mg/g, while the system with only oxide-chitosan had an adsorption capacity of only 1.56 mg/g; it was also found that these adsorption values were relatively constant from pH 3 to 9 for the metal-containing version, and from 3 to 7 for the oxide-chitosan version. After the high extreme, the adsorption capacity decreased significantly and had little impact on the adsorption when  $\text{Cl}^-$ ,  $\text{SO}_4^{2-}$  and  $\text{NO}_3^-$  ions were present, but  $\text{HCO}_3^-$  reduced the adsorption capability. When the Langmuir isotherm was modeled, the

maximum adsorption capability was of 3.33 mg/g at 303 K, and  $\Delta G$  was negative in all temperatures modeled (303, 313, and 323 K) with a small  $\Delta S = 0.05$ , indicating a spontaneous process (Viswanathan *et al.* 2014). A closed system was also used for the fluoride removal, but herein, instead of  $\text{SiO}_2$ , bentonite was used in the generation of the base sorbent. This system presented an adsorption capacity at pH 5 and 30 °C of 2.87 mg/g, and when modeled with a Langmuir isotherm, the maximum adsorption capacity was of 8.6 mg/g at 30 °C, decreasing as temperature increased. Contrary to the previous system, this presented a decrease of capacity moving in both extremes of pH, as the performance at 3 was as low as at 9, a similar behavior with co-existing ions, with the carbonate ions affecting the adsorption more. Finally, the system was tested for 10 cycles of reuse using 0.5 M NaOH as a regeneration solution. A stable adsorption was maintained for 8 cycles, where only the 17% capacity was lost gradually, which indicates the good performance of the system through time (Zhang *et al.* 2014d).

A more ambitious system was prepared in chitosan beads containing a combination of activated carbon and montmorillonite ((Ca<sub>0.13</sub>Na<sub>0.34</sub>K<sub>0.03</sub>) [Al<sub>3.04</sub>Fe(III)<sub>0.41</sub>Mg<sub>0.49</sub>Ti<sub>0.01</sub>] [Si<sub>7.98</sub>Al<sub>0.02</sub>]O<sub>20</sub>(OH)<sub>4</sub>, PubChem CID: 71586775). The objective of this combination was to remove metals, but also some cationic and anionic organic pollutants in a one-step system. For this Zn, metoprolol (MTP, C<sub>15</sub>H<sub>25</sub>NO<sub>3</sub>, PubChem CID: 4171) and clofibric acid (CBA, C<sub>10</sub>H<sub>11</sub>ClO<sub>3</sub>, PubChem CID: 2797) were selected to act as a metal mode, a cationic beta blocker, and an anionic anti-cholesterol. The adsorption capacity was tested in a solution of the model substances with an initial concentration of 1.5 mmol/L with pH 6.5 at 25 °C using 200 mg of the system and controls. The results showed that the composites had indeed a better adsorption of the samples, but the most effective adsorbent was the chitosan with 1.5% of activated carbon, with an adsorption maximum of 10, 26, and 21 mg/g for Zn(II), MTP, and CBA, respectively; while the three components system had an adsorption of 10, 19, and 16 mg/g, respectively. Interestingly, for the anionic model, the montmorillonite-chitosan system presented the best performance with 30 mg/g for MTP, which was not the behavior when the base materials were tested alone, and activated carbon performed better (Bouyahmed *et al.* 2018). Overall, this system was able to capture all type of pollutants in good proportions, which has to be the ultimate goal of remediation systems.

As it has been shown, chitosan is easily molded into beads that can be packed into columns, while keeping a high surface area; another structure that can be considered for similar system design are foams that can be obtained when different polymers are mixed, entangled, and/or crosslinked. An example of this design is a foam composite generated with polyurethane and chitosan, which was tested for adsorption of an acid dye, acid violet 48 (C<sub>37</sub>H<sub>38</sub>N<sub>2</sub>Na<sub>2</sub>O<sub>9</sub>S<sub>2</sub>, PubChem CID: 11969493). Performance of the foam was studied varying pH, initial concentrations, and chitosan composition variance from 5 to 20% (w/w). The Langmuir isotherm model showed that the maximum adsorption capability was of 29.6 mg/g when the chitosan concentration was 20%, and decreasing as the concentration decreased; meanwhile, the best adsorption was at pH 3, decreasing gradually up to pH 8, and plummeting in a higher pH range (Lee *et al.* 2009).

Cellulose-chitosan composites are also interesting, as they are cheap and abundant raw materials, and, as seen in the previously and in this section, they have a large variety of sorbates, which can also be further improved with structure, group addition, or composite generations. An example of fiber combinations for a homogeneous membrane generation was completed using butyl methylimidazolium chloride [BMIm<sup>+</sup>Cl<sup>-</sup>] ionic liquid in a recovery variation of the process. This system was used to adsorb a cyanotoxin

called microcystin-LR (MC,  $C_{49}H_{74}N_{10}O_{12}$ , PubChem CID: 445434), which is one of the 80 reported variants of microcystins, but is linked with liver cancer and is closely monitored by the U.S. EPA (U.S. Environmental Protection Agency 2012). For the composite formation, a 10% solution was generated in the ionic liquid in the range 100 to 110 °C and using a 75% deacetylated chitosan to reach a final concentration of the dry composite between 20 and 67%, wherein the solutions were stirred for about 6 to 8 h. When a pure cellulose membrane was tested with no adsorption of MC, when the 20% was evaluated the adsorption capacity obtained by a pseudo-second order model was of 42 mg/g, while the 67% presented an adsorption capacity of 96 mg/g. An interesting point in this work is that the increase in chitosan also came with a swelling increase of 29.2% when 20 and 67% were compared. Lastly, reusability of the membrane was determined by putting the charged membrane in ultrapure water, resulting in the release of all the adsorbed MC and allowing the system to re-adsorb at the similar concentration on a second use (Tran *et al.* 2013).

**Table 3.** Chitosan-derived Materials and Pollutants Adsorbed

Material	Pollutant	Capacity [mg/g]	Regeneration	Reference
Chitosan Beads with carboxymethyl groups	Cu(II)	130	0.1 M HCl	Yan <i>et al.</i> 2011
Chitosan with epichlorohydrin and triphosphate	Cu(II)	130.72	0.1 HCl and HNO <sub>3</sub>	Laus <i>et al.</i> 2010
	Cd(II)	83.75		
	Pb(II)	166.94		
Chitosan iron coated flakes	As(III)	16.15	0.1 M NaOH	Gupta <i>et al.</i> 2009
	As(V)	22.47		
Iron draped glutaraldehyde crosslinked chitosan granules	As(III)	2.32		
	As(V)	2.24		
Chitosan beads impregnated with Fe-Mn oxide	As(III)	54.2	0.5 M NaOH	Qi <i>et al.</i> 2015
	As(V)	39.1		
Chitosan spun hollow fiber with iron oxide nanoparticles	Se(IV)	15.62		Seyed Dorraji <i>et al.</i> 2017
Magnetic chitosan with EDTA	Cd(II)	168.5	2 M HNO <sub>3</sub>	Zhao <i>et al.</i> 2015a
	Pb(II)	213.41		
	Co(II)	72.84		
	Ni(II)	81.05		
Magnetic chitosan with DTPA	Cd(II)	175.47		
	Pb(II)	181.92		
	Co(II)	66		
	Ni(II)	69.66		
Magnetic carboxymethyl chitosan/branched PEI	Pb(II)	114.7	0.1 M EDTA	Wang <i>et al.</i> 2017
Magnetic chitosan/graphene oxide	Methylene blue	180.83		Fan <i>et al.</i> 2012

	Ciprofloxacin	282.9	Methanol	Wang <i>et al.</i> 2016
Magnetic chitosan/ graphene oxide/tetractylammonium bromide	Cr(VI)	145.35	HCl	Li <i>et al.</i> 2014
Chitosan beads with triphosphate and hydrous zirconium oxide	F-	22.1		Cho <i>et al.</i> 2016
	Pb(II)	46.1		
Zirconium (IV)-chitosan	Cr(VI)	175	0.01 M NaOH	Zhang <i>et al.</i> 2013a
	V(V)	208		Zhang <i>et al.</i> 2014a
ZnO nanoparticles coated with chitosan	Pb(II)	476.1	0.01 EDTA	Saad <i>et al.</i> 2018
	Cd(II)	135.1		
	Cu(II)	117.6		
Silica gel-chitosan	F-	1.55		Viswanathan <i>et al.</i> 2014
Silica gel-chitosan with La(III)	F-	4.9		
Bentonite-chitosan with La(III)	F-	8.54	0.5 M NaOH	Zhang <i>et al.</i> 2014d
Chitosan beads/ activated carbon	Zn(II)	10		Bouyahmed <i>et al.</i> 2018
	Metoprolol	26		
	Clofibric acid	21		
Chitosan beads/montmorillonite	Zn(II)	6		
	Metoprolol	30		
	Clofibric acid	8		
Chitosan beads/activated carbon/montmorillonite	Zn(II)	10		
	Metoprolol	19		
	Clofibric acid	16		
Chitosan/polyurethane foam	Acid violet	29.6		Lee <i>et al.</i> 2009
Cellulose/chitosan (20%)	Microcystin- LR	42	H <sub>2</sub> O	Tran <i>et al.</i> 2013
Cellulose/chitosan (67%)		96		

As the use of ionic liquids is still a work in progress, another approach to combining these two natural polymers was by imbedding cellulose nanocrystals (CNC) in a chitosan matrix and then freeze-drying and compacting the material, which was crosslinked with glutaraldehyde for further stability. This system was tested for the removal of three dyes: Victoria Blue 2B (VB, C<sub>29</sub>H<sub>32</sub>ClN<sub>3</sub>, PubChem CID: 16599), Methyl Violet 2B (MV, C<sub>25</sub>H<sub>30</sub>ClN<sub>3</sub>, PubChem CID: 11057), and Rhodamine 6G (R6G, C<sub>28</sub>H<sub>31</sub>ClN<sub>2</sub>O<sub>3</sub>, PubChem CID: 13806). The maximum removal was found when pH was at 5 but was stable up to 9 for the VB and R6G, but it decreased for MV. Initial concentration also had an impact on the removal percentage, as it saturates faster; for an initial concentration of 1 mg/L, the removal efficiency was of 91, 70, and 98% for MV, R6G, and VB, respectively, but when the concentration was 10 mg/L, the percentage decreased to 48, 13, and 88%. Part of the

comparison was the impact of the crosslinking of the chitosan, assuming that it had an impact on MV and R6G adsorption but not on VB, which can be explained by the greater contribution of the hydrogen bonding mechanism employed by the latter, instead of electrostatic interactions where the sulfate, amino, and acetyl groups are the driving force (Karim *et al.* 2014).

This section has overviewed some approaches taken by researchers to improve water by adsorption with a low-cost biopolymer that possesses charged surface groups. These groups are the main driving force in adsorption for a lot of the cases considered. The groups also are a crucial factor when structure is desired, as these interactions with the media present the opportunity of precipitate in the generation of beads when pH is changed drastically and are anchoring points for the chemical and ionic crosslinks between the materials.

### Alginate

Alginates are also linear polymers consisting of (1→4) β-D-mannuronic acid (M) and α-L-guluronic acid (G), which are part of the structural components of algae and are an exopolymer of bacteria matrixes (Fig. 4). The blocks that are formed with the monomers depend highly on the origin and provide the resulting alginate with different properties, as the ease of hydrolysis and crosslinking depends on those. The blocks can be obtained by hydrolysis and fractionation, as consecutive G or M residues (GGGGGG or MMMMMM). These have low solubility and are more resistant to the attack of extreme pH or enzymes; meanwhile alternated blocks (GMGMGM) are degraded more quickly (Lee and Mooney 2012).

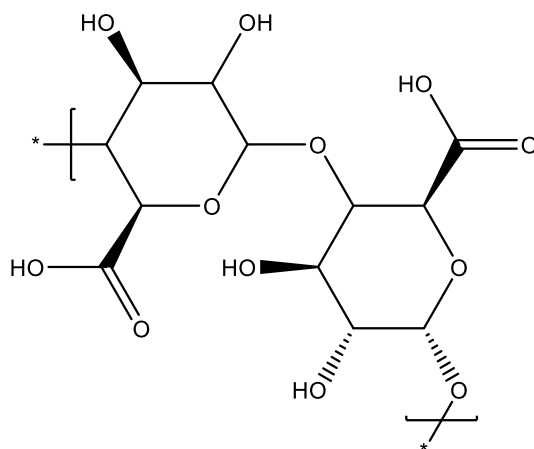


**Fig. 4.** Structure of alginates monomers

The attractiveness in the use of alginate, apart from the low toxicity, relatively low cost, and biocompatibility, is the mild gelation that occurs when divalent cations are present in the media (that presented in decreasing affinity order are Pb > Cu > Cd > Ba > Sr > Ca > Co, Ni, Zn > Mn) or when pH is below the pK<sub>a</sub> value of the uronic acids (3 to 3.5). It is important to highlight that only G-blocks are believed to be responsible for crosslinking while interacting with divalent cations; as the natural source dictates this G/M ratio, it is always important to characterize this to understand the physical and chemical characteristics of the generated hydrogels (Lee and Mooney 2012; Pawar and Edgar 2012).

Another interesting behavior of these resulting hydrogels is that they present a huge water uptake, which frequently has been used to maintain stable conditions for encapsulation and improvement of the persistency of sensitive molecules or systems such as cells. Similarly, the molecular weight of the raw material will have an impact on the properties, as when low molecular weight is used, the polymer solution or hydrogels generated can be plasticly modified and have been widely used to inject into the muscles or ingested orally for drug delivery and personal medicine; but when high molecular weight is preferred, higher mechanical properties and viscosity are provided, which lead to better water resistance and durability (Yang *et al.* 2011; Pawar and Edgar 2012).

A simple, direct, and effective way to use this polymer to improve the purity of water was tested by the addition of alginate and calcium to a sample water as a coagulant system and therefore reduce turbidity. In this study, 3 samples were tested with initial turbidities of 10, 80, and 150 NTU obtained by adding smectite clay; for treatment, concentrations of calcium ranged from 30 to 200 mg/L and alginate from 0.001 to 10 mg/L with low viscosity. For most of the samples, concentrations as small as 80 mg/L of calcium were used, and alginate concentrations varied from sample to sample; for 150 NTU, the lowest concentration to obtain an NTU of 1 or lower was 2 mg/L, while for 80 NTU the lowest alginate concentration was of 0.4 mg/L. For 10 NTU, two alginates were tested with low and high viscosities; herein, the low molecular weight was unable to reduce the turbidity below 4 NTU, but the high molecular weight accomplished it with a concentration of 2 mg/L and 120 mg/L of calcium. The most significant contribution of this system is that it works at neutral pH conditions, while aluminum, which is the most common coagulant, has to change pH to alkali conditions to work and produce a higher volume of slurry compared to the alginate treatment; therefore, alginate can act as a more feasible alternative that would also simplify downstream processes (Devrimci *et al.* 2012).

A more standard process to eliminate pollutants is the Polymer Assisted Filtration (PAF), where a polymer is pre-dissolved to enhance the precipitation of ions in a solution and then be removed by filtration. For this application, the polymer should have some inherent interaction with the ions, but nowadays, synthetic polymers are mainly used, even when these could have a certain toxicity or low solubility. Looking for alternatives, an alginate with M/G ratio of 1:1.5 and MW between 12 to 80 kDa was studied to eliminate divalent ions such as Pb(II), Cu(II), Zn(II), and Ni(II). Herein, it was observed that alginate was able to eliminate the Pb(II), Cu(II), and Zn(II) in concentrations as low as  $4 \times 10^{-2}$  M, but Ni(II) was adsorbed between 3 to 5 orders of magnitude less than the other metals, which was explained because of the soft ion nature of the Ni(II), which prefers to bind with ligands with softer interactions. The regeneration of the alginate was also demonstrated in acid conditions with times between 2 to 20 min depending on the pH (Fatin-Rouge *et al.* 2006).

For a less specific treatment, alginate proved to be able to separate oil and water efficiently for emulsification when a surface modification with dodecanol was performed to obtain a hydrophobic system. The emulsion was obtained using sunflower oil at 10 wt% and with the synthesized alginate having a substitution ratio of 8.47%. It was found that with only 0.8%, the emulsion was stable for up to one month, presenting no creaming or face visible phase separation and with less viscosity than the sodium alginate by itself (Yang *et al.* 2012), presenting it as a good system to separate oil when it could be incorporated to a complex composite.

As mentioned before, alginate has the inherent ability to generate beads when divalent cations are in the media. Exploiting this property, beads were generated with silver

particles (AgNP) using three different approaches: 1) entrapping premade AgNP, 2) reduction of Ag<sup>+</sup> in premade beads, and 3) a simultaneous gelation and reduction. The systems were then tested for bactericidal performance in a column through which 10<sup>5</sup> to 10<sup>6</sup> CFU *E. coli*/mL flowed. The results showed that the systems with the reduction *in situ* the CFU was decreased to non-measurable quantities in only 1 min of retention in the column, but the reduction in premade beads liberated high quantities of ions, up to 22 ppm, which was not the case in the simultaneous gelation and reduction-derived beads. This last observation implies that the latter might have a longer life-time, which is highly desirable for feasible water purification systems (Lin *et al.* 2013).

Even when beads are the most common structure generated by alginate coagulation, hollow fibers can also be prepared successfully; an example is the hollow fibers generated with TiO<sub>2</sub> for a photocatalytic reactor that was tested with the degradation of methyl orange. These fibers were tested wet and dried by supercritical CO<sub>2</sub> exchange. The fibers contained 41.7% of TiO<sub>2</sub>, and the dry fibers had better permeability than the theoretical calculation predicted, with a BET of 94 m<sup>2</sup>/g instead of 46, a pore volume of 0.46 mL/g instead of 0.36, and a mean pore radius was of 9.7 nm, while the prediction was of 16 nm. From an initial concentration of 6.4 mg/L, the efficiency of removal in flow without UV irradiation was of 0.08 mg/L, but with the UV was of 0.64 mg/L, which is much higher than what was obtained with the oxide nanoparticles alone. This was related to the high surface area, the adsorption to the alginate matrix, and the better dispersion of the nanoparticles due to the moieties from the alginate (Papageorgiou *et al.* 2012).

Iron oxides have also been used with alginate on account of their magnetic properties and adsorption capability. One example of the first property is a system developed in which alginate nanogel carrying tetra- sodium thiacalix[4]arene tetrasulfonate and synthesized nanoparticles for easier recuperation in metal water treatment. When solutions with 50 ppm of Co(II), Cd(II), Pb(II), Cu(II), Ni(II), and Cr(III) were tested with a pH of 7, the adsorptions ranged between 87 and 96.5%, with an apparent increase in adsorption when the magnetic particles were present compared to the system without them; the order of interaction was Pb(II) > Cd(II) > Cu(II) > Cr(III) > Co(II) > Ni(II) (Lakouraj *et al.* 2014). Meanwhile, the capture by adsorption was tested with As(III) and As(V) in alginate beads impregnated with iron oxide; herein, two loads were studied, 10, 20, and 30% of hydrous iron oxide using a constant concentration of 1 g/L in solutions that contained only one of the two arsenic species. Results showed that the total removal for As(III) was higher when the load was 30% but the rate of adsorption was lower, with 10% being the fastest. As for As(V), 20% was the best adsorption performance, but only around 60% was adsorbed. Also, phosphate salts appeared to have an effect on the adsorption, as the removal efficiency was lower when these ions were present. For the Langmuir model isotherms, the maximum adsorption capacity was 393.7 mg/g for As(III) and 200.4 mg/g for As(V). Finally, regeneration was possible with agitation in a 0.05 M NaOH solution for 24 h and continued to work for 8 cycles; no significant loss in efficiency was observed for both arsenic species, but bead mass decreased between 15 to 20% after the cycles for As(III) and As(V), respectively (Sigdel *et al.* 2016).

Another tested alginate composite for arsenic removal consisted of beads imbedded with zirconium oxide. This system was also tested with Cu(II), and the effects of the mixing of both arsenic and copper were tested, as well; separately, maximum adsorption capabilities were 32.3, 28.5, and 69.9 mg/g for As(III), As(V), and Cu(II), respectively, and when mixed, the As(V) was enhanced and more than doubling adsorption, while As(III) adsorption decreased, and no significant effect in Cu(II) adsorption was observed.

Initial concentration and pH had a larger effect on copper adsorption than in the arsenic species, with optimum conditions at 300 mg/L and a pH of 9. The main contribution of this system is the simultaneous adsorption of cations and anions from wastewaters (Kwon *et al.* 2016).

In the above studies, a specific oxide was used for the arsenic removal, but solid waste material that contains oxides can be used, also. To demonstrate this, a residue from an electroplating industry containing Fe, Ni, Cu, and Cr oxides was prepared in alginate beads and tested in sample waters. The optimum pH for this system was found to be 8, with 48 h to reach the plateau in a solution with an initial concentration of 15 mg/L. The Langmuir model maximum adsorption capacities were 126.5 mg/g for As(III) and 41.6 mg/g for As(V), which are about 60% higher than that of the raw material, leading to an improvement in the uses of waste products in other industries for water treatment (Escudero *et al.* 2009).

Ceramics have also been impregnated in alginate beads for organics and metals adsorption. For example, attapulgite ( $\text{Al}_2\text{H}_{29}\text{Mg}_2\text{O}_{15}\text{Si}_4^-$ , PubChem CID: 56842194) was encapsulated via freeze-drying, cross-linked with a calcium solution, and later tested for Cu(II) and Cd(II) adsorption. When the ratio load was 1:4 between the clay and alginate, the Langmuir modeling showed that the maximum adsorption capacity of this material was 119 and 160 mg/g, respectively. The pH seemed to have no impact when it was higher than 4, but at lower pH, the adsorption decreased. The optimal concentration for Cu(II) was 200 mg/L, while for Cd(II), it was 400 mg/L. Finally, the recyclability was tested with mild acid washing (0.2 M HCl) for 1 h; the copper adsorption efficiency was decreased by 32% after the second cycle and remained constant for the following 4 cycles; meanwhile, cadmium adsorption increased 26%, which was explained by the exchange of calcium from the material with more active sites for adsorption and possibly by the release of Ca ions, which transform the active sites to alginic acid. This is also consistent with a 23% weight loss in the first acid washing (Wang *et al.* 2018).

While for organics, imbedded nano-goethite in a fixed ratio of 3:1 alginate: clay was used for the adsorption of Congo red ( $\text{C}_{32}\text{H}_{22}\text{N}_6\text{Na}_2\text{O}_6\text{S}_2$ , PubChem CID: 11313). For this system, the optimum pH was 3 with a maximum adsorption capability of 181.1 mg/g. For reusability, 0.1 M NaOH was tested for 5 cycles with a desorption efficiency of 94%, but a loss of efficiency was observed after 4 cycles, decreasing from 85% to 76%, which is still acceptable for multiple uses (Munagapati and Kim 2017). Another commonly used clay is bentonite; when beads carrying it were tested for methylene blue adsorption, it was found that the optimal pH was between 7 to 10 with a maximum adsorption capability estimated by Langmuir isotherm of 799.4 mg/g. Herein, the efficiency loss after 6 cycles with acid washings in water pH 3, was only 7%; since the initial efficiency was a high value of 94%, the system was judged to be promising for the removal of the cationic dye MB (Djebri *et al.* 2016).

As activated carbon is one of the main adsorbents available, the use of other forms of carbon serve as an attractive alternative to replace this market; they have some of the same effects, but when nanomaterials are used, some can leak to water streams, resulting in micro-pollution. To prevent this, carbon nanotubes were immersed in alginate (1:1.5) and then wet spun and freeze-dried; performance was evaluated for Cu(II) adsorption in a solution with 20 mg/L, an ionic strength of 0.1 M using  $\text{NaNO}_3$ , and a pH between 2 and 7. It was found that good adsorption was present for the composite in all pH ranges, but it reached an optimal performance at pH 5 of 83.3%; higher pH presented precipitation of the copper species. Lastly, the maximum adsorption capability was modeled by Langmuir

isotherms and was determined to be 84.9 mg/g, which was higher than previous studies using the separate components and other natural derivatives as waste yeast, lignin, or activated sludge (Li *et al.* 2010). Another carbon-containing system, alginate-bentonite-activated carbon beads, were tested for methylene blue adsorption; herein, it was observed that after pH 6, maximum adsorption was reached and was stable to higher potentials. Interestingly, Langmuir isotherm models were made at three different temperatures 30, 40, and 50 °C having a maximum adsorption capability of 757.0, 982.5, and 994.1 mg/g, respectively. The first one was lower than a simple bentonite-alginate composite (Djebri *et al.* 2016), but there was a clear relationship between the increase in temperature and the adsorption capacity of the system. Also, the Gibbs free energy was increased from -5.92 to -5.72 kJ/mol, presenting a higher tendency to adsorb at lower temperatures; this indicates that there were other phenomena involved in the adsorption than physisorption, which is always a spontaneous process. Finally, regeneration was tested with methanol washes for 6 cycles, and adsorbance efficiency decreased from 94.4 to 75.4%, which are good values for the rehabilitation of contaminated water (Benhouria *et al.* 2015).

Like the previous cases, combinations with other polysaccharides or synthetic polymers can help gain better properties, generating composites with improved interactions with the pollutants. For example, three freeze-dried alginate-CNF (7:1) aerogels were generated for oil/water separation with a difference of how freezing was done to the mixture: direct refrigeration, unidirectional freezing, or bidirectional. Herein, cellulose was used only as a mechanical reinforcer, but also it helped to improve the hydrophobicity as hydroxyl groups were added and silanized, too. In this work, the structure of the aerogel was the main difference, with the bidirectionally frozen aerogel performing better when compression cycles were applied with almost non-stress reduction or plastic deformation compared with the others after 10 cycles. The contact angle for oil in this aerogel was 0° and of 148.7° for water, assessing the superhydrophobic nature of it, and when this aerogel was tested for the selectively pump oils from a water mixture, it showed adsorption capacities between 15 and 35 g/g for hexane, hexadecane, silicon oil, pump oil, toluene, colza oil, and chloroform in this order, with the same results for up to 10 cycles when regeneration was obtained by mechanical squeezing with 80% strain (Yang *et al.* 2018).

Meanwhile, alginate-chitosan beads were generated for divalent ion adsorption. These beads were generated by spraying an alginate-chitosan solution into a 0.15 M CuCl<sub>2</sub> solution and then exchanging the Cu(II) ions for H<sup>+</sup> in a 0.1 M HCl solution; these beads were tested for Cu(II), Co(II), and Cd(II), having a maximum adsorption capacity of 8.39, 3.18, and 6.63 mg/g, respectively and reaching saturation around 10 min in solutions with 5 mM of the chloride from of the metal (Gotoh *et al.* 2004). Similarly, nano-chitosan-alginate-cellulose (2:8:1) nano-beads were generated and tested for Pb(II) ions adsorption. Optimal adsorption conditions were found to be pH 6, initial concentration of 62.5 mg/L, dosage of 4 g and temperature of 50 °C; regeneration of the beads was also obtained using 0.1 M HCl solutions. The nano-chitosan comes from the addition of tripolyphosphate as an ionic pre-crosslinker to the chitosan solution before mixing with alginate and cellulose, which generates nanoparticles with a sharp distribution peak at 100 nm when observed in DLS. Langmuir isotherms were calculated, but no correlation was found, suggesting a different adsorption mechanism, which fit in a Freundlich model with an *n* value of 1.4916 (Vijayalakshmi *et al.* 2017). It is important to remember that this model is used when the energy term (*b*) in the Langmuir model is a function of surface storage, suggesting a heterogeneous phenomenon and using *n* as a constant that describes the shift from linearity, with 1 being the value that indicates linearity (Novotny 2003).

Also, polymers synthesized in the alginate matrix have been studied for metal removal. For example, alginate-polyaniline nanofibers were tested for Cr(VI); here calcium was not used as a crosslinker, as H-bonding was done with the N groups of the aniline structure. This system was able to eliminate 78.6% from a solution with an initial concentration of 100 mg/L of Cr(VI) in 60 min. The system efficiency also showed to be highly dependent on pH, decreasing efficiency as the pH increased from 2 to 10. Furthermore, the optimal dosage of material was found to be 150 mg. When other ions were tested in the solution, a decrease in the adsorption of the metal was observed when bicarbonate ions were present, but no significant loss was observed with chloride, sulphates, or nitrate ions. The maximum adsorption capability was modeled with Langmuir isotherms with values of 73.3, 74.5, and 75.8 mg/g at 303, 313, and 323 K, respectively and  $\Delta G$  of -10.48, -10.43, and -10.0 kJ/mol for each. Regeneration was also obtained with a 0.5 M NaOH solution with non-significant loss after 3 cycles, indicating that the system can be used as an alternative for the removal of this ion (Karthik and Meenakshi 2015).

One of the main advantages of the synthesis *in situ* of the polymer for the composite is that physical entanglement and van der Waals interactions will be the main forces holding the composite together, leaving available the inherent functional groups of the polymers; *i.e.* the carboxylic and hydroxyl groups of the alginate, which could then be leveraged for adsorbing the pollutants. Examples of this are beads of sodium alginate and poly[2-acrylamido-2-methylpropane-1-propanesulfonic acid] (PAMPS) which were evaluated for the adsorption of methylene blue (MB), Congo red (CR), methylene violet (MV, C<sub>14</sub>H<sub>12</sub>N<sub>2</sub>O<sub>5</sub>, PubChem CID: 73024), amaranth red (AR, C<sub>20</sub>H<sub>11</sub>N<sub>2</sub>Na<sub>3</sub>O<sub>10</sub>S<sub>3</sub>, PubChem CID: 5359521), and metal ions such as Cu(II), Pb(II), Cd(II), and Ni(II). The tested system had a Young's modulus of 191 kPa, a compression strength of 48 kPa, and a water uptake of approximately 30%. For MB adsorption, pH did not seem to have a major impact on the adsorption efficiency; on the contrary, the initial concentration of MB had an effect, increasing removal capacity as the concentration increased. When the Langmuir model isotherm was used, the maximum adsorption capacity was 2273 mg/g, which was close to the experimental values. When tested with the other dyes, AR and CR, which are anionic, it did not present a measurable adsorption, mainly due to the electrostatic repulsion; while cationic dye MV presented an adsorption of 2105 mg/g, which valued closely to the 2977 mg/g of MB. For the metal ions, adsorption capacity was 2042 mg/g for Pb(II), with lower values of 254, 50, and 843 mg/g for Cu(II), Ni(II), and Cd(II), respectively. Finally, recyclability of MB adsorption was tested for 5 cycles using NaCl as a desorbing agent, reaching a removal ratio of 90%, which leads to a possible industrial application as a broad quantity of cationic species adsorbed in high amounts (Shao *et al.* 2018).

As previously mentioned, alginate presents the advantage of being highly hygroscopic, enabling the use of encapsulated microorganisms for bioremediation. Some examples of this are the use of *Zoogloea ramigera* for Cu(II) removal in filters with different flow rates; the best removal obtained was of 94.3% of a solution with 50 mg/L and using 20 g of the sorbent with a flow of 3.6 mL/min and maintaining this efficiency after flowing 2700 mL. The only downside of this system was that mass transfer was slower than with the alginate beads, taking between 100 and 200 min to reach the maximum capacity. Recovery of the Cu(II) was obtained by washing with 0.005 M H<sub>2</sub>SO<sub>4</sub> and a pH of 2, which allowed for a reutilization of the system (Sag *et al.* 1995). Similar systems can be generated with multiple organisms; for example, microalgae *Chlorella vulgaris* was co-

immobilized with the bacteria *Azospirillum brasilense* and was used for the removal of ammonium and phosphorus ions.

**Table 4.** Alginate-derived Materials and Pollutants Adsorbed

Material	Pollutant	Capacity [mg/g]	Regeneration	Reference
Alginate beads with iron oxide	As(III)	393.7	0.05 M NaOH	Sidgel <i>et al.</i> 2016
	As(V)	200.4		
Alginate beads with zirconium oxide	As(III)	32.3		Kwon <i>et al.</i> 2016
	As(V)	28.5		
	Cu(II)	69.9		
Alginate beads with Fe, Ni, Cu, and Cr oxides	As(III)	126.5		Escudero <i>et al.</i> 2009
	As(V)	41.6		
Alginate beads with attapulgite	Cu(II)	119	0.2 M HCl	Wang <i>et al.</i> 2018
	Cd(II)	160		
Alginate beads with nano-goethite	Congo red	181.1	0.1 M NaOH	Munagapati <i>et al.</i> 2017
Alginate beads with bentonite	Methylene blue	799.4	H <sub>2</sub> O pH 3	Djebri <i>et al.</i> 2016
Alginate with carbon nanotubes	Cu(II)	84.88		Li <i>et al.</i> 2010
Alginate beads with bentonite and activated carbon	Methylene blue	756.97	Methanol	Benhouria <i>et al.</i> 2015
Alginate-chitosan beads	Cu(II)	8.39		Gotoh <i>et al.</i> 2004
	Co(II)	3.18		
	Cd(II)	6.63		
Alginate-polyaniline nanofibers	Cr(VI)	73.34	0.5 M NaOH	Karthik <i>et al.</i> 2015
Alginate beads with PAMPS	Methylene blue	2272.73	NaCl	Shao <i>et al.</i> 2018
	Methylene violet	2105		
	Pb(II)	2042		
	Cu(II)	254		
	Ni(II)	50		
	Cd(II)	843		

When an initial concentration of ammonium was of 3 mg/L, 93% was eliminated in the first 2 days and 99% after the 6<sup>th</sup> day. Meanwhile, phosphorous at concentrations above 20 mg/L presented no change in concentration, but in a solution of 15 mg/L, 75% was eliminated in 2 days with no further change. When both ions were present, 91% of ammonium was eliminated after 2 days, but no change in phosphorous concentrations was

observed; this suggests a higher affinity to the ammonium than to phosphorous. It is important to say that the use of alginates allowed for the use of these organisms in continuous and semi-continuous systems, so when the sample water was recirculated, drops in phosphorous concentrations were observed after the 3<sup>rd</sup> cycle, indicating some mass transfer phenomena occurring (De-Bashan *et al.* 2002).

An advantage of bioremediation is the use of intrinsic biochemical routes and defense mechanisms of the bacteria to accumulate the pollutants and easily recuperate them. For instance, mercury was stored by *Enterobacter* sp. that was entrapped in alginate beads. For this experiment, 30 g of the wet sorbent were used in a solution with 5 mg/L of HgCl<sub>2</sub> at 30 °C and in a more complex water sample obtained from an industrial discharge in India and enriched with 7.3 mg/L of Hg(II). The reusability of the beads was assessed by 3 washes in ultrapure water. Complete removal was obtained in both samples after 72 h with the bacteria immobilized in the beads, while free bacteria only removed 69%, and the beads alone 19%. No more than two cycles were permitted, as for the fourth efficiency decreased to a 49%. The loss of efficiency was attributed to the loss of cells from the washes with ultrapure water. The mercury here was found stored as nanoparticles (3.75 ± 0.03 nm) at the cytoplasm of the bacteria with a change of Hg(II) to Hg(0), due to the presence of reductase found in this organism, thus showing the advantage of using more complicated biosystems for water remediation when treating toxic pollutants (Sinha and Khare 2012).

This section showed advantages of using inherent properties of the polysaccharides, such as alginate, that can be exploited to provide structure, for direct adsorption, or as carriers of other components including nanoparticles, polymers, or microorganisms, presenting more options of hygroscopic materials for water treatment.

### Hemicelluloses

Hemicelluloses are another class of widely abundant heteropolymers, as they constitute about 25 to 35% of wood mass (Smook 2016). The major monomeric units in the polymers are hexoses (D-glucose, D-mannose, and D-galactose), pentoses (L-arabinose, D-xylose), and uronic acids (D-glucuronic acid, 4-O-methyl-D-glucuronic acid, and D-galacturonic acid) (Gírio *et al.* 2010; Salam *et al.* 2011a). These monomers form branched chains with both  $\alpha$  and  $\beta$  linkages with lower molecular weights than the other polysaccharides. These formed polymers can be divided into four groups: xylans, mannans, xyloglucans, and mixed-linkage  $\beta$ -glucans.

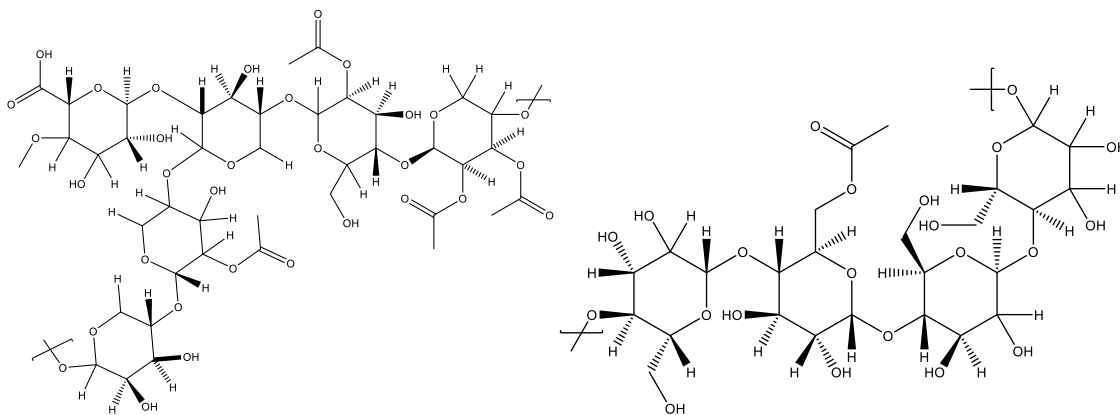


Fig. 5. Structures of xylan (left) and glucomannan (right)

Among these groups, xylans the most abundant (Fig. 5, left), as they represent the major components of hemicelluloses in hardwoods and about half of the tissue in cereal grains (Wang *et al.* 2013; Sixta 2006); while mannan-type, such as glucomannans (Fig. 5, right) and galactoglucomannans, are mainly found in the secondary cell wall of softwoods (Gírio *et al.* 2010).

The main disadvantage that these polysaccharides present is their high solubility in water; therefore, a great portion of them are lost in the downstream processes of pulping, turning them into residue that is usually burned to obtain energy. Nevertheless, some work has been done to obtain added-value products targeting water remediation systems. For example, the modification of xylan with organic acids, such as citrate, succinic anhydride, and sodium monochloroacetate, was performed to increase the carboxyl content 2x in the three cases and to increase the water absorption from 200% in natural xylan to 500% when modification with citrate was done (Salam *et al.* 2011a). This modification with citric acid, with and without catalyst (sodium hypophosphite, SHP), was then used to study the adsorption capability of this material for Cu(II) and methyl orange. The adsorption experiments were done using a slurry of the material with the following standard solutions: 500 mg/L of Cu(NO<sub>3</sub>)<sub>2</sub> at room temperature, pH 4.5, and 400 rpm for 24 h; methyl orange was done with 20 mg/L pH 2.5 for the same time at room temperature. Herein, the study showed that the catalyst increased the crosslink reaction instead of enhancing the carboxyl group content, and consequently the carboxylated xylan without the catalyst had the better adsorption capacity with 83.8 mg/g of Cu(II) and 1.69 mg/g methyl orange when the weight ratio of citric acid/xylan was 3.6. In contrast, the unmodified xylans had a binding capacity of 11.4 and << 0.1, respectively, for Cu(II) and MO, demonstrating the potential to use these hemicelluloses that were modified with green chemistry and that can provide hydrogels with high water intake and can be easily degraded after usage (Wang *et al.* 2013).

Another work with hemicelluloses used pressurized hot water extracted polysaccharides from *Pinus wallichiana* and modified all the hydroxyls to improve the adsorption of malachite green (MG, C<sub>23</sub>H<sub>25</sub>ClN<sub>2</sub>, PubChem CID: 11294). Herein, C6 was first acetylated, while C3 and C2 were carboxylated via aldehyde formation. Adsorption capability was tested with 5 g of the sorbent in a solution with 100 mg/L of MG at 50 °C. After confirmation of the adsorbance capacity, ranges of pH (3 to 9), temperature (20 to 90 °C), and concentration (10 to 120 mg/L) were also studied. The optimal concentration was found to be 98.2 mg/g at 70 °C and pH 6.5. Reusability was also tested for 16 cycles, where 67% of the capacity was possible, removing a total amount of 1294 g/g in the 16 cycles. Finally, kinetics and thermodynamics were studied. The Langmuir isotherm model showed a maximum adsorption capacity of 456.2 mg/g with the following thermodynamic parameters at 343 K:  $\Delta G$  of -16.62 kJ/mol,  $\Delta H$  of 49.9 kJ/mol, and  $\Delta S$  of 172.02 J/mol K. This demonstrates the great capacity of hemicellulose for use as an adsorbent for this dye or similar cationic organic molecules (Gautam *et al.* 2018).

Similar to the polysaccharides mentioned above, composites can play an important role in enhancing the adsorption capacity of hemicelluloses. For example, konjac glucomannan was crosslinked via calcium ions with graphene oxide and tested for the adsorption of methyl orange and methyl blue. In this work adsorption capacity was modeled with Langmuir and Freundlich isotherms, finding that the latter gave a better estimate with maximum capacities of 51.6 and 92.3 mg/g for MO and MB, respectively, and  $n$  value higher than 1. Interestingly, the composite swelled approximately one third less than the one without the graphene, but adsorption of the dyes was almost doubled, which was attributed to  $\pi$ - $\pi$  stacking and ionic interactions with the oxide and the available

hydroxyl groups (Gan *et al.* 2015). In the same way, MB was adsorbed to corn stover hemicelluloses hydrogels containing a variety of swellable clay (Laponite XLG,  $\text{Mg}_{5.34}\text{Li}_{0.66}\text{Si}_8\text{O}_{20}(\text{OH})_4\text{Na}_{0.66}$ ) to improve the adsorption capability. In this case, the cross-linkage was done with polyethylene glycol diglycidyl ether (PEGDE). Concentrations of each component were varied to understand the mechanical and rheological behavior, but adsorption was performed only in the hydrogels that had 1.5 M PEGE/ 1 M hemicelluloses and with 2 M of clay. Adsorption experiments were carried out with 100 mg of a freeze-dried sample in a solution at 25 °C and pH ranging from 2 to 9 to find the optimal conditions. The pH study results show that efficiency was low in acidic conditions, but when pH 6 was reached, adsorption stabilized at the maximum efficiency. For the modeling, Freundlich and Langmuir equations were tested in the isotherms; results varied, as the hydrogels without clay fit the a Freundlich model, while the one with incorporated clay fit the Langmuir monolayer model with a maximum adsorption capacity calculated of 148.8 mg/g (Cheng *et al.* 2016). This last result makes evident how nanocomposites can improve the adsorption capacity by changing the mechanism in which the pollutant interacts with the hydrogels; in both cases, water adsorption was reduced, but mechanical stability was achieved by simple crosslinking of the hemicelluloses.

As previously mentioned, one of the main drawbacks of the use of hemicelluloses is their low molecular weight compared to other polysaccharides, such as cellulose. Therefore, the mechanical properties of materials prepared with these polysaccharides are somehow inferior compared to others such as cellulose; to remediate this, the incorporation of other polymers, such as chitosan, can improve the final mechanical properties. A crosslinked aerogel with tri-carboxylated hemicellulose-chitosan (1:1) has been developed and tested for swelling stability in water and saline solutions. This system presents only 8% mass loss in water and a gain of 9.3% in the saline solution, also having a tensile strength of 1.61 N/mm<sup>2</sup>. An interesting point is that the volume expansion was 110% in water and 240% in saline solutions, but the mass adsorbed was only 80 g of water and 100 g of salts, meaning that the salts improved the swelling by rearranging the hydrogel without degrading the material, as no mass loss was observed, demonstrating that the composite can be used for water treatment in different conditions (Salam *et al.* 2011b). A similar system was generated by grafting pentetic acid (DTPA,  $\text{C}_{14}\text{H}_{23}\text{N}_3\text{O}_{10}$  PubChem CID: 3053) to hemicelluloses and then crosslinking with chitosan; this hydrogel was tested for the adsorption of Pb(II), Cu(II), and Ni(II) ions and swelling in saline conditions. The results showed that this system was stiffer than the one obtained with carboxylated hemicellulose, as salt uptake was 0.30 g/g, but there were similar losses and gains in water and saline solutions. Meanwhile for the metallic ions, the best conditions were at pH 5 and initial concentration of 5 mg/L, having a maximum adsorption of 2.9, 0.95, and 1.37 mg/g for Pb(II), Cu(II), and Ni(II), respectively (Ayoub *et al.* 2013). A more complex hemicellulose-chitosan was generated by adding  $\text{TiO}_2$  to the hydrogel to further improve the adsorption of metals. In this case the crosslinking was made by Schiff base linkages between the aldehyde groups of the hemicellulose (xylan) and the amines from chitosan. This hydrogel had a great water intake of 1507% g/g in water and 821% g/g in the saline solution, which is greater than the two previous studies; Langmuir isotherms modeled the adsorption of the metallic ions, giving maximum adsorption capacities for Cu(II), Cr(VI), Ni(II), Cd(II), and Hg(II) of 158.7, 97.1, 96.2, 78.1, and 76.3 mg/g, respectively. Analysis of thermodynamic and kinetic data revealed that the adsorption was spontaneous and endothermic, with  $\Delta G$  between -7 and -1.55 kJ/mol and positive  $\Delta H$  (Wu *et al.* 2014). These three studies made it clear that the combination of hemicelluloses and chitosan can

help to improve water uptake and stability, allowing the use of hemicelluloses in more complex systems for water treatment.

While chitosan is great for the adsorption of metals due to the amine functional groups, other synthetic polymers can also help in the stability of hemicelluloses, and the generation of materials is applicable to pollutant capture. For instance, butyl acrylate and acrylamide were used jointly to generate hemicellulose-containing latex (HCL), which was studied for the adsorption of MB. An interesting finding with this system was that adsorption was constant between pH 3 to 7 (30.4 mg/g), and in more alkali conditions adsorption increased, reaching a maximum at pH 13 of 97.3 mg/g; this was explained as the more negative surface charge that the composite acquired at lower proton concentration was found.

**Table 5.** Hemicelluloses-derived Materials and Pollutants Adsorbed

Material	Pollutant	Capacity [mg/g]	Regeneration	Reference
Carboxylated xylan with sodium hypophosphite	Cu(II)	83.8		Wang <i>et al.</i> 2013
	Methyl orange	1.69		
C6-acetylated, C2, C3-carboxylated hemicelluloses	Malachite green	456.23		Gautam <i>et al.</i> 2018
Glucomannan with graphene oxide	Methyl orange	51.6		Gan <i>et al.</i> 2015
	Methyl blue	92.3		
Hemicelluloses with PEGDE carrying laponite	Methylene blue	148.8		Cheng <i>et al.</i> 2016
Hemicelluloses -g-pentetic acid with chitosan	Pb(II)	2.9		Ayoub <i>et al.</i> 2013
	Cu(II)	0.95		
	Ni(II)	1.37		
Hemicellulose-chitosan with TiO <sub>2</sub>	Cu(II)	158.7		Wu <i>et al.</i> 2014
	Cr(VI)	97.1		
	Ni(II)	96.2		
	Cd(II)	78.1		
	Hg(II)	76.3		
Hemicellulose-containing latex	Methylene blue	42.73		Zhang <i>et al.</i> 2015b
O-acetyl galactoglucomannan -g- methacrylate	As(V)	48.17		Dax <i>et al.</i> 2014
	Cr(VI)	40		

The adsorption followed tightly the Langmuir isotherm models, showing a maximum adsorption capability at 25 °C of 42.7 mg/g (Zhang *et al.* 2015b). Furthermore, methacrylate was grafted to O-acetyl galactoglucomannan, which was used to generate hydrogels for arsenic and chromium removal. The hydrogel generated with these materials

was able to uptake 15 times its initial weight in water after 120 min; the maximum adsorption of the pollutants was observed at pH 9, which ensures that As and Cr must be in their anionic forms. The maximum adsorption obtained with the system was 48.2 mg/g for As(V) with similar results for the Cr(VI), which was constant for Cr(VI) for two more batches but was reduced in one third for As(V) in the subsequent tests (Dax *et al.* 2014).

Even though the low molecular weight of the hemicelluloses could present a problem for application in more complex materials generation, the addition of functional groups or using crosslinking agents provides an increase in the network generation within the hydrogels. This network generation provides a feasible approach to obtaining materials that can improve water quality using an abundant and underused resource such as the hemicelluloses.

#### *Starch: Amylose and amylopectin*

Another important polysaccharide blend is starch, which is produced in plants, tuber crops, and roots for storage of energy (between 16 and 24% mass content) and constitutes an important element in the human diet (Hoover 2001; Sajilata *et al.* 2006). Starch is composed of two main glucose-based polysaccharides: amylose and amylopectin; the first is a linear structure of glucose residues linked by  $\alpha$ -D-(1  $\rightarrow$  4) glycosidic bonds (Fig. 6), which ordinarily constitute between 15 to 20 % of total starch. Amylopectin is a branched structure with both  $\alpha$ -D-(1  $\rightarrow$  4) and  $\alpha$ -D-(1  $\rightarrow$  6) glycosidic bonds and in which side chains are typically 20 to 25 glucose units (Hoover 2001; Singh *et al.* 2010).

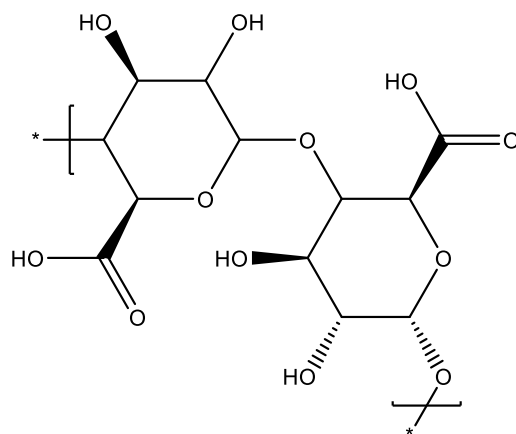


**Fig. 6.** Two glucose molecules joined by  $\alpha$  1, 4 linkage, which originates backbone of amylose and amylopectin

Their composition is the same as cellulose, but the difference in the bond orientation ( $\alpha$  vs.  $\beta$ ) causes an important difference in how both polymers pack in the natural environment. Starch polymers form helices instead of fibers, and these aggregate into granules with 70% of amorphous structure, while the other 30% form a crystalline region in the granules which consists primarily of amylopectin. This difference in cluster formation and in the amorphous proportion makes the starch more susceptible to enzyme degradation than cellulose chains (Sajilata *et al.* 2006).

Just as in cellulose, the hydroxyl groups in the polymeric backbone of starch permit the formation of highly hygroscopic materials while also allowing the use of hydroxyl groups as reactive points to add moieties to improve the uptake of pollutants or specific molecules. For example, starch was poly-carboxylated at C6 by nitrogen oxides and used

to generate a hydrogel that was tested to adsorb Cu(II). The maximum adsorption capacity was 128.3 mg/g, which was obtained with 2 h contact at 40 °C, pH 7, and 50 mg/L initial concentration, following a Langmuir isotherm. A chelation binding mechanism where coordination between the copper, and the carboxyl, hydroxyl, and keto groups of the hydrogel was suggested to be the predominant phenomenon (Chauhan *et al.* 2010). Similarly, N-(3-chloro-2-hydroxypropyl) trimethyl ammonium chloride (CHPTAC) was incorporated into starch as a cationic moiety. This material was tested as a flocculant in 0.25% w/w silica suspensions and compared with other commercial options, showing a decrease from 13 NTU to approximately 4 NTU at neutral conditions and performing better than most of the commercially available options, proving to be a low-cost material with good performance as an option for wastewater treatment systems (Pal *et al.* 2005).

In the previous cases, cationic groups were added to the surface of hydrogels, and layered double hydroxide (LDH), also called hydrotalcite clay, was used to obtain negative surface charges (Zubair *et al.* 2017). An example of this is the use of starch-NiFe-LDH composites in two proportions (1:1 and 1:2) for the removal of methyl orange. The optimum conditions for adsorption were found to be pH 3, initial dosage of 10 mg/L, 180 min, and low concentrations of initial MO dissolved; meanwhile, for the modeling of the isotherms, the Freundlich model was found to fit better than the Langmuir, indicating a heterogeneous adsorption that was favorable, as  $1/n$  was lower than 1, with a maximum adsorption capacity of 388 and 358 mg/g, respectively, which was reproducible for 4 cycles using a 0.1 M NaOH solution for regeneration (Zubair *et al.* 2018).

A less specific adsorption mechanism has been shown by carbon nanotubes. To improve the biocompatibility of these materials, starch is a good alternative that has many advantages. In the following case, carbon nanotubes were covalently linked to starch (14.3 %) and iron oxide nanoparticles for facilitating the removal from solutions. This system was then tested for the removal of methylene blue and methyl orange in solutions containing 500 mg/L of the material with 373.9 and 327.3 mg/L of the MB and MO, respectively. An adsorption of 135 mg/g for MO and 94 mg/g for MB was obtained for the samples with starch in 10 min of contact, whereas, in the absence of starch, the removal capacity was approximately half of the uptake with starch, and it took approximately 30 min. As planned with the magnetic nanoparticles, these sorbents were quickly separated from the solution, with a visible diminution of the color concentration, which presents a good alternative for the elimination of organic pollutants by either adsorption to the nanotubes and starch or by using different catalytic nanoparticles that can be grown onto the carbon nanotubes such as ZnO, Ag, or TiO<sub>2</sub> (Chang *et al.* 2011).

Composites with polysaccharides also serve as an alternative to use either as a continuous phase or as a dispersed phase with special properties or moieties. Like the hemicelluloses, chitosan is a predilect material due to the difference in surface groups and the high abundance of it. Examples of composites of starch/chitosan are reported in the literature. For instance, a cationic starch was composited with chitosan and tested as a flocculant. The starch was prepared by microwave irradiation with sodium hydroxide and 2,3-epoxypropyltrimethylammonium chloride, resulting in a DS of 0.31. The material was then crosslinked with chitosan in the presence of a crosslinker. The optimal conditions for the synthesis were a temperature of crosslinking at 70 °C, a ratio of 5:1 cationic starch: chitosan, and a ratio of 0.75 mL/g of catalyzer for 1.5 h. This system performed better in clarifying water at 5 °C and pH 5 with efficiencies around 88%; this provides a new alternative for flocculation in atypical systems (You *et al.* 2009). A similar composite was generated with starch and chitosan, but instead of the cationic starch, citrate-

modified starch was used to further crosslink the chitosan to the starch molecules and generate a hydrogel with high water and saline adsorption. An important finding in this study was that the temperature used for the cross linkage had an effect on the properties of the swelling and tensile strength, increasing from 1.44 to 1.81 N/mm<sup>2</sup> for the latter and from 1940 to 2780% w/w from water adsorption when temperature changed from 100 to 120 °C. This behavior was similar in the saline solution, but larger mass loss was found in the foam generated at 120 °C, showing how the properties can be adjusted as desired by changing temperature conditions and maintaining pH, ratio, and solid-liquid proportions. One of the main advantages of this strategy is that the incorporation of the citrate as a crosslinker increased the thermal stability, water adsorption, and strength while decreasing weight loss compared to normal starch-chitosan composites (Salam *et al.* 2010).

As noted, starch is usually grafted to allow interactions with the other materials; for this, latexes are great materials to consider, as they can be used as an interface or as a point to graft from the polymer to form the composites. An example of the first strategy is a composite that was generated with starch grafted with poly-acrylic acid and CNC. This system aimed to be a fast removal agent of methylene blue (MB), for which the pH was studied as the isoelectric point of the material changed as the concentration of CNC increased. The optimal CNC concentration for maximum adsorption was found to be 5% at a pH 5; this adsorption was modeled by Langmuir isotherms as 2240 mg/g with around 90% of total removal in 1 h. Reusability was also tested, finding that when it was immersed in a solution with pH 1, 60% of the adsorbed material was released and available for reusability; similar results were observed for the only grafted hydrogel that did not contain the CNC, but maximum adsorption was only of 2040 mg/g (Gomes *et al.* 2015). When sodium humate was used for the composite instead of CNC, the obtained system was able to form complexes with Cu(II). Herein different added percentages were tested (0, 5, 10, 15, and 20); from these, the best performance was found in the hydrogel containing 5% in a pH range of 2.7 to 5 and a maximum adsorption capacity modeled by Langmuir isotherm of 2.83 mg/g, which decreased as the content of sodium humate increased, which also gave some support to the hypothesis that the adsorption mechanisms were ion-exchange and chelation with the carboxylic groups. Lastly, regeneration was evaluated with 0.1 M NaOH, which, similar to the adsorption, was better in hydrogels containing sodium humate. Adsorption even improved after the first cycle, but after 4 cycles the efficiency had decreased by almost 40% (Zheng *et al.* 2010). Another system that used the grafted polymers as an interface was one with polyacrylamide grafted starch that contained clay (bentonite, kaolinite, or sercite). These were only tested for water absorption capacity, which reached 4000 g H<sub>2</sub>O/g in 120 min, which apparently was mostly influenced by the presence of kaolinite, as the composite with only this clay absorbed almost 2500 g/g on its own but needed the three to enhance swelling (Wu *et al.* 2000).

Meanwhile, the “grafted from” approach can use different monomers to obtain sidechains with different properties and surface interactions. For example, aniline was used to form a hydrogel for the removal of reactive dyes, Reactive Black 5 (RB, C<sub>26</sub>H<sub>21</sub>N<sub>5</sub>Na<sub>4</sub>O<sub>19</sub>S<sub>6</sub>, PubChem CID: 44134920) and Reactive Violet 4 (RV, C<sub>20</sub>H<sub>16</sub>CuN<sub>3</sub>Na<sub>3</sub>O<sub>15</sub>S<sub>4</sub>, PubChem CID: 129818966). The composite was able to remove 99% of RB and 98% of RV at pH 3 from solutions with 0.5 mM of the dyes; higher pH resulted in lower adsorption efficiency, with only 65% at pH 9. This was explained by the dissociation of the sodium from the sulfur groups at low pH, increasing the adsorption. When isotherms were performed, the Toth model fit the data better than the Langmuir or Freundlich, giving maximum adsorption capacities of 808 mg/g of RB and 667 mg/g of

RV. A benefit of this study is an adsorption study done with a dye bath effluent containing RB (0.5 mM), RV (0.5 mM), sodium chloride (355 mM), sodium carbonate (61 mM), sodium hydroxide (6.5 mM), and acetic acid (6.5 mM) with pH 5, which is closer to a mixture that could represent a real scenario. With this solution, the removal efficiency was 87% and the isotherm fit into a modified Freundlich model, which changed the concentration term for an absorbance term; this gave an adsorption capacity of 1.97 mg/g. Finally, desorption was tested for reusability with a 0.1 M NaOH solution, which was 93% for RV, 94.2% for RB, and only 89.4% for the dye solution; when tested again for sorption, a reduction of 4% was observed, which is considered negligible, showing the good performance of the composite which is inexpensive and eco-friendly (Janaki *et al.* 2012). Similarly for dye adsorption, N,N-Diethylamino ethyl methacrylate was grafted from starch to remove Direct Red 81 (DR, C<sub>29</sub>H<sub>19</sub>N<sub>5</sub>Na<sub>2</sub>O<sub>8</sub>S<sub>2</sub>, PubChem CID: 9570117). Different grafting yields were tested, and the best one had a 50% yield, with an adsorbent concentration of 2.5 g/L and pH 1, obtaining a 95.6% efficiency after 50 min; the isotherm was modeled by Langmuir, giving a maximum adsorption capacity of 112 mg/g (Abdel-Halim 2013).

**Table 6.** Starch-derived Materials and Pollutants Adsorbed

Material	Pollutant	Capacity (mg/g)	Regeneration	Reference
C6-carboxylated starch hydrogel	Cu(II)	128.26		Chauhan <i>et al.</i> 2010
Starch NiFe-LDH composite	Methyl orange	358.42	0.1 M NaOH	Zubair <i>et al.</i> 2018
Carbon nanotubes-starch/iron oxide	Methylene blue	94		Chang <i>et al.</i> 2011
	Methyl orange	327.33		
Starch-g-polyacrylic acid	Methylene blue	2043	H <sub>2</sub> O pH 1	Gomes <i>et al.</i> 2015
Starch-g-polyacrylic acid/CNC		2236		
Starch-g-polyacrylic acid/sodium humate	Cu(II)	2.83	0.1 M NaOH	Zheng <i>et al.</i> 2010
Aniline/starch	Reactive black 5	808.11	0.1 M NaOH	Janaki <i>et al.</i> 2012
	Reactive violet 4	667.09		
Starch-g-N,N-Diethylamino ethyl methacrylate	Direct red 81	112		Abdel-Halim <i>et al.</i> 2013
Starch/Polyvinyl alcohol	Fe(II)	37.07	2 M HCl	Chowdhury <i>et al.</i> 2015
	As(III)	22.11	2 M NaOH	

“Grafting from” can also be used for metal removal; for example, polyvinyl alcohol was used in different starches, wheat-flour, rice-powder corn-starch, and maize-starch. The

corn-starch composite performed best in the adsorption of Fe(II) and As(III) with 37.1 and 22.1 mg/g, respectively, and was reused for up to 3 cycles with efficiencies between 95 and 88%; herein, a 2 M HCl solution was used for Fe(II) desorption and a 2 M NaOH solution for As(III). Also, this composite presented 600% swelling when placed in water, which helped when tests of metals adsorption were performed using neutral pH and concentrations of 100 mg/L were given using 0.5 g of the sorbent; herein, adsorptions were of ~20, 22, 37, 7.5, 18, 4, and 22 mg/g for Cr(VI), Mn(II), Fe(II), Ni(II), Cu(II), Pb(II), and As(III), respectively (Chowdhury *et al.* 2015).

As presented, starch is a low-cost option for the development of hydrogels, with high water adsorption and pollutant removal capacity. Simple chemistry can be used to adjust the surfaces generated and improve composite interactions for chelation and adsorption of metals and dyes, respectively.

### Cyclodextrins

Cyclodextrins are cyclic oligosaccharides formed by  $\alpha$ -1,4-glucopyranose units (Fig. 7), that have inherent properties of biocompatibility and non-toxicity. These cyclic molecules are obtained by the enzymatic degradation of starch by cyclodextrin glucanotransferase (CGTase) enzyme, which can result in structures containing six ( $\alpha$ ), seven ( $\beta$ ), or eight ( $\gamma$ ) units (Villiers 1891; del Valle 2004; Kurkov and Loftsson 2013).

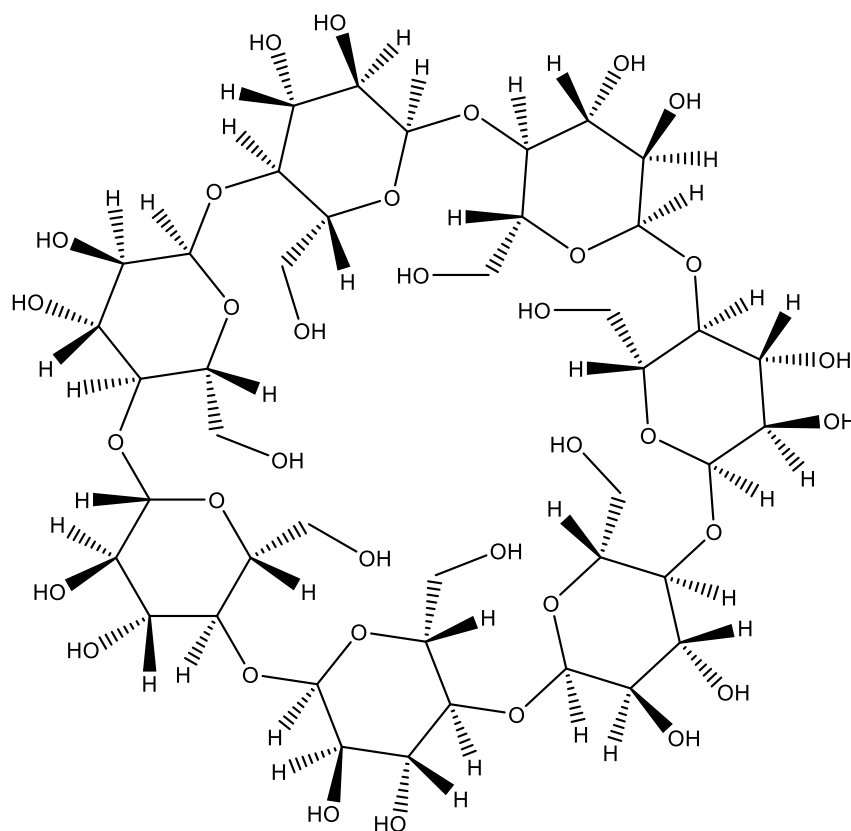


Fig. 7. Structure of  $\beta$ -cyclodextrin

The glucose units here are spatially immobilized in a  ${}^4C_1$ -chair conformation, which gives the structure the shape of a truncate cone with an internal cavity with diameters between 6 to 10 Å. Because of this conformation, the primary hydroxyl groups end up

oriented to the exterior of the cone, making the exterior part highly hydrophilic and the interior hydrophobic. Meanwhile, the secondary hydroxyls are on the edges of the cavity forming H-bonds between them, leading the non-bonding electron pairs to be oriented towards the cavity interior, conferring a Lewis-like base character (Szejtli *et al.* 1982; Szejtli 1998; Cova *et al.* 2018).

Due to the structure of cyclodextrin (CD), it has between three to five times more resistance to hydrolysis than linear polymers, and as the hydroxyl groups are used to form the H-bond, they also have a lower solubility. The number of units has an impact on these properties, as well; for example,  $\beta$ -CD is known to be more rigid and less soluble than the other two possible CDs, as they use all the secondary oxygens to stabilize the ring compared to the  $\alpha$ -CD, which only forms 4 of 6 possible bonds and is more rigid because of the seven units, which make it less flexible and more planar than  $\gamma$ -CD. Similarly, the half-life of the structure of  $\beta$ -CD is approximately 15 h in an aqueous solution at 70 °C and pH 1.1; this is 1.5 times greater than  $\gamma$ -CD and 1.5 times less than  $\alpha$ -CD (Kurkov and Loftsson 2013).

As previously mentioned, the structure of the CD provides a hydrophobic cavity that can form highly stable host-guest complexes with alkyl chains or aromatic compounds. These complexes are stabilized by different electrostatic Van der Waals, charge-transfer interactions, and other H-bonds that could be formed between the guest molecules and the oxygens in the ring or the primary hydroxylic groups. All of these interactions can then be used for the improvement of solubility, capture, or control of organics, volatiles, and antioxidant molecules (Saenger and Steiner 1998; Liu and Guo 2004; Guo *et al.* 2005; Kurkov and Loftsson 2013; Cova *et al.* 2018). The high structural and thermal stability of  $\beta$ -CD has made it the predominant cyclodextrin on the market, causing the production cost to go down and increasing the availability of derivatives with almost 86% of the market in medicine (Kurkov and Loftsson 2013).

For environmental applications, the low molecular weight of  $\beta$ -CD (1135 Da) makes it important to generate composites for its use in aqueous media. One of the most widespread approaches is the generation of a polymer with epichlorohydrin or other agents capable of esterification (Gidwani and Vyas 2014; Morin-Crini and Crini 2013; Morin-Crini *et al.* 2018). The main objective when crosslinking is to increase size and efficiency without loss by steric effects. An example of a study using this analysis is one that a Canadian group performed where 5 types of crosslinker agents were used to examine the effectiveness in decolorizing a solution with phenolphthalein ( $3.6 \times 10^{-5}$  M in 0.1 M sodium hydrogen carbonate buffer pH 10.5); the crosslinkers used were epichlorohydrin (EP), sebacoyl chloride (SCL), terephthaloyl chloride (TCL), glutaraldehyde (GLU), and poly-(acrylic acid) (PAA). From these, the TCL with proportions 1:1, the GLU 1:3, and 1:15 molar ratio was the one with a better performance, with 72.4, 68.7, and 64.6 % of accessible  $\beta$ -CD in the polymer, respectively. Even when accessibility varied between the systems,  $\Delta G$  from all copolymers ranged between -27.6 and -30.9 kJ/mol, demonstrating the favorable complex formation between the aromatic compound and the  $\beta$ -CD (Mohamed *et al.* 2012). Another group tried tetrafluoroterephthalonitrile as a linker and compared it with polymers with epichlorohydrin and activated carbon; this system was tested for the adsorption of 0.1 mM bisphenol-A solutions. The system generated with high surface porosity had an efficiency of 80%, sustaining it for 5 cycles, while the same polymer without a porous formation had an efficiency around 30%, like the epichlorohydrin-linked system. The activated carbon systems ranged between 60 to 10% efficiency. For a better understanding of the binding, the porous system was tested to adsorb other compounds,

bisphenol S, 2-naphthol, 1-naphthyl amine, 2,4-dichlorophenol, metolachlor, ethinyl oestradiol, and propranolol hydrochloride. In all of these, removal efficiencies ranged from 70 to 90%, outperforming activated carbon and EP-CD (Alsbaiee *et al.* 2016).

Differences in the CD can also modify the adsorption behavior of molecules in the polymer with the same crosslinker. For instance, the use of 2-hydroxypropyl  $\beta$ -CD (HPCDP), random methyl- $\beta$ -CD (RMCDP), or a blend with  $\beta$ -CD polymer for the removal of pollutants show different removal efficiencies depending on the selected pesticide when spheres with EP were prepared. The 4 systems (RMCDP, HPCDP,  $\beta$ CD, and the Multiplex) were studied for adsorbance of 10 aromatic pesticide (fomesafen, bromacil, simazine, atrazine, fenamiphos, fipronil, benalaxyl, butene-fipronil, pretilachlor, and butachlor) and all fit Langmuir isotherms. The mixture of the different CD proved to be the most effective, with maximum adsorption capacities greater in almost all cases but the benalaxyl, where HPCDP had a maximum of 28.0 mg/g, while the multiplex had 22.7 mg/g (Liu *et al.* 2011). When compared to the pristine polymers, the addition of moieties did not always help to improve, as  $\beta$ CD had a better adsorption of fomesafen, simazine, and pretilachlor, but HPCDP was better for bromacil, fenamiphos, fipronil, and benalaxyl, leaving the rest working better with the random methylated material. This means that interactions are guided by different mechanisms, and the inclusion of aliphatic moieties can improve adsorption and to form better complexes when the surface is chemically uneven.

The main focus of the use of these hydrophobic materials for water treatment in studies is when dyes and other aromatic structures are to be removed. For example, in a study in 2008, CDP with EP was used to eliminate Basic Blue 3 (BB3,  $C_{33}H_{32}ClN_3$ , PubChem CID: 17407), basic violet 3 (BV3,  $C_{25}H_{30}ClN_3$ , PubChem CID: 11057), and basic violet 10 (BV10,  $C_{28}H_{31}ClN_2O_3$ , PubChem CID: 6694) from standard solutions with concentration 40 mg/L. These polymers had a maximum adsorption capacity of 42.4, 35.8, and 53.2 mg/g, respectively, when modeled by Langmuir isotherms. A clear relationship between the adsorbent mass (that allows and estimation of the number of hydrophobic cavities available) with the removal of pollutants was found. This suggests a chemisorption of the dyes from the hydrophobic cavities in the polymer (Crini 2008). Similarly, azo dyes with more elaborate structures were studied, but with polymers were crosslinked with 4,4-methylene-bisphenyldiisocyanate (MDI) or hexamethylenediisocyanate (HMDI). Generally, the one with the phenolic groups had a better adsorption capacity than the linear one, probably due to the increase of immobilization by  $\pi$ - $\pi$  interactions; the tested dyes were Evans Blue (EB,  $C_{34}H_{24}N_6Na_4O_{14}S_4$ , PubChem CID: 9566057) and Chicago Sky Blue (CSB,  $C_{34}H_{24}N_6Na_4O_{16}S_4$ , PubChem CID: 5359775). The ideal pH for these systems was 3, and the maximum adsorption capacities were 9.6 and 7.6 mg/g for the HMDI derivate and 10.59 and 12.09 mg/g respectively for the MDI polymer (Yilmaz *et al.* 2010).

As observed, the linkers can provide advantages in the interactions with the pollutants, but those linkers can also serve as points to further design the polymer. For example, four polymers were generated using toluene diisocyanate (TDI), isophorone diisocyanate (IPDI), hexamethylene diisocyanate (HMDI), and carbonyl diimidazole (CDI) as a cross-linker and then the material was doped with  $TiO_2$  for the photocatalytic reaction of the adsorbed pollutants. From this, the polymer that used TDI had the best retention of total organic carbon (TOC), with a maximum of 93% (Khaoulani *et al.* 2015).

Another commonly used approach to increase molecular weight and facilitate the recovery of the CD from solutions is the generation of a composite with magnetic particles, especially  $Fe_3O_4$  nanoparticles, as they are easily synthesized and can be adsorbed to the  $\beta$ -CD without changing their potential to eliminate pollutants. An example of the use of this

system was to degrade bisphenol-A (BPA) and malachite green (MG); for these experiments, 100 mg of the composite were immersed in solutions with 20 mg/L of BPA or 9.27 mg/L of MG. The system was able to photodegrade 70% of BPA, and when reused 6 times, degradation decreased to 64.2%; meanwhile for GM, almost a complete removal was obtained, decreasing to 90.1% after 6 cycles (Kumar *et al.* 2015). Other experiments were also performed to test the adsorptions of different organics and metal ions. For example, 1-naphthylamine (60 mg/L) was tested at different pH, ionic strength, concentrations, and  $\beta$ -CD content; the ideal conditions were between 5.5 and 7.5, with ionic strength  $< 0.05$ , initial sorbent concentration of 1 g/L, and  $\beta$ -CD content  $> 6.84$ . Different concentrations were tested and fit the Langmuir isotherm, with a maximum adsorption concentration of 144.7 mg/g and thermodynamic parameters of  $-4.7$  kJ/mol for  $\Delta G$ ,  $50.6$  J/mol K for  $\Delta S$ , and  $\Delta H$  of  $10.7$  kJ/mol at 303 K. In this same article, adsorption of Cu(II) was tested in solutions with an initial concentration of 10 mg/L; when the pH was varied, ideal conditions were found to be at  $\text{pH} \geq 8$ , and recycling was completed 5 times after washing with  $\text{HNO}_3$  ( $\text{pH} \sim 2$ ), decreasing from an initial adsorption of 9.04 mg/g to 8.6 mg/g. When these data were fit to the Langmuir model, the maximum adsorption capacity was 9.04 mg/g, the same as achieved in the experimental data (Li *et al.* 2013). Similarly, 1-naphthol and Co(II) were tested separately and in a mixed solution. In this set of experiments, the grafted amount of  $\beta$ -CD was 115 mg/g, and concentrations of 1-naphthol and Co(II) were 50 mg/L and 10 mg/L, respectively. For Co(II), optimal conditions were: pH above 8.3, 2 h of contact, and a maximum adsorption capacity 38.0 mg/g at 293 K; for 1-naphthol, optimal contact time was of 4 hours, at a pH of 9, with an effect on adsorption due to ionic strength after this pH, presenting a better adsorption at 0.7 mol/L NaCl, the fitting into the Langmuir model by the isotherms with a maximum adsorption capacity of 235.1 mg/g at 293 K. Probably the most interesting analysis of this paper is the effect of each of these on the adsorption of the CD-nanoparticle. It was observed that the concentration of the organic had an effect on the adsorption of Co(II), peaking when 80 mg/L of 1-naphthol was present; this is attributed to the adsorption of the hydrophobic part of the alcohol into the cavities, while the hydroxyl groups were available to form active sites with the ion. In lower concentrations, the tri-complex formation was not saturated in the surface, while at higher concentrations of naphthol, the complex naphthol-Co(II) were formed in solution, decreasing the capacity to adsorb into the material. On the other hand, changes in the concentration of Co(II) did not affect the capacity of the 1-naphthol to get captured by the CD, sustaining the idea of the capture of the alcohol by hydrophobic interactions (Zhang *et al.* 2014c).

Another element that has been shown to adsorb into the magnetic CD composite is the rare earth Eu(III); this was tested at pH 3.5 and 5, where the ionic species were present for adsorption and using an initial concentration of  $2.3 \times 10^{-4}$  mg/L. Also, different ionic strengths were tested observing no significant effect due to the change of salt concentrations. When the adsorption isotherms were fit to a Langmuir model, the maximum adsorption capacities were calculated as  $3.31 \times 10^{-4}$  and  $5.49 \times 10^{-4}$  mg/g for pH 3.5 and 5, respectively; these values were highly efficient considering their price and eco-friendly production compared to clay and other commercial sorbents (Guo *et al.* 2015).

Like the other polymers, the addition of CD moieties helps to extract heavy metals from wastewaters. For example, a carboxymethyl- $\beta$ -CD was polymerized with EP, used to coprecipitate with  $\text{Fe}_3\text{O}_4$  nanoparticles, and used to extract Pd(II), Cd(II), and Ni(II). The system was shown to be dependent on pH, ionic strength, and temperature; optimal pH seemed to be  $> 5.5$  for all cases with higher temperatures, and ionic strength decreased the

adsorption capacity. The Langmuir model fit the isotherms through maximum adsorption capacities of 64.5, 27.7, and 13.2 mg/g for Pd(II), Cd(II), and Ni(II), respectively. When reversibility was studied, three eluent solutions were tested: 0.01 M nitric acid, 0.1 M Na<sub>2</sub>EDTA, and 0.02 M phosphoric acid; nitric acid and EDTA were better eluents for Pb(II), and the phosphoric acid for Ni(II). Overall, Pb(II) was easier to remove from the sorbent, followed by Cd(II), and lastly Ni(II). Pb(II) was able to be reused for adsorption for up to 4 cycles without significant loss, proving to be an easy, convenient, and efficient nanocomposite for the removal of ions (Badruddoza *et al.* 2013).

Although Fe<sub>3</sub>O<sub>4</sub>-CD is a nanomaterial with high surface area, it can be improved when the composite is built-up with other high surface colloidal particles, such as silica or graphene. When this was studied and tested for microcystin-LR adsorption, a cyanotoxin related to liver cancer consisting of a 7 amino acid cycle, it was observed that any composite with  $\alpha$ ,  $\beta$ , or  $\gamma$ -CD adsorbed into the materials between 16 to 19% w/w, but only the one on the graphene surface had a good capture performance, with removal capacities of 80, 140, and 160 mg/g for  $\alpha$ ,  $\beta$ , and  $\gamma$ -CD, respectively (Sinha and Jana 2015). The main contribution of this paper is the use of cyclodextrin to remove complex molecules, such as microcystin-LR in a high surface nanomaterial, combining specific properties of each material: complex formation with CD and microcystin, high surface area by the graphene and the magnetic properties for the removal of the Fe<sub>3</sub>O<sub>4</sub> nanoparticles.

Just like graphene, multiwalled carbon nanotubes (MWCNT) can be used to support  $\beta$ -CD and increase the contact area; this grafting is achieved in reactors where only N<sub>2</sub> atmosphere is permitted while heating, avoiding its degradation or the formation of oxides. This high surface material was used to remove polychlorinated biphenyls (PBCs) from a solution with an initial concentration of 4.1 mg/L, pH 3.5, ionic strength 0.01 M NaClO<sub>4</sub>, and *T* of 20 °C; the PBCs tested were 4,4'-dichlorobiphenyls (4,40-DCB) and 2,3,3'-trichlorobiphenyl (2,3,30-TCB) that when fitted to the Langmuir isotherm models had a maximum adsorption capacity of 261 and 235 mg/g, respectively. The effects of pH and ionic force were also tested but were found to have little to no influence on the adsorption between pH 3 to 10 and concentrations ranging from 0.001 to 0.05 M (Shao *et al.* 2010). Similar to the previous case, the MWCNT can be further composited with other nanoparticles, such as iron oxides, to enhance adsorption and add properties to the sorbent like magnetic properties for its separation. In one study, this was used to eliminate 1-naphthylamine; when fitted to a Langmuir model, the maximum adsorption capacity of the system was 200 mg/g. It was also found that pH had an effect on the adsorption, as it was only when the pH was higher than the pK<sub>a</sub> that there was significant adsorption was observed, especially after pH 5.5. Interestingly, when a higher initial concentration was used (60 mg/L instead of 32 mg/L), a decrease in adsorption was observed after pH 8.5, which was explained due to an electron-donor-acceptor interaction and Lewis acid-base interaction between the CNT and the 1-naphthylamine after this pH value (Hu *et al.* 2011).

Another alternative to increase both contact area and recovery after the adsorption, is the use of polymer fibers as substrates to immobilize the CD. Following the scope of the review, natural fibers have been used for their abundance, mechanical properties, and high surface area (Prabaharan and Gong 2008; Lin and Dufresne 2013; Zhang *et al.* 2013b; Medronho *et al.* 2013; Dong *et al.* 2014; Ruiz-Palomero *et al.* 2015; Ghorpade *et al.* 2017). Cellulose is the most abundant polysaccharide and can be used to enhance the water adsorption of materials as well as for an easy recovery of hydrogels or films. An example of this composite using nanofibrils was used for the adsorption of phenol; herein, adsorption was done using different structures (fibers, membranes, and aerogels) with

different initial weight concentrations (1 to 3%). From these, the best performance was obtained with the 3% aerogel, as the porosity of the obtained material increased significantly the surface area, favoring the adsorption kinetics. This result was more apparent when isotherms were made with the 3% materials, where the maximum adsorption was of 13.9 mg/g for the aerogel, 3.67 mg/g for the membrane, and 5.93 mg/g for the fibers. Adsorption also decreased as the temperature increased from 20 to 40 °C, and when the pH was above 9, dependency of the adsorption to these parameters was shown (Zhang *et al.* 2015a).

Another method to obtain high surface materials is by electrospinning, which generate mats that can also be modified with CD to adsorb pollutants; an example of this was done by electrospinning regenerated cellulose acetate fibers which were modified with CDs ( $\alpha$ ,  $\beta$ , and  $\gamma$ ) by citric acid and sodium hypophosphite hydrate (SHPI) and were used to adsorb toluene. This regenerated material had an average diameter distribution between 226.5 and 364.5 nm, with the best adsorption rate given by the  $\gamma$ -CD modified fibers with 86% in 180 min at 60 °C (Yuan *et al.* 2017).

As previously mentioned, cellulose is easily modifiable to adsorb metals; therefore, if these modifications are partnered with cyclodextrin, a material with wider adsorption capability can be obtained. To verify this, cellulose powder was grafted with glycidyl methacrylate monomers, with  $\beta$ -CD, and quaternary ammonium groups and used to remove Cr(VI) from aqueous solutions. When the Langmuir isotherm was modeled, a maximum adsorption capacity of 61.0 mg/g was found, with an optimum pH range between 3.5 to 6 and a slight decrease in adsorption when other ions were present between 1 to 7% depending on the ion diversity. Reusability was possible using sodium hydroxide (0.5 mg/L) as a desorption agent for up to 5 cycles with minimal loss of efficiency (Zhou *et al.* 2011a).

One way to improve the adsorption is to promote the exposure of the cavity from  $\beta$ -CD; for this, different alternatives have been tested, but the use of “click” chemistry stands out as it uses aqueous and green chemistry. For example, a membrane from acetate nanocellulose – azide- $\beta$ -CD was electrospun and used to remove phenanthrene; in this set of experiments, it was observed that the grafting of the CD modified the spinnability of the nanofibers, as more roughness was seen in the microscopies, but the final membrane was still obtained with continuous fibers. When tested for the adsorption of the aromatic compound, it was observed that the final concentration after 480 h was 5% for the modified membrane and 15% for the unmodified membrane, demonstrating the enhanced activity due to the hydrophobic cavities attached with the  $\beta$ -CD (Celebioglu *et al.* 2014).

A reduction of the modification steps can be done when chitosan is used, due to its advantage of keeping the desired properties of polysaccharides while a nitrogen is already placed in the structure for use as an anchoring point for a modified cyclodextrin. This application has been used to test the adsorption of methyl orange; for the design of the material, maleoyl chains were used as linkers between the chitosan and CD, followed with glutaraldehyde to generate a stable structure. The adsorption was made using 10 mg of the adsorbent with 50 mL of solution with different concentrations, pH, and temperature from which it was found that the optimal conditions were at pH 5, room temperature (25 °C), and dosage of 200 mg/L; when this was fitted into a Langmuir isotherm, the maximum adsorption capacity was of 392 mg/g, one of the highest reported (Jiang *et al.* 2018b). Even though this system showed good performance, higher surface area can be obtained when the modified chitosan is attached to another material; examples of this are the use of a similarly prepared chitosan/ $\beta$ -CD attached to magnetic nanoparticles and graphene for it

removal and stabilization. This was tested to remove methylene blue, which had a better performance at higher pH values, reaching a maximum adsorption capacity calculated at 84.3 mg/g (Fan *et al.* 2013). Another example was the adsorption of  $\beta$ -CD/chitosan to cellulose yarns generated by spinning; however, in this case, the  $\beta$ -CD was previously TEMPO-oxidized and immobilized to chitosan that was available in the surface of the yarn by EDC/NHS. This system was used to adsorb 17  $\alpha$ -ethinyl estradiol (EE2) and followed by surface plasmon resonance (SPR) and by UV-Vis measurements with solutions at pH 7.4 in a 50 mM phosphate buffer with concentrations of 0, 0.1875, 0.375, 0.75, and 1.25  $\mu$ g/mL; the system presented an immobilization of EE2 in SPR of 0.15 degrees, which correspond to an adsorption of 2.5 mg/g (Orelma *et al.* 2018).

Synthetic polymers can also provide some properties that can be explored for other applications; similar to the regenerated cellulose (Yuan *et al.* 2017), electrospun polyethylene terephthalate (PET) mats were modified with different cyclodextrins and were tested for the adsorption of phenanthrene, with no significant difference between CD efficiency. However, the addition of them was found to enhance the removal of the compound from aqueous solutions (Kayaci *et al.* 2013). Poly(methyl methacrylate) was also electrospun with  $\beta$ -CD in different concentrations (10, 25, 50% w/w) without any chemical modification; these mats were then tested for the adsorption of organic vapors (styrene, toluene, and aniline) which was later quantified by direct pyrolysis mass spectrometry. In all cases, changes in the degradation were only observable when CD was present, and the intensity increased as the percent grafted increase, assuring the interaction between the oligosaccharide and the solvents. Interestingly, the ways they interact differ in some degree, as aniline interacted in only one degradation peak, which sustains the theory of inclusion complex formation. Styrene had a broader interaction with  $\beta$ -CD, possibly due to inclusion complex formation, but also due to adsorption mechanism. Finally, toluene had two temperature peaks, which indicates also the formation of complex and some other kind of interactions (Uyar *et al.* 2010).

As a last example, poly(urethane) was also copolymerized with  $\beta$ -CD and used to test the sorption of chlorinated aromatic compounds, which are a main source of concern; the tested compounds were pentachlorophenol (PCP,  $C_6Cl_5OH$ , PubChem CID: 992), 2,4-dichlorophenol ( $C_6H_4Cl_2O$ , PubChem CID: 8449), and 2,4-dichlorophenoxy acetic acid ( $C_8H_6Cl_2O_3$ , PubChem CID: 1486). Here, the cross-linkage was done using two components: methylenediphenyl diisocyanate (MDI) and dicyclohexylmethane-4,4'-diisocyanate (CDI), which apparently have some differences when the isotherms were generated at 295 K and pH 9. For this case, the Sips isotherm model, which is a corrected version of the Langmuir isotherm, was used. For pentachlorophenol, the maximum adsorption capacities were 14.9 and 22.9 mg/g for the CDI and MDI crosslinked material; the low capacity was probably due to the size of the pollutant compared with the cavity of  $\beta$ -CD. The capacities for the other aromatics were: for 2,4-dichlorophenol, 98.9 and 6.4 mg/g for MDI and CDI, respectively, and for 2,4-dichlorophenoxy acetic acid, 119.3 and 250.8 mg/g for the same polymers (Wilson *et al.* 2011). All the above examples show how cyclodextrins can be widely used for the removal of pollutants, especially because they possess the capacity to capture aromatic molecules in hydrophobic cavities.

**Table 7.** Cyclodextrin-derived Materials and Pollutants Adsorbed

Material	Pollutant	Capacity [mg/g]	Regeneration	Reference
2-hydroxypropyl $\beta$ -cyclodextrin with EP	Benalaxyl	27.99		Liu <i>et al.</i> 2011
2-hydroxypropyl/methyl/ pristine $\beta$ -cyclodextrins with EP		22.74		
Cyclodextrin polymer with EP	Basic blue 3	42.4		Crini <i>et al.</i> 2008
	Basic violet 3	35.8		
	Basic violet 10	53.2		
Cyclodextrin polymer with MDI	Evans blue	10.59		Yilmaz <i>et al.</i> 2010
	Chicago sky blue	12.09		
Cyclodextrin polymer with HMDI	Evans blue	9.58		
	Chicago sky blue	7.63		
$\beta$ -cyclodextrin with Fe <sub>3</sub> O <sub>4</sub> nanoparticles	Naphthylamine	144.74		Li <i>et al.</i> 2013
	Cu(II)	9.04		
	1-naphthol	235.06		Zhang <i>et al.</i> 2014c
	Co(II)	38.03		
Eu(III)	5.49 * 10 <sup>-4</sup>		Guo <i>et al.</i> 2015	
Carboxymethyl $\beta$ -cyclodextrin polymer with EP	Pb(II)	64.5	0.01 M HNO <sub>3</sub> / 0.1 M Na <sub>2</sub> EDTA /0.02 M H <sub>3</sub> PO <sub>4</sub>	Badruddoza <i>et al.</i> 2013
	Cd(II)	27.7		
	Ni(II)	13.2		
$\alpha$ -cyclodextrin/graphene/ Fe <sub>3</sub> O <sub>4</sub>	Microcystin-LR	80		Sinha and Jana, 2015
$\beta$ -cyclodextrin/graphene/ Fe <sub>3</sub> O <sub>4</sub>		140		
$\gamma$ -cyclodextrin/graphene/ Fe <sub>3</sub> O <sub>4</sub>		160		
Multiwalled carbon nanotubes/ $\beta$ -cyclodextrin	4,4'-dichlorobiphenyl	261		Shao <i>et al.</i> 2010
	2,3,3'-trichlorobiphenyl	235		
Multiwalled carbon nanotubes/ $\beta$ -cyclodextrin/ iron oxide	1-naphthylamine	200		Hu <i>et al.</i> 2011

$\beta$ -cyclodextrin/ cellulose nanofibers	Phenol	5.93		Zhang <i>et al.</i> 2015a
$\beta$ -cyclodextrin/ cellulose aerogels		13.93		
$\beta$ -cyclodextrin/ cellulose membranes		3.67		
Cellulose powder-g- glycidyl methacrylate/ ammonium/ $\beta$ - cyclodextrin	Cr(VI)	61.05	NaOH	Zhou <i>et al.</i> 2011a
Chitosan/ cyclodextrin/ glutaraldehyde	Methyl orange	392		Jiang <i>et al.</i> 2018
Chitosan/ cyclodextrin/ graphene/ magnetic nanoparticles	Methylene blue	84.32		Fan <i>et al.</i> 2013
Polyurethane/ cyclodextrin with MDI	Pentachlorophenol	22.9		Wilson <i>et al.</i> 2011
	2,4- dichlorophenoxy acetic acid	119.26		
	2,4-dichlorophenol	98.94		
Polyurethane/ cyclodextrin with CDI	Pentachlorophenol	14.38		
	2,4- dichlorophenoxy acetic acid	250.84		
	2,4-dichlorophenol	6.42		

## Final Remarks

In conclusion, the recent development of adsorbents from polysaccharides seems to be a feasible approach for generating materials of low cost and high performance with a wide variety of possible functionalization that can further improve the interactions between pollutants and fibers. Among the different polysaccharides, cellulose and chitosan have been the most studied, which derives from their wide availability and the deep knowledge on processing technologies held by the scientific community. Furthermore, surface modification of these polysaccharides for adding new functional groups with little environmental impact, such as TEMPO oxidation, has been the method of choice for modification of the polysaccharide surfaces and improvement of the targeting of water contaminants. When surface modification using greener chemistry is not an option, the generation of composite materials by combining polysaccharides with other polymers containing the functional groups is a low-cost approach that can provide great impact in

removing the wide variety of pollutants, such as metallic and organic ions, pesticides, dyes, dissolved organic pollutants such as toxins, and oils.

The formation of composites with other polysaccharides (*i.e.* cyclodextrins), nanoparticles, clays, or even other complex polymers can further increase the substrate surface area, while adding additional functionalities that will increase their selectivity, such as catalytic properties.

The low-cost, reusability and extended life cycle of polysaccharide materials are key points that all research must consider when developing composites, in particular for their utilization in water remediation. Even though some synthetic polymers have shown improved potential to be utilized for the uptake of water pollutants, the complexity and toxicity, as well as the high cost of the involved chemistry has made them less attractive. Additionally, most of them involve organic solvents as media for polymer functionalization, which offers more reasons to opt for the natural polysaccharides as the option of choice.

The main challenge that polysaccharide-derived materials must address is the recycling of the adsorbent, as well as the manufacturing cost. This could be addressed by either slowing down degradation or increasing the pollutant uptake per cycle. On the one hand there is potential to increase the manufacturer's profitability by adding value to the capacity of the manufacturer. On the other hand it is possible to increase the material's life for the end users.

Regarding cost analysis of composite materials based in natural polymers, it can be argued that production costs will be higher in the case of composite materials and/or modified polysaccharides. However, efforts are being made to lower these prices on a daily basis based on optimization of current production methods. Furthermore, the superior performance of the (nano) composites materials open a clear pathway in which the captured pollutant can be purified or re-integrated to upstream production, providing some return in the process besides the obvious environmental benefits of the water quality improvement. For these reasons, natural fibers are exiting materials to develop and improve so that the commercial application of versatile systems with low cost that improve water quality and increase life expectancy can be possible in the near future.

## ACKNOWLEDGEMENTS

This publication was supported by the Alabama Agricultural Experiment Station, and the Hatch program of the National Institute of Food and Agriculture, United States Department of Agriculture. The School of Forestry and Wildlife Sciences at Auburn University financial support to complete this work is greatly appreciated.

## REFERENCES CITED

- Abdel-Halim, E. S. (2013). "Preparation of starch/poly(N,N-diethylaminoethyl methacrylate) hydrogel and its use in dye removal from aqueous solutions," *Reactive and Functional Polymers* 73(11), 1531-1536. DOI: 10.1016/j.reactfunctpolym.2013.08.003
- Adeleye, A. S., Conway, J. R., Garner, K., Huang, Y., Su, Y., and Keller, A. A. (2016). "Engineered nanomaterials for water treatment and remediation : Costs , benefits ,

- and applicability,” 286, 640–662.
- Algarra, M., Isabel, M., Alonso, B., María, C., Casado, J., and Benavente, J. (2014). “Characterization of an engineered cellulose based membrane by thiol dendrimer for heavy metals removal,” 253, 472–477.
- Ali, I. (2012). “New generation adsorbents for water treatment,” *Chemical Reviews*, 112(10), 5073–5091. DOI: 10.1021/cr300133d
- Ali, I., and Gupta, V. K. (2007). “Advances in water treatment by adsorption technology,” *Nature Protocols*, Nature Publishing Group, 1(6), nprot.2006.370. DOI: 10.1038/nprot.2006.370
- Alsbaiee, A., Smith, B. J., Xiao, L., Ling, Y., Helbling, D. E., and Dichtel, W. R. (2016). “Rapid removal of organic micropollutants from water by a porous  $\beta$ -cyclodextrin polymer,” *Nature*, Nature Publishing Group, 529(7585), 190–194. DOI: 10.1038/nature16185
- Ayoub, A., Venditti, R. A., Pawlak, J. J., Salam, A., and Hubbe, M. A. (2013). “Novel hemicellulose-chitosan biosorbent for water desalination and heavy metal removal,” *ACS Sustainable Chemistry and Engineering*, 1(9), 1102–1109. DOI: 10.1021/sc300166m
- Badruddoza, A. Z. M., Shawon, Z. B. Z., Tay, W. J. D., Hidajat, K., and Uddin, M. S. (2013). “Fe 3O 4/cyclodextrin polymer nanocomposites for selective heavy metals removal from industrial wastewater,” *Carbohydrate Polymers*, Elsevier Ltd., 91(1), 322–332. DOI: 10.1016/j.carbpol.2012.08.030
- Benhouria, A., Islam, M. A., Zaghouane-Boudiaf, H., Boutahala, M., and Hameed, B. H. (2015). “Calcium alginate-bentonite-activated carbon composite beads as highly effective adsorbent for methylene blue,” *Chemical Engineering Journal*, Elsevier B.V., 270, 621–630. DOI: 10.1016/j.cej.2015.02.030
- Bhowmik, K. L., Deb, K., Bera, A., Debnath, A., and Saha, B. (2018). “Interaction of anionic dyes with polyaniline implanted cellulose: Organic  $\pi$ -conjugated macromolecules in environmental applications,” *Journal of Molecular Liquids*, Elsevier B.V., 261, 189–198. DOI: 10.1016/j.molliq.2018.03.128
- Bouyahmed, F., Cai, M., Reinert, L., Duclaux, L., Dey, R., Youcef, H., Lahcini, M., Muller, F., and Delpeux-Ouldriane, S. (2018). “A Wide Adsorption Range Hybrid Material Based on Chitosan, Activated Carbon and Montmorillonite for Water Treatment,” *C*, 4(2), 35. DOI: 10.3390/c4020035
- Calcagnile, P., Caputo, I., Cannoletta, D., Bettini, S., Valli, L., and Demitri, C. (2017). “A bio-based composite material for water remediation from oily contaminants,” 134, 374–382.
- Camel, V., and Bermond, A. (1998). “The use of ozone and associated oxidation processes in drinking water treatment,” *Water Research*, 32(11), 3208–3222. DOI: 10.1016/S0043-1354(98)00130-4
- Carpenter, A. W., de Lannoy, C.-F., and Wiesner, M. R. (2015). “Cellulose nanomaterials in water treatment technologies,” *Environmental Science & Technology*, 49(9), 5277–5287. DOI: 10.1021/es506351r
- Celebioglu, A., Demirci, S., and Uyar, T. (2014). “Cyclodextrin-grafted electrospun cellulose acetate nanofibers via ‘click’ reaction for removal of phenanthrene,” *Applied Surface Science*, Elsevier B.V., 305, 581–588. DOI: 10.1016/j.apsusc.2014.03.138
- Chang, P. R., Zheng, P., Liu, B., Anderson, D. P., Yu, J., and Ma, X. (2011). “Characterization of magnetic soluble starch-functionalized carbon nanotubes and its

- application for the adsorption of the dyes,” *Journal of Hazardous Materials*, Elsevier B.V., 186(2–3), 2144–2150. DOI: 10.1016/j.jhazmat.2010.12.119
- Chauhan, G. S., Guleria, L., and Sharma, R. (2005). “Synthesis, characterization and metal ion sorption studies of graft copolymers of cellulose with glycidyl methacrylate and some comonomers,” *Cellulose*, 12(1), 97–110. DOI: 10.1023/B:CELL.0000049349.66326.5e
- Chauhan, K., Chauhan, G. S., and Ahn, J. H. (2010). “Novel polycarboxylated starch-based sorbents for Cu<sup>2+</sup> ions,” *Industrial and Engineering Chemistry Research*, 49(6), 2548–2556. DOI: 10.1021/ie9009952
- Chen, P. Y., McKittrick, J., and Meyers, M. A. (2012). “Biological materials: Functional adaptations and bioinspired designs,” *Progress in Materials Science*, Elsevier Ltd, 57(8), 1492–1704. DOI: 10.1016/j.pmatsci.2012.03.001
- Cheng, H., Feng, Q., Liao, C., Liu, Y., Wu, D., and Wang, Q. (2016). “Removal of methylene blue with hemicellulose/clay hybrid hydrogels,” *Chinese Journal of Polymer Science*, 34(6), 709–719. DOI: 10.1007/s10118-016-1788-2
- Cho, D. W., Jeon, B. H., Jeong, Y., Nam, I. H., Choi, U. K., Kumar, R., and Song, H. (2016). “Synthesis of hydrous zirconium oxide-impregnated chitosan beads and their application for removal of fluoride and lead,” *Applied Surface Science*, Elsevier B.V., 372, 13–19. DOI: 10.1016/j.apsusc.2016.03.068
- Chowdhury, M. N. K., Ismail, A. F., Beg, M. D. H., Hegde, G., and Gohari, R. J. (2015). “Polyvinyl alcohol/polysaccharide hydrogel graft materials for arsenic and heavy metal removal,” *New Journal of Chemistry*, Royal Society of Chemistry, 39(7), 5823–5832. DOI: 10.1039/c5nj00509d
- Cova, T. F. G. G., Murtinho, D., Pais, A. A. C. C., and Valente, A. J. M. (2018). “Combining cellulose and cyclodextrins: fascinating designs for materials and pharmaceuticals,” *Frontiers in Chemistry*, 6(July), 271. DOI: 10.3389/fchem.2018.00271
- Crini, G. (2008). “Kinetic and equilibrium studies on the removal of cationic dyes from aqueous solution by adsorption onto a cyclodextrin polymer,” *Dyes and Pigments*, 77(2), 415–426. DOI: 10.1016/j.dyepig.2007.07.001
- D’Halluin, M., Rull-Barrull, J., Bretel, G., Labrugère, C., Le Grogneq, E., and Felpin, F. X. (2017). “Chemically modified cellulose filter paper for heavy metal remediation in water,” *ACS Sustainable Chemistry and Engineering*, 5(2), 1965–1973. DOI: 10.1021/acssuschemeng.6b02768
- Davila-Rodriguez, J. L., Escobar-Barrios, V. A., and Rangel-Mendez, J. R. (2012). “Removal of fluoride from drinking water by a chitin-based biocomposite in fixed-bed columns,” *Journal of Fluorine Chemistry*, 140, 99–103. DOI: 10.1016/j.jfluchem.2012.05.019
- Davila-Rodriguez, J. L., Escobar-Barrios, V. A., Shirai, K., and Rangel-Mendez, J. R. (2009). “Synthesis of a chitin-based biocomposite for water treatment: Optimization for fluoride removal,” *Journal of Fluorine Chemistry*, 130(8), 718–726. DOI: 10.1016/j.jfluchem.2009.05.012
- Dax, D., Chávez, M. S., Xu, C., Willför, S., Mendonça, R. T., and Sánchez, J. (2014). “Cationic hemicellulose-based hydrogels for arsenic and chromium removal from aqueous solutions,” *Carbohydrate Polymers*, 111, 797–805. DOI: 10.1016/j.carbpol.2014.05.045
- De-Bashan, L. E., Moreno, M., Hernandez, J. P., and Bashan, Y. (2002). “Removal of ammonium and phosphorus ions from synthetic wastewater by the microalgae

- Chlorella vulgaris* coimmobilized in alginate beads with the microalgae growth-promoting bacterium *Azospirillum brasilense*,” *Water Research*, 36(12), 2941–2948. DOI: 10.1016/S0043-1354(01)00522-X
- Devrimci, H. A., Yuksel, A. M., and Sanin, F. D. (2012). “Algal alginate: A potential coagulant for drinking water treatment,” *Desalination*, Elsevier B.V., 299, 16–21. DOI: 10.1016/j.desal.2012.05.004
- Djebri, N., Boutahala, M., Chelali, N. E., Boukhalfa, N., and Zeroual, L. (2016). “Enhanced removal of cationic dye by calcium alginate/organobentonite beads: Modeling, kinetics, equilibriums, thermodynamic and reusability studies,” *International Journal of Biological Macromolecules*, Elsevier B.V., 92, 1277–1287. DOI: 10.1016/j.ijbiomac.2016.08.013
- Dong, C., Qian, L. Y., Zhao, G. L., He, B. H., and Xiao, H. N. (2014). “Preparation of antimicrobial cellulose fibers by grafting  $\beta$ -cyclodextrin and inclusion with antibiotics,” *Materials Letters*, Elsevier, 124, 181–183. DOI: 10.1016/j.matlet.2014.03.091
- Dotto, G. L., Santos, J. M. N. dos, Rosa, R., Pinto, L. A. A., Pavan, F. A., and Lima, E. C. (2015). “Fixed bed adsorption of Methylene Blue by ultrasonic surface modified chitin supported on sand,” *Chemical Engineering Research and Design*, Institution of Chemical Engineers, 100, 302–310. DOI: 10.1016/j.cherd.2015.06.003
- Du, Y., Lv, X. T., Wu, Q. Y., Zhang, D. Y., Zhou, Y. T., Peng, L., and Hu, H. Y. (2017). “Formation and control of disinfection byproducts and toxicity during reclaimed water chlorination: A review,” *Journal of Environmental Sciences*, 58, 51–63. DOI: 10.1016/j.jes.2017.01.013
- Dwivedi, A. D., Dubey, S. P., Hokkanen, S., Fallah, R. N., and Sillanpää, M. (2014). “Recovery of gold from aqueous solutions by taurine modified cellulose: An adsorptive-reduction pathway,” *Chemical Engineering Journal*, Elsevier B.V., 255, 97–106. DOI: 10.1016/j.cej.2014.06.017
- Dwivedi, A. D., Permana, R., Singh, J. P., Yoon, H., Chae, K. H., Chang, Y. S., and Hwang, D. S. (2017). “Tunichrome-Inspired Gold-Enrichment Dispersion Matrix and Its Application in Water Treatment: A Proof-of-Concept Investigation,” *ACS Applied Materials and Interfaces*, 9(23), 19815–19824. DOI: 10.1021/acsami.7b03064
- Escudero, C., Fiol, N., Villaescusa, I., and Bollinger, J. C. (2009). “Arsenic removal by a waste metal (hydr)oxide entrapped into calcium alginate beads,” *Journal of Hazardous Materials*, 164(2–3), 533–541. DOI: 10.1016/j.jhazmat.2008.08.042
- Faisal, A. A. H., Sulaymon, A. H., and Khaliefa, Q. M. (2017). “A review of permeable reactive barrier as passive sustainable technology for groundwater remediation,” *International Journal of Environmental Science and Technology*, Springer Berlin Heidelberg, 1–16. DOI: 10.1007/s13762-017-1466-0
- Fan, L., Luo, C., Sun, M., Li, X., Lu, F., and Qiu, H. (2012). “Preparation of novel magnetic chitosan/graphene oxide composite as effective adsorbents toward methylene blue,” *Bioresource Technology*, Elsevier Ltd, 114, 703–706. DOI: 10.1016/j.biortech.2012.02.067
- Fan, L., Luo, C., Sun, M., Qiu, H., and Li, X. (2013). “Synthesis of magnetic  $\beta$ -cyclodextrin-chitosan/graphene oxide as nano-adsorbent and its application in dye adsorption and removal,” *Colloids and Surfaces B: Biointerfaces*, Elsevier B.V., 103, 601–607. DOI: 10.1016/j.colsurfb.2012.11.023
- Fan, Y., Saito, T., and Isogai, A. (2009). “TEMPO-mediated oxidation of  $\beta$ -chitin to prepare individual nanofibrils,” *Carbohydrate Polymers*, Elsevier Ltd, 77(4), 832–

838. DOI: 10.1016/j.carbpol.2009.03.008
- Fatin-Rouge, N., Dupont, A., Vidonne, A., Dejeu, J., Fievet, P., and Foissy, A. (2006). "Removal of some divalent cations from water by membrane-filtration assisted with alginate," *Water Research*, 40(6), 1303–1309. DOI: 10.1016/j.watres.2006.01.026
- Feng, S., Bagia, C., and Mpourmpakis, G. (2013). "Determination of proton affinities and acidity constants of sugars," *Journal of Physical Chemistry A*, 117(24), 5211–5219. DOI: 10.1021/jp403355e
- Fu, F., Dionysiou, D. D., and Liu, H. (2014). "The use of zero-valent iron for groundwater remediation and wastewater treatment: A review," *Journal of Hazardous Materials*, Elsevier B.V., 267, 194–205. DOI: 10.1016/j.jhazmat.2013.12.062
- Gan, L., Shang, S., Hu, E., Yuen, C. W. M., and Jiang, S. X. (2015). "Konjac glucomannan/graphene oxide hydrogel with enhanced dyes adsorption capability for methyl blue and methyl orange," *Applied Surface Science*, Elsevier B.V., 357, 866–872. DOI: 10.1016/j.apsusc.2015.09.106
- Gautam, D., Kumari, S., Ram, B., Chauhan, G. S., and Chauhan, K. (2018). "A new hemicellulose-based adsorbent for malachite green," *Journal of Environmental Chemical Engineering*, Elsevier, 6(4), 3889–3897. DOI: 10.1016/j.jece.2018.05.029
- Ghorpade, V. S., Yadav, A. V., and Dias, R. J. (2017). "Citric acid crosslinked  $\beta$ -cyclodextrin/carboxymethylcellulose hydrogel films for controlled delivery of poorly soluble drugs," *Carbohydrate Polymers*, Elsevier Ltd., 164, 339–348. DOI: 10.1016/j.carbpol.2017.02.005
- Gidwani, B., and Vyas, A. (2014). "Synthesis, characterization and application of Epichlorohydrin- $\beta$ -cyclodextrin polymer," *Colloids and Surfaces B: Biointerfaces*, Elsevier B.V., 114, 130–137. DOI: 10.1016/j.colsurfb.2013.09.035
- Girio, F. M., Fonseca, C., Carvalheiro, F., Duarte, L. C., Marques, S., and Bogel-Lukasik, R. (2010). "Hemicelluloses for fuel ethanol: A review," *Bioresource Technology*, Elsevier Ltd, 101(13), 4775–4800. DOI: 10.1016/j.biortech.2010.01.088
- Glaze, W. H., Kang, J.-W., and Chapin, D. H. (1987). "The chemistry of water treatment processes involving ozone, hydrogen peroxide and ultraviolet radiation," Taylor & Francis.
- Gomes, R. F., de Azevedo, A. C. N., Pereira, A. G. B., Muniz, E. C., Fajardo, A. R., and Rodrigues, F. H. A. (2015). "Fast dye removal from water by starch-based nanocomposites," *Journal of Colloid and Interface Science*, Elsevier Inc., 454, 200–209. DOI: 10.1016/j.jcis.2015.05.026
- Gopi, S., Balakrishnan, P., Pius, A., and Thomas, S. (2017). "Chitin nanowhisker (ChNW)-functionalized electrospun PVDF membrane for enhanced removal of Indigo carmine," *Carbohydrate Polymers*, Elsevier Ltd., 165, 115–122. DOI: 10.1016/j.carbpol.2017.02.046
- Gotoh, T., Matsushima, K., and Kikuchi, K. I. (2004). "Preparation of alginate-chitosan hybrid gel beads and adsorption of divalent metal ions," *Chemosphere*, 55(1), 135–140. DOI: 10.1016/j.chemosphere.2003.11.016
- Grem, I. C. da S., Lima, B. N. B., Carneiro, W. F., Queirós, Y. G. de C., and Mansur, C. R. E. (2013). "Chitosan microspheres applied for removal of oil from produced water in the oil industry," *Polímeros Ciência e Tecnologia*, 23(6), 705–711. DOI: 10.4322/polimeros.2014.008
- Guo, X., Abdala, A. A., May, B. L., Lincoln, S. F., Khan, S. A., and Prud'homme, R. K. (2005). "Novel associative polymer networks based on cyclodextrin inclusion compounds," *Macromolecules*, 38(7), 3037–3040. DOI: 10.1021/ma050071o

- Guo, Z., Li, Y., Pan, S., and Xu, J. (2015). "Fabrication of Fe<sub>3</sub>O<sub>4</sub>@cyclodextrin magnetic composite for the high-efficient removal of Eu(III)," *Journal of Molecular Liquids*, Elsevier B.V., 206, 272–277. DOI: 10.1016/j.molliq.2015.02.034
- Gupta, A., Chauhan, V. S., and Sankaramakrishnan, N. (2009). "Preparation and evaluation of iron-chitosan composites for removal of As(III) and As(V) from arsenic contaminated real life groundwater," *Water Research*, Elsevier Ltd, 43(15), 3862–3870. DOI: 10.1016/j.watres.2009.05.040
- Gurgel, L. V. A., Júnior, O. K., Gil, R. P. de F., and Gil, L. F. (2008). "Adsorption of Cu(II), Cd(II), and Pb(II) from aqueous single metal solutions by cellulose and mercerized cellulose chemically modified with succinic anhydride," *Bioresource Technology*, 99(8), 3077–3083. DOI: 10.1016/j.biortech.2007.05.072
- Han, J., Xin, J., Zheng, X., Kolditz, O., and Shao, H. (2016). "Remediation of trichloroethylene-contaminated groundwater by three modifier-coated microscale zero-valent iron," *Environmental Science and Pollution Research*, 23(14), 14442–14450. DOI: 10.1007/s11356-016-6368-z
- Haruta, M. (1997). "Size- and support-dependency in the catalysis of gold," *Catalysis Today*, 36(1), 153–166. DOI: 10.1016/S0920-5861(96)00208-8
- Hatton, F. L., Malmström, E., and Carlmark, A. (2015). "Tailor-made copolymers for the adsorption to cellulosic surfaces," *European Polymer Journal*, 65, 325–339. DOI: 10.1016/j.eurpolymj.2015.01.026
- Hitzfeld, B. C., Hoger, S. J., and Dietrich, D. R. (2000). "Cyanobacterial toxins: Removal during drinking water treatment, and human risk assessment cyanobacteria," *Environmental Health Perspectives* 108(1), 113–122.
- Hokkanen, S., Bhatnagar, A., Repo, E., Lou, S., and Sillanpää, M. (2016). "Calcium hydroxyapatite microfibrillated cellulose composite as a potential adsorbent for the removal of Cr(VI) from aqueous solution," *Chemical Engineering Journal* 283, 445–452. DOI: 10.1016/j.cej.2015.07.035
- Hokkanen, S., Repo, E., and Sillanpää, M. (2013). "Removal of heavy metals from aqueous solutions by succinic anhydride modified mercerized nanocellulose," *Chemical Engineering Journal* 223, 40–47. DOI: 10.1016/j.cej.2013.02.054
- Hokkanen, S., Repo, E., Suopajarvi, T., Liimatainen, H., Niinimaa, J., and Sillanpää, M. (2014). "Adsorption of Ni(II), Cu(II) and Cd(II) from aqueous solutions by amino modified nanostructured microfibrillated cellulose," *Cellulose* 21(3), 1471–1487. DOI: 10.1007/s10570-014-0240-4
- Hoover R. (2001). "Composition, molecular structure, and physicochemical properties of tuber and root starches: A review," *Carbohydr Polymer* 45(3), 2001.
- Hu, J., Shao, D., Chen, C., Sheng, G., Ren, X., and Wang, X. (2011). "Removal of 1-naphthylamine from aqueous solution by multiwall carbon nanotubes/iron oxides/cyclodextrin composite," *Journal of Hazardous Materials* 185(1), 463–471. DOI: 10.1016/j.jhazmat.2010.09.055
- Hult, E. L., Larsson, P. T., and Iversen, T. (2002). "A comparative CP/MAS<sup>13</sup>C-NMR study of the supermolecular structure of polysaccharides in sulphite and kraft pulps," *Holzforchung* 56(2), 179–184. DOI: 10.1515/HF.2002.030
- Ilharco, L. M., Garcia, A. R., Lopes da Silva, J., and Vieira Ferreira, L. F. (1997). "Infrared approach to the study of adsorption on cellulose: Influence of cellulose crystallinity on the adsorption of benzophenone," *Langmuir* 13(15), 4126–4132. DOI: 10.1021/la962138u
- Isobe, N., Chen, X., Kim, U. J., Kimura, S., Wada, M., Saito, T., and Isogai, A. (2013).

- “TEMPO-oxidized cellulose hydrogel as a high-capacity and reusable heavy metal ion adsorbent,” *Journal of Hazardous Materials* 260, 195–201. DOI: 10.1016/j.jhazmat.2013.05.024
- IUPAC. (2014). *Compendium of Chemical Terminology (the “Gold Book”), IUPAC Compendium of Chemical Terminology*, (M. Nič, J. Jiráč, B. Košata, A. Jenkins, and A. McNaught, eds.), Blackwell Scientific Publications, Oxford. DOI: 10.1351/goldbook
- Jain, P., Varshney, S., and Srivastava, S. (2016). “Functionalized nanobiomaterials: high-performance sorbents for chromium remediation from water streams,” *International Journal of Environmental Science and Technology* 13(12), 2893-2904. DOI: 10.1007/s13762-016-1115-z
- Janaki, V., Vijayaraghavan, K., Oh, B. T., Lee, K. J., Muthuchelian, K., Ramasamy, A. K., and Kamala-Kannan, S. (2012). “Starch/polyaniline nanocomposite for enhanced removal of reactive dyes from synthetic effluent,” *Carbohydrate Polymers* 90(4), 1437–1444. DOI: 10.1016/j.carbpol.2012.07.012
- Jiang, J., Ye, W., Yu, J., Fan, Y., Ono, Y., Saito, T., and Isogai, A. (2018a). “Chitin nanocrystals prepared by oxidation of  $\alpha$ -chitin using the O<sub>2</sub>/laccase/TEMPO system,” *Carbohydrate Polymers* 189(August 2017), 178–183. DOI: 10.1016/j.carbpol.2018.01.096
- Jiang, Y., Liu, B., Xu, J., Pan, K., Hou, H., Hu, J., and Yang, J. (2018b). “Cross-linked chitosan/ $\beta$ -cyclodextrin composite for selective removal of methyl orange: Adsorption performance and mechanism,” *Carbohydrate Polymers* 182(July 2017), 106–114. DOI: 10.1016/j.carbpol.2017.10.097
- Jin, L., Sun, Q., Xu, Q., and Xu, Y. (2015). “Adsorptive removal of anionic dyes from aqueous solutions using microgel based on nanocellulose and polyvinylamine,” *Bioresource Technology* 197, 348–355. DOI: 10.1016/j.biortech.2015.08.093
- Kardam, A., Raj, K. R., Srivastava, S., and Srivastava, M. M. (2014). “Nanocellulose fibers for biosorption of cadmium, nickel, and lead ions from aqueous solution,” *Clean Technologies and Environmental Policy* 16(2), 385–393. DOI: 10.1007/s10098-013-0634-2
- Karim, Z., Claudpierre, S., Grahn, M., Oksman, K., and Mathew, A. P. (2016). “Nanocellulose based functional membranes for water cleaning: Tailoring of mechanical properties, porosity and metal ion capture,” *Journal of Membrane Science* 514, 418–428. DOI: 10.1016/j.memsci.2016.05.018
- Karim, Z., Mathew, A. P., Grahn, M., Mouzon, J., and Oksman, K. (2014). “Nanoporous membranes with cellulose nanocrystals as functional entity in chitosan: Removal of dyes from water,” *Carbohydrate Polymers* 112, 668–676. DOI: 10.1016/j.carbpol.2014.06.048
- Karthik, R., and Meenakshi, S. (2015). “Removal of Cr(VI) ions by adsorption onto sodium alginate-polyaniline nanofibers,” *International Journal of Biological Macromolecules*, Elsevier B.V., 72, 711–717. DOI: 10.1016/j.ijbiomac.2014.09.023
- Kayaci, F., Aytac, Z., and Uyar, T. (2013). “Surface modification of electrospun polyester nanofibers with cyclodextrin polymer for the removal of phenanthrene from aqueous solution,” *Journal of Hazardous Materials* 261, 286–294. DOI: 10.1016/j.jhazmat.2013.07.041
- Khaoulani, S., Chaker, H., Cadet, C., Bychkov, E., Cherif, L., Bengueddach, A., and Fourmentin, S. (2015). “Wastewater treatment by cyclodextrin polymers and noble metal/mesoporous TiO<sub>2</sub> photocatalysts,” *Comptes Rendus Chimie, Academie des*

- sciences, 18(1), 23–31. DOI: 10.1016/j.crci.2014.07.004
- Kim, D. H., Cha, J. H., Hong, S. H., Kim, D. Y., and Kim, C. W. (2009). “Control of corrosive water in advanced water treatment plant by manipulating calcium carbonate precipitation potential,” *Korean Journal of Chemical Engineering*, 26(1), 90–101. DOI: 10.1007/s11814-009-0015-z
- Kim, Y., Kon, Y., Kim, S., Harbottle, D., and Lee, J. W. (2017). “Nanostructured potassium copper hexacyanoferrate-cellulose hydrogel for selective and rapid cesium adsorption,” *Chemical Engineering Journal* 313, 1042–1050. DOI: 10.1016/j.cej.2016.10.136
- Klemm, D., Heublein, B., Fink, H. P., and Bohn, A. (2005). “Cellulose: Fascinating biopolymer and sustainable raw material,” *Angewandte Chemie - International Edition* 44(22), 3358–3393. DOI: 10.1002/anie.200460587
- Kumar, A., Guo, C., Sharma, G., Pathania, D., Naushad, M., Kalia, S., and Dhiman, P. (2016). “Magnetically recoverable ZrO<sub>2</sub>/Fe<sub>3</sub>O<sub>4</sub>/chitosan nanomaterials for enhanced sunlight driven photoreduction of carcinogenic Cr(VI) and dechlorination & mineralization of 4-chlorophenol from simulated waste water,” *RSC Advances* 6(16), 13251–13263. DOI: 10.1039/c5ra23372k
- Kumar, A., Sharma, G., Naushad, M., and Thakur, S. (2015). “SPION/β-cyclodextrin core-shell nanostructures for oil spill remediation and organic pollutant removal from waste water,” *Chemical Engineering Journal* 280, 175–187. DOI: 10.1016/j.cej.2015.05.126
- Kumar Dutta, P., Dutta, J., and Tripathi, V. S. (2004). “Chitin and chitosan: Chemistry, properties and applications,” *Journal of Scientific & Industrial Research*, 63(January), 20–31. DOI: 10.1002/chin.200727270
- Kurkov, S. V., and Loftsson, T. (2013). “Cyclodextrins,” *International Journal of Pharmaceutics*, 453(1), 167–180. DOI: 10.1016/j.ijpharm.2012.06.055
- Kwon, O. H., Kim, J. O., Cho, D. W., Kumar, R., Baek, S. H., Kurade, M. B., and Jeon, B. H. (2016). “Adsorption of As(III), As(V) and Cu(II) on zirconium oxide immobilized alginate beads in aqueous phase,” *Chemosphere* 160, 126–133. DOI: 10.1016/j.chemosphere.2016.06.074
- Lakouraj, M. M., Mojerlou, F., and Zare, E. N. (2014). “Nanogel and superparamagnetic nanocomposite based on sodium alginate for sorption of heavy metal ions,” *Carbohydrate Polymers* 106(1), 34–41. DOI: 10.1016/j.carbpol.2014.01.092
- Langlais, B., Reckhow, D. A., and Brink, D. R. (1991). *Ozone in Water Treatment: Application and Engineering, Cooperative research report*, CRC Press, Boca Raton, FL, USA.
- Laus, R., Costa, T. G., Szpoganicz, B., and Fávere, V. T. (2010). “Adsorption and desorption of Cu(II), Cd(II) and Pb(II) ions using chitosan crosslinked with epichlorohydrin-triphosphate as the adsorbent,” *Journal of Hazardous Materials*, 183(1–3), 233–241. DOI: 10.1016/j.jhazmat.2010.07.016
- Lawrance, G. A. (2013). *Introduction to Coordination Chemistry*, Wiley, New York, NY.
- Lee, H. C., Jeong, Y. G., Min, B. G., Lyoo, W. S., and Lee, S. C. (2009). “Preparation and acid dye adsorption behavior of polyurethane/chitosan composite foams,” *Fibers and Polymers*, 10(5), 636–642. DOI: 10.1007/s12221-010-0636-1
- Lee, K. Y., and Mooney, D. J. (2012). “Alginate: Properties and biomedical applications,” *Progress in Polymer Science (Oxford)* 37(1), 106–126. DOI: 10.1016/j.progpolymsci.2011.06.003
- Lee, K. Y., Quero, F., Blaker, J. J., Hill, C. A. S., Eichhorn, S. J., and Bismarck, A.

- (2011). "Surface only modification of bacterial cellulose nanofibres with organic acids," *Cellulose*, 18(3), 595–605. DOI: 10.1007/s10570-011-9525-z
- Lemlikchi, W., Sharrock, P., Mecherri, M. O., Fiallo, M., and Nzihou, A. (2012). "Treatment of textile waste waters by hydroxyapatite co-precipitation with adsorbent regeneration and reuse," *Waste and Biomass Valorization*, 3(1), 75–79. DOI: 10.1007/s12649-011-9096-0
- Li, J., Chen, C., Zhao, Y., Hu, J., Shao, D., and Wang, X. (2013). "Synthesis of water-dispersible Fe<sub>3</sub>O<sub>4</sub>β-cyclodextrin by plasma-induced grafting technique for pollutant treatment," *Chemical Engineering Journal* 229, 296–303. DOI: 10.1016/j.cej.2013.06.016
- Li, J., Zuo, K., Wu, W., Xu, Z., Yi, Y., Jing, Y., Dai, H., and Fang, G. (2018). "Shape memory aerogels from nanocellulose and polyethyleneimine as a novel adsorbent for removal of Cu(II) and Pb(II)," *Carbohydrate Polymers* 196(April), 376–384. DOI: 10.1016/j.carbpol.2018.05.015
- Li, L., Luo, C., Li, X., Duan, H., and Wang, X. (2014). "Preparation of magnetic ionic liquid/chitosan/graphene oxide composite and application for water treatment," *International Journal of Biological Macromolecules* 66, 172–178. DOI: 10.1016/j.ijbiomac.2014.02.031
- Li, Y., Liu, F., Xia, B., Du, Q., Zhang, P., Wang, D., Wang, Z., and Xia, Y. (2010). "Removal of copper from aqueous solution by carbon nanotube/calcium alginate composites," *Journal of Hazardous Materials* 177(1–3), 876–880. DOI: 10.1016/j.jhazmat.2009.12.114
- Lin, N., and Dufresne, A. (2013). "Supramolecular hydrogels from in situ host-guest inclusion between chemically modified cellulose nanocrystals and cyclodextrin," *Biomacromolecules*, 14(3), 871–880. DOI: 10.1021/bm301955k
- Lin, S., Huang, R., Cheng, Y., Liu, J., Lau, B. L. T., and Wiesner, M. R. (2013). "Silver nanoparticle-alginate composite beads for point-of-use drinking water disinfection," *Water Research* 47(12), 3959–3965. DOI: 10.1016/j.watres.2012.09.005
- Liu, D., Zhu, Y., Li, Z., Tian, D., Chen, L., and Chen, P. (2013). "Chitin nanofibrils for rapid and efficient removal of metal ions from water system," *Carbohydrate Polymers* 98(1), 483–489. DOI: 10.1016/j.carbpol.2013.06.015
- Liu, H., Cai, X., Wang, Y., and Chen, J. (2011). "Adsorption mechanism-based screening of cyclodextrin polymers for adsorption and separation of pesticides from water," *Water Research* 45(11), 3499–3511. DOI: 10.1016/j.watres.2011.04.004
- Liu, L., and Guo, Q. X. (2004). "Use of quantum chemical methods to study cyclodextrin chemistry," *Journal of Inclusion Phenomena and Macrocyclic Chemistry*, 50(1), 95–103. DOI: Doi 10.1007/10.1007/S10847-003-8847-3
- Liu, P., Borrell, P. F., Božič, M., Kokol, V., Oksman, K., and Mathew, A. P. (2015). "Nanocelluloses and their phosphorylated derivatives for selective adsorption of Ag<sup>+</sup>, Cu<sup>2+</sup> and Fe<sup>3+</sup> from industrial effluents," *Journal of Hazardous Materials*, 294, 177–185. DOI: 10.1016/j.jhazmat.2015.04.001
- Liu, P., Oksman, K., and Mathew, A. P. (2016). "Surface adsorption and self-assembly of Cu(II) ions on TEMPO-oxidized cellulose nanofibers in aqueous media," *Journal of Colloid and Interface Science* 464, 175–182. DOI: 10.1016/j.jcis.2015.11.033
- Luo, X., Lei, X., Xie, X., Yu, B., Cai, N., and Yu, F. (2016). "Adsorptive removal of Lead from water by the effective and reusable magnetic cellulose nanocomposite beads entrapping activated bentonite," *Carbohydrate polymers*, 151, 640–648. DOI: 10.1016/j.carbpol.2016.06.003

- Luo, X., Zhang, G., Wang, X., and Gu, P. (2013). "Research on a pellet co-precipitation micro-filtration process for the treatment of liquid waste containing strontium," *Journal of Radioanalytical and Nuclear Chemistry*, 298(2), 931–939. DOI: 10.1007/s10967-013-2495-x
- Ma, H., Hsiao, B. S., and Chu, B. (2012). "Ultrafine cellulose nanofibers as efficient adsorbents for removal of UO<sub>2</sub><sup>2+</sup> in water," *ACS Macro Letters*, 1(1), 213–216. DOI: 10.1021/mz200047q
- Maatar, W., and Boufi, S. (2015). "Poly(methacrylic acid-co-maleic acid) grafted nanofibrillated cellulose as a reusable novel heavy metal ions adsorbent," *Carbohydrate Polymers* 126, 199–207. DOI: 10.1016/j.carbpol.2015.03.015
- Mahfoudhi, N., and Boufi, S. (2017). "Nanocellulose as a novel nanostructured adsorbent for environmental remediation: a review," *Cellulose* 24(3), 1171–1197. DOI: 10.1007/s10570-017-1194-0
- Mao, Y., Guo, D., Yao, W., Wang, X., Yang, H., Xie, Y. F., Komarneni, S., Yu, G., and Wang, Y. (2018). "Effects of conventional ozonation and electro-peroxone pretreatment of surface water on disinfection by-product formation during subsequent chlorination," *Water Research*, 130, 322–332. DOI: 10.1016/j.waters.2017.12.019
- Medronho, B., Andrade, R., Vivod, V., Ostlund, A., Miguel, M. G., Lindman, B., Voncina, B., and Valente, A. J. M. (2013). "Cyclodextrin-grafted cellulose: Physico-chemical characterization," *Carbohydrate Polymers* 93(1), 324–330. DOI: 10.1016/j.carbpol.2012.08.109
- Melone, L., Rossi, B., Pastori, N., Panzeri, W., Mele, A., and Punta, C. (2015). "TEMPO-oxidized cellulose cross-linked with branched polyethyleneimine: Nanostructured adsorbent sponges for water remediation," *ChemPlusChem*, 80(9), 1408–1415. DOI: 10.1002/cplu.201500145
- Meraz, K. A. S., Vargas, S. M. P., Maldonado, J. T. L., Bravo, J. M. C., Guzman, M. T. O., and Maldonado, E. A. L. (2016). "Eco-friendly innovation for nejayote coagulation-flocculation process using chitosan: Evaluation through zeta potential measurements," *Chemical Engineering Journal* 284, 536–542. DOI: 10.1016/j.cej.2015.09.026
- Meyers, M. A., Chen, P. Y., Lin, A. Y. M., and Seki, Y. (2008). "Biological materials: Structure and mechanical properties," *Progress in Materials Science*, 53(1), 1–206. DOI: 10.1016/j.pmatsci.2007.05.002
- Mishima, T., Hisamatsu, M., York, W. S., Teranishi, K., and Yamada, T. (1998). "Adhesion of  $\beta$ -D-glucans to cellulose," *Carbohydrate Research*, 308(3–4), 389–395. DOI: 10.1016/S0008-6215(98)00099-8
- Mohamed, M. H., Wilson, L. D., Pratt, D. Y., Guo, R., Wu, C., and Headley, J. V. (2012). "Evaluation of the accessible inclusion sites in copolymer materials containing  $\beta$ -cyclodextrin," *Carbohydrate Polymers* 87(2), 1241–1248. DOI: 10.1016/j.carbpol.2011.09.011
- Morin-Crini, N., and Crini, G. (2013). "Environmental applications of water-insoluble  $\beta$ -cyclodextrin-epichlorohydrin polymers," *Progress in Polymer Science* 38(2), 344–368. DOI: 10.1016/j.progpolymsci.2012.06.005
- Morin-Crini, N., Winterton, P., Fourmentin, S., Wilson, L. D., Fenyvesi, É., and Crini, G. (2018). "Water-insoluble  $\beta$ -cyclodextrin-epichlorohydrin polymers for removal of pollutants from aqueous solutions by sorption processes using batch studies: A review of inclusion mechanisms," *Progress in Polymer Science* 78, 1–23. DOI: 10.1016/j.progpolymsci.2017.07.004

- Munagapati, V. S., and Kim, D. S. (2017). "Equilibrium isotherms, kinetics, and thermodynamics studies for congo red adsorption using calcium alginate beads impregnated with nano-goethite," *Ecotoxicology and Environmental Safety* 141(August 2016), 226–234. DOI: 10.1016/j.ecoenv.2017.03.036
- Nevárez, L. A. M., Casarrubias, L. B., Celzard, A., Fierro, V., Muñoz, V. T., Davila, A. C., Lubian, J. R. T., and Sánchez, G. G. (2011). "Biopolymer-based nanocomposites: effect of lignin acetylation in cellulose triacetate films," *Science and Technology of Advanced Materials*, 12(4), 045006. DOI: 10.1088/1468-6996/12/4/045006
- Novotny, V. (2003). *Water Quality: Diffuse Pollution and Watershed Management*, John Wiley & Sons, Inc., New York, NY.
- Nyberg, U., Andersson, B., Aspegren, H., and Ødegaard, H. (1994). "The use of polymer in the pre-precipitation step of a wastewater treatment system for extended nutrient removal," in: *Chemical Water and Wastewater Treatment III: Proceedings of the 6th Gothenburg Symposium 1994 June 20 -- 22, 1994 Gothenburg, Sweden*, R. Klute and H. H. Hahn, (eds.), Springer Berlin Heidelberg, Berlin, Heidelberg, 211–219. DOI: 10.1007/978-3-642-79110-9\_15
- Oh, D. X., Kim, S., Lee, D., and Hwang, D. S. (2015). "Tunicate-mimetic nanofibrous hydrogel adhesive with improved wet adhesion," *Acta Biomaterialia* 20, 104–112. DOI: 10.1016/j.actbio.2015.03.031
- Olivera, S., Muralidhara, H. B., Venkatesh, K., Guna, V. K., Gopalakrishna, K., and Kumar K., Y. (2016). "Potential applications of cellulose and chitosan nanoparticles/composites in wastewater treatment: A review," *Carbohydrate Polymers* 153, 600–618. DOI: 10.1016/j.carbpol.2016.08.017
- Orelma, H., Filpponen, I., Johansson, L.-S., Laine, J., and Rojas, O. J. (2011). "Modification of cellulose films by adsorption of CMC and chitosan for controlled attachment of biomolecules," *Biomacromolecules*, 12(12), 4311–4318. DOI: 10.1021/bm201236a
- Orelma, H., Filpponen, I., Johansson, L. S., Österberg, M., Rojas, O. J., and Laine, J. (2012). "Surface functionalized nanofibrillar cellulose (NFC) film as a platform for immunoassays and diagnostics," *Biointerphases*, 7(1–4), 1–12. DOI: 10.1007/s13758-012-0061-7
- Orelma, H., Virtanen, T., Spoljaric, S., Lehmonen, J., Seppälä, J., Rojas, O. J., and Harlin, A. (2018). "Cyclodextrin-functionalized fiber yarns spun from deep eutectic cellulose solutions for nonspecific hormone capture in aqueous matrices," *Biomacromolecules*, 19(2), 652–661. DOI: 10.1021/acs.biomac.7b01765
- Pal, S., Mal, D., and Singh, R. P. (2005). "Cationic starch: An effective flocculating agent," *Carbohydrate Polymers* 59(4), 417–423. DOI: 10.1016/j.carbpol.2004.06.047
- Papageorgiou, S. K., Katsaros, F. K., Favvas, E. P., Romanos, G. E., Athanasekou, C. P., Beltsios, K. G., Tziaila, O. I., and Falaras, P. (2012). "Alginate fibers as photocatalyst immobilizing agents applied in hybrid photocatalytic/ultrafiltration water treatment processes," *Water Research* 46(6), 1858–1872. DOI: 10.1016/j.watres.2012.01.005
- Paul, V. J. (2008). "Global warming and cyanobacterial harmful algal blooms," in: *Cyanobacterial Harmful Algal Blooms: State of the Science and Research Needs*, H. K. Hudnell, (ed.), Springer New York, NY, 239–257. DOI: 10.1007/978-0-387-75865-7\_11
- Pavinatto, F. J., Caseli, L., and Oliveira, O. N. (2010). "Chitosan in nanostructured thin films," *Biomacromolecules*, 11(8), 1897–1908. DOI: 10.1021/bm1004838
- Pawar, S. N., and Edgar, K. J. (2012). "Alginate derivatization: A review of chemistry,

- properties and applications,” *Biomaterials* 33(11), 3279–3305. DOI: 10.1016/j.biomaterials.2012.01.007
- Prabaharan, M., and Gong, S. (2008). “Novel thiolated carboxymethyl chitosan-g- $\beta$ -cyclodextrin as mucoadhesive hydrophobic drug delivery carriers,” *Carbohydrate Polymers*, 73(1), 117–125. DOI: 10.1016/j.carbpol.2007.11.005
- Qi, J., Zhang, G., and Li, H. (2015). “Efficient removal of arsenic from water using a granular adsorbent: Fe-Mn binary oxide impregnated chitosan bead,” *Bioresource Technology* 193, 243–249. DOI: 10.1016/j.biortech.2015.06.102
- Renard, E., Barnathan, G., Deratani, A., and Seville, B. (1997). “Polycondensation of cyclodextrins with epichlorohydrin. Influence of reaction conditions on the polymer structure,” *Macromol. Symp.* 122, 229–234. DOI: 10.1002/masy.19971220136
- Rinaudo, M. (2006). “Chitin and chitosan: Properties and applications,” *Progress in Polymer Science* 31(7), 603–632. DOI: 10.1016/j.progpolymsci.2006.06.001
- Rosenblum, L., Zaffiro, A., Adams, W. A., and Wendelken, S. C. (2017). “Effect of chlorination by-products on the quantitation of microcystins in finished drinking water,” *Toxicon*, 138, 138–144. DOI: 10.1016/j.toxicon.2017.08.023
- Ruiz-Palomero, C., Soriano, M. L., and Valcárcel, M. (2015). “ $\beta$ -Cyclodextrin decorated nanocellulose: A smart approach towards the selective fluorimetric determination of danofloxacin in milk samples,” *Analyst* 140(10), 3431–3438. DOI: 10.1039/c4an01967a
- Saad, A. H. A., Azzam, A. M., El-Wakeel, S. T., Mostafa, B. B., and Abd El-latif, M. B. (2018). “Removal of toxic metal ions from wastewater using ZnO@Chitosan core-shell nanocomposite,” *Environmental Nanotechnology, Monitoring and Management*, 9, 67–75. DOI: 10.1016/j.enmm.2017.12.004
- Saeki, H., Sasaki, M., Komatsu, K., Miura, A., and Matsuda, H. (2009). “Oil spill remediation by using the remediation agent JE1058BS that contains a biosurfactant produced by *Gordonia* sp. strain JE-1058,” *Bioresource Technology* 100(2), 572–577. DOI: 10.1016/j.biortech.2008.06.046
- Saenger, W., and Steiner, T. (1998). “Cyclodextrin inclusion complexes : Host  $\pm$  Guest interactions and hydrogen-bonding networks,” *Acta Crystallographica Section A: Foundations of Crystallography*, 54(6), 798–805. DOI: 10.1107/S0108767398010733
- Sag, Y., Nourbakhsh, M., Aksu, Z., and Kutsal, T. (1995). “Comparison of Ca-alginate and immobilized *Z. ramigera* as sorbents for copper(II) removal,” 30(2), 175–181. DOI: 10.1016/0032-9592(95)80009-3
- Saito, T., and Isogai, A. (2004). “TEMPO-mediated oxidation of native cellulose. The effect of oxidation conditions on chemical and crystal structures of the water-insoluble fractions,” *Biomacromolecules*, 5(5), 1983–1989. DOI: 10.1021/bm0497769
- Sajilata, M. G., Singhal, R. S., and Kulkarni, P. R. (2006). “Resistant starch - A review,” *Comprehensive Reviews in Food Science and Food Safety*, 5(1), 1–17. DOI: 10.1111/j.1541-4337.2006.tb00076.x
- Salam, A., Pawlak, J. J., Venditti, R. A., and El-tahlawy, K. (2011a). “Incorporation of carboxyl groups into xylan for improved absorbency,” *Cellulose*, 18(4), 1033–1041. DOI: 10.1007/s10570-011-9542-y
- Salam, A., Pawlak, J. J., Venditti, R. A., El-tahlawy, K., and Carolina, N. (2010). “Synthesis and characterization of starch citrate - chitosan foam with superior water and saline absorbance properties,” *Biomacromolecules*, 11(6), 1453–1459.
- Salam, A., Venditti, R. A., Pawlak, J. J., and El-tahlawy, K. (2011b). “Crosslinked

- hemicellulose citrate – chitosan aerogel foams,” *Carbohydrate Polymers* 84(4), 1221–1229. DOI: 10.1016/j.carbpol.2011.01.008
- Sankar, M. U., Aigal, S., Maliyekkal, S. M., Chaudhary, A., Anshup, Kumar, A. A., Chaudhari, K., and Pradeep, T. (2013). “Biopolymer-reinforced synthetic granular nanocomposites for affordable point-of-use water purification,” *Proceedings of the National Academy of Sciences*, 110(21), 8459–8464. DOI: 10.1073/pnas.1220222110
- Saravanan, D., Gomathi, T., and Sudha, P. N. (2013). “Sorptions studies on heavy metal removal using chitin/bentonite biocomposite,” *International Journal of Biological Macromolecules* 53, 67–71. DOI: 10.1016/j.ijbiomac.2012.11.005
- Sato, A., Wang, R., Ma, H., Hsiao, B. S., and Chu, B. (2011). “Novel nanofibrous scaffolds for water filtration with bacteria and virus removal capability,” *Journal of Electron Microscopy*, 60(3), 201–209. DOI: 10.1093/jmicro/dfr019
- Sehaqui, H., de Larraya, U. P., Liu, P., Pfenninger, N., Mathew, A. P., Zimmermann, T., and Tingaut, P. (2014). “Enhancing adsorption of heavy metal ions onto biobased nanofibers from waste pulp residues for application in wastewater treatment,” *Cellulose*, 21(4), 2831–2844. DOI: 10.1007/s10570-014-0310-7
- Seyed Dorraji, M. S., A.R., A.-G., Hanifehpour, Y., Woo Joo, S., Figoli, A., Carraro, M., and Tasselli, F. (2017). “Performance of chitosan based nanocomposite hollow fibers in the removal of selenium ( IV ),” *Chemical engineering research and design*, 117, 309–317.
- Shao, D., Sheng, G., Chen, C., Wang, X., and Nagatsu, M. (2010). “Removal of polychlorinated biphenyls from aqueous solutions using  $\beta$ -cyclodextrin grafted multiwalled carbon nanotubes,” *Chemosphere* 79(7), 679–685. DOI: 10.1016/j.chemosphere.2010.03.008
- Shao, Z. J., Huang, X. L., Yang, F., Zhao, W. F., Zhou, X. Z., and Zhao, C. S. (2018). “Engineering sodium alginate-based cross-linked beads with high removal ability of toxic metal ions and cationic dyes,” *Carbohydrate Polymers* 187, 85–93. DOI: 10.1016/j.carbpol.2018.01.092
- Sharma, P. R., Chattopadhyay, A., Sharma, S. K., Geng, L., Amiralian, N., Martin, D., and Hsiao, B. S. (2018a). “Nanocellulose from spinifex as an effective adsorbent to remove cadmium(II) from water,” *ACS Sustainable Chemistry and Engineering*, 6(3), 3279–3290. DOI: 10.1021/acssuschemeng.7b03473
- Sharma, P. R., Chattopadhyay, A., Sharma, S. K., and Hsiao, B. S. (2017a). “Efficient Removal of  $\text{UO}_2^{2+}$  from water using carboxycellulose nanofibers prepared by the nitro-oxidation method,” *Industrial & Engineering Chemistry Research*, 56(46), 13885–13893. DOI: 10.1021/acs.iecr.7b03659
- Sharma, P. R., Chattopadhyay, A., Zhan, C., Sharma, S. K., Geng, L., and Hsiao, B. S. (2018b). “Lead removal from water using carboxycellulose nanofibers prepared by nitro-oxidation method,” *Cellulose* 25(3), 1961–1973. DOI: 10.1007/s10570-018-1659-9
- Sharma, P. R., Joshi, R., Sharma, S. K., and Hsiao, B. S. (2017b). “A simple approach to prepare carboxycellulose nanofibers from untreated biomass,” *Biomacromolecules*, 18(8), 2333–2342. DOI: 10.1021/acs.biomac.7b00544
- Shrivastava, V. . S. (2010). “Metallic and organic nanomaterials and their use in pollution control: A Review,” *Archives of Applied Science Research*, 2(6), 82–92.
- Shuaiyang, W., Huiling, L., Junli, R., Chuanfu, L., Feng, P., and Runcang, S. (2013). “Preparation of xylan citrate - A potential adsorbent for industrial wastewater treatment,” *Carbohydrate Polymers* 92(2), 1960–1965. DOI:

- 10.1016/j.carbpol.2012.11.079
- Shukla, S. K., Mishra, A. K., Arotiba, O. A., and Mamba, B. B. (2013). "Chitosan-based nanomaterials: A state-of-the-art review," *International Journal of Biological Macromolecules* 59, 46–58. DOI: 10.1016/j.ijbiomac.2013.04.043
- Sigdel, A., Park, J., Kwak, H., and Park, P. K. (2016). "Arsenic removal from aqueous solutions by adsorption onto hydrous iron oxide-impregnated alginate beads," *Journal of Industrial and Engineering Chemistry* 35, 277–286. DOI: 10.1016/j.jiec.2016.01.005
- Singh, J., Dartois, A., and Kaur, L. (2010). "Starch digestibility in food matrix: a review," *Trends in Food Science and Technology* 21(4), 168–180. DOI: 10.1016/j.tifs.2009.12.001
- Singha, A. S., and Guleria, A. (2014). "Chemical modification of cellulosic biopolymer and its use in removal of heavy metal ions from wastewater," *International Journal of Biological Macromolecules* 67, 409–417. DOI: 10.1016/j.ijbiomac.2014.03.046
- Sinha, A., and Jana, N. R. (2015). "Separation of microcystin-LR by cyclodextrin-functionalized magnetic composite of colloidal graphene and porous silica," *ACS Applied Materials and Interfaces*, 7(18), 9911–9919. DOI: 10.1021/acsami.5b02038
- Sinha, A., and Khare, S. K. (2012). "Mercury bioremediation by mercury accumulating *Enterobacter* sp. cells and its alginate immobilized application," *Biodegradation*, 23(1), 25–34. DOI: 10.1007/s10532-011-9483-z
- Sixta, H. (2006). *Handbook of Pulp*, H. Holik, (ed.), Wiley Online Library. WILEY-VCH Verlag GmbH & Co. KGaA, Weinheim.
- Smith, C. A., and Wood, E. J. (1997). *Moléculas Biológicas*, Escalona y Garcia., H., Aguilar Ortega, M.T., (ed.), Addison-Wesley Iberoamericana, Mexico.
- Smook, G. (2016). *Handbook for Pulp and Paper Technologist*, Kocurek, M., (ed.), 4th edition, TAPPI Press.
- Snyder, A., Bo, Z., Moon, R., Rochet, J. C., and Stanciu, L. (2013). "Reusable photocatalytic titanium dioxide-cellulose nanofiber films," *Journal of Colloid and Interface Science* 399, 92–98. DOI: 10.1016/j.jcis.2013.02.035
- Sookne, A. M., and Harris, M. (1941). "Surface characteristics of cotton fibers, as indicated by electrophoretic studies," *Journal of Research of the National Bureau of Standards*, 26(1), 65. DOI: 10.6028/jres.026.041
- Stana-Kleinschek, K., Strnad, S., and Ribitsch, V. (1999). "Surface characterization and adsorption abilities of cellulose fibers," *Polymer Engineering & Science*, 39(8), 1412–1424. DOI: 10.1002/pen.11532
- Struszczyk, M. H. (2002). "Chitin and Chitosan," *Polimery* 47(5), 316–325. DOI: 10.1002/0471440264.pst052
- Suopajarvi, T., Liimatainen, H., Karjalainen, M., Upola, H., and Niinimäki, J. (2015). "Lead adsorption with sulfonated wheat pulp nanocelluloses," *Journal of Water Process Engineering* 5, 136–142. DOI: 10.1016/j.jwpe.2014.06.003
- Syahmani, S., Iriani, R., Sanjaya, R. E., and Leny. (2018). "Potency of Chitin as an Adsorbent in Black Water Treatment Process at Peatland Environment," in: *Advances in Social Science, Education and Humanities Research (ASSEHR)*, Atlantis Press, 316–321.
- Szejtli, J. (1998). "Introduction and General Overview of Cyclodextrin Chemistry," *Chemical Reviews*, 98(5), 1743–1754. DOI: 10.1021/cr970022c
- Szejtli, J., Zsádon, B., Fenyvesi, É., and Tüdös, F. (1982). "Sorbents of cellulose basis capable of forming inclusion complexes and a process for the preparation thereof,"

- Szejtli, J., Zsardon, B., Fenyvesi, E., Horvath, N. O., Tudos, F. (1980). "Sorbents of cellulose basis capable of forming inclusion complexes and a process for the preparation thereof," U.S. Patent No. 4,357,468.
- The European Commission. (2015). *Commission Directive 2015/1787 of 6 October 2015 amending Annexes II and III to Council Directive 98/83/EC on quality of water intended for human consumption*, European Union, 6–17.
- Todde, G., Jha, S. K., Subramanian, G., and Shukla, M. K. (2018). "Adsorption of TNT, DNAN, NTO, FOX7, and NQ onto cellulose, chitin, and cellulose triacetate. Insights from density functional theory calculations," *Surface Science* 668, 54–60. DOI: 10.1016/j.susc.2017.10.004
- Tomson, M. B., and Vignona, L. (1984). "Precipitation of Phosphate Minerals in Waste Water Treatment Systems," in: *Phosphate Minerals*, J. O. Nriagu and P. B. Moore, (eds.), Springer Berlin Heidelberg, Berlin, Heidelberg, 386–399. DOI: 10.1007/978-3-642-61736-2\_13
- Tran, C. D., Duri, S., Delneri, A., and Franko, M. (2013). "Chitosan-cellulose composite materials: Preparation, characterization and application for removal of microcystin," *Journal of Hazardous Materials*, 253, 355–366.
- Trujillo-Reyes, J., Peralta-Videa, J. R., and Gardea-Torresdey, J. L. (2014). "Supported and unsupported nanomaterials for water and soil remediation: Are they a useful solution for worldwide pollution?," *Journal of Hazardous Materials*, 280, 487–503. DOI: 10.1016/j.jhazmat.2014.08.029
- Tyagi, P. K., Singh, R., Vats, S., and Kumar, D. (2012). "Nanomaterials Use in Wastewater Treatment," in: *International Conference on Nanotechnology and Chemical Engineering (ICNCS'2012) December 21-22, 2012 Bangkok (Thailand)*, Bangkok, 65–68.
- U.S. Environmental Protection Agency. (2006). *Revision to the unregulated contaminant monitoring rule (UCMR 4) for public water systems and announcement of public meeting*, Federal Register, Washington DC, USA, 1–28.
- U.S. Environmental Protection Agency. (2012). "Cyanobacteria and Cyanotoxins : Information for Drinking Water Systems," *United States Environmental Protection Agency*, (EPA-810F11001), 1–9.
- U.S. Environmental Protection Agency. (2017). *National Primary Drinking Water Regulations: Announcement of the Results of EPA's Review of Existing Drinking Water Standards and Request for Public Comment and/or Information on Related Issues*, Washington DC, USA, 3518–3552.
- Uyar, T., Havelund, R., Nur, Y., Balan, A., Hacaloglu, J., Toppare, L., Besenbacher, F., and Kingshott, P. (2010). "Cyclodextrin functionalized poly(methyl methacrylate) (PMMA) electrospun nanofibers for organic vapors waste treatment," *Journal of Membrane Science* 365(1–2), 409–417. DOI: 10.1016/j.memsci.2010.09.037
- del Valle, E. M. M. (2004). "Cyclodextrins and their uses: A review," *Process Biochemistry*, 39(9), 1033–1046. DOI: 10.1016/S0032-9592(03)00258-9
- Vijayalakshmi, K., Devi, B. M., Latha, S., Gomathi, T., Sudha, P. N., Venkatesan, J., and Anil, S. (2017). "Batch adsorption and desorption studies on the removal of lead (II) from aqueous solution using nanochitosan/sodium alginate/microcrystalline cellulose beads," *International Journal of Biological Macromolecules*, 104, 1483–1494. DOI: 10.1016/j.ijbiomac.2017.04.120
- Villiers, A. (1891). "Sur la fermentation de la fécule par l'action du ferment butyrique," *Compt. Rend. Acad. Sci*, 112, 536–538.

- Viswanathan, N., Pandi, K., and Meenakshi, S. (2014). "Synthesis of metal ion entrapped silica gel/chitosan biocomposite for defluoridation studies," *International Journal of Biological Macromolecules* 70, 347–353. DOI: 10.1016/j.ijbiomac.2014.06.010
- Wang, F., Yang, B., Wang, H., Song, Q., Tan, F., and Cao, Y. (2016). "Removal of ciprofloxacin from aqueous solution by a magnetic chitosan grafted graphene oxide composite," *Journal of Molecular Liquids* 222, 188–194. DOI: 10.1016/j.molliq.2016.07.037
- Wang, Y., Feng, Y., Zhang, X. F., Zhang, X., Jiang, J., and Yao, J. (2018). "Alginate-based attapulgite foams as efficient and recyclable adsorbents for the removal of heavy metals," *Journal of Colloid and Interface Science* 514, 190–198. DOI: 10.1016/j.jcis.2017.12.035
- Wang, Y., Li, Y., Liu, S., and Li, B. (2015a). "Fabrication of chitin microspheres and their multipurpose application as catalyst support and adsorbent," *Carbohydrate Polymers* 120, 53–59. DOI: 10.1016/j.carbpol.2014.12.005
- Wang, Y., Pei, Y., Xiong, W., Liu, T., Li, J., Liu, S., and Li, B. (2015b). "New photocatalyst based on graphene oxide/chitin for degradation of dyes under sunlight," *International Journal of Biological Macromolecules* 81, 477–482. DOI: 10.1016/j.ijbiomac.2015.08.037
- Wang, Y., Wu, D., Wei, Q., Wei, D., Yan, T., Yan, L., Hu, L., and Du, B. (2017). "Rapid removal of Pb(II) from aqueous solution using branched polyethylenimine enhanced magnetic carboxymethyl chitosan optimized with response surface methodology," *Scientific Reports*, 7(1), 1–11. DOI: 10.1038/s41598-017-09700-5
- Ware, G. W., and Whitacre, Da. M. (Eds.). (2006). *Reviews of Environmental Contamination and Toxicology Vol 188*, Springer, New York, NY. DOI: 10.1007/978-0-387-78444-1
- Wilson, A. (2017). "Do algal blooms threaten drinking water We are closer to an answer now Do algal blooms threaten drinking water sources in Alabama?," in: *2017 ADEM Drinking Water Surface Water Meeting*.
- Wilson, L. D., Mohamed, M. H., and Berhaut, C. L. (2011). "Sorption of aromatic compounds with copolymer sorbent materials containing  $\beta$ -cyclodextrin," *Materials*, 4(9), 1528–1542. DOI: 10.3390/ma4091528
- Wittaya, T. (2012). "Rice Starch-Based Biodegradable Films: Properties Enhancement," in: *Structure and Function of Food Engineering*, 103–134. DOI: <http://dx.doi.org/10.5772/47751>
- World Health Organization. (2014). "Guidelines for drinking-water quality, 2011," *Switzerland: WHO Library Cataloguing-in-Publication Data, Fourth Google Scholar*, 1, 595. DOI: 10.1016/S1462-0758(00)00006-6
- World Health Organization. (2017). "WHO | Water safety and quality," *WHO*, World Health Organization, <[http://www.who.int/water\\_sanitation\\_health/water-quality/en/](http://www.who.int/water_sanitation_health/water-quality/en/)> (Nov. 21, 2017).
- Wu, J., Lin, J., Zhou, M., and Wei, C. (2000). "Synthesis and properties of starch-graft-polyacrylamide/clay superabsorbent composite," *Macromolecular Rapid Communications*, 21(15), 1032–1034. DOI: 10.1002/1521-3927(20001001)21:15<1032::AID-MARC1032>3.0.CO;2-N
- Wu, J. X., Zhang, J., Kang, Y. L., Wu, G., Chen, S. C., and Wang, Y. Z. (2018). "Reusable and Recyclable Superhydrophilic Electrospun Nanofibrous Membranes with in Situ Co-cross-linked Polymer-Chitin Nanowhisker Network for Robust Oil-in-Water Emulsion Separation," *ACS Sustainable Chemistry and Engineering*, 6(2),

- 1753–1762. DOI: 10.1021/acssuschemeng.7b03102
- Wu, S., Hu, J., Wei, L., Du, Y., Shi, X., Deng, H., and Zhang, L. (2014). “Construction of porous chitosan-xylan-TiO<sub>2</sub> hybrid with highly efficient sorption capability on heavy metals,” *Journal of Environmental Chemical Engineering*, 2(3), 1568–1577. DOI: 10.1016/j.jece.2014.07.001
- Xiang, Z., Gao, W., Chen, L., Lan, W., Zhu, J. Y., and Runge, T. (2016). “A comparison of cellulose nanofibrils produced from *Cladophora glomerata* algae and bleached eucalyptus pulp,” *Cellulose* 23(1), 493–503. DOI: 10.1007/s10570-015-0840-7
- Xie, K., Zhang, Y., and Chen, S. (2010). “Synthesis and characterization of reactive polyhedral oligomeric silsesquioxanes (R-POSS) containing multi-N-methylol groups,” *Journal of Organometallic Chemistry* 695(5), 687–691. DOI: 10.1016/j.jorganchem.2009.12.001
- Xie, K., Zhao, W., and He, X. (2011). “Adsorption properties of nano-cellulose hybrid containing polyhedral oligomeric silsesquioxane and removal of reactive dyes from aqueous solution,” *Carbohydrate Polymers* 83(4), 1516–1520. DOI: 10.1016/j.carbpol.2010.09.064
- Xu, P., Zeng, G. M., Huang, D. L., Feng, C. L., Hu, S., Zhao, M. H., Lai, C., Wei, Z., Huang, C., Xie, G. X., and Liu, Z. F. (2012). “Use of iron oxide nanomaterials in wastewater treatment: A review,” *Science of the Total Environment* 424, 1–10. DOI: 10.1016/j.scitotenv.2012.02.023
- Xu, R., Mao, J., Peng, N., Luo, X., and Chang, C. (2018). “Chitin/clay microspheres with hierarchical architecture for highly efficient removal of organic dyes,” *Carbohydrate Polymers* 188(November 2017), 143–150. DOI: 10.1016/j.carbpol.2018.01.073
- Yan, H., Dai, J., Yang, Z., Yang, H., and Cheng, R. (2011). “Enhanced and selective adsorption of copper(II) ions on surface carboxymethylated chitosan hydrogel beads,” *Chemical Engineering Journal* 174(2–3), 586–594. DOI: 10.1016/j.cej.2011.09.064
- Yang, J. S., Jiang, B., He, W., and Xia, Y. M. (2012). “Hydrophobically modified alginate for emulsion of oil in water,” *Carbohydrate Polymers* 87(2), 1503–1506. DOI: 10.1016/j.carbpol.2011.09.046
- Yang, J. S., Xie, Y. J., and He, W. (2011). “Research progress on chemical modification of alginate: A review,” *Carbohydrate Polymers* 84(1), 33–39. DOI: 10.1016/j.carbpol.2010.11.048
- Yang, J., Xia, Y., Xu, P., and Chen, B. (2018). “Super-elastic and highly hydrophobic / superoleophilic sodium alginate / cellulose aerogel for oil / water separation,” *Cellulose* 25(6), 3533–3544. DOI: 10.1007/s10570-018-1801-8
- Yang, R., Aubrecht, K. B., Ma, H., Wang, R., Grubbs, R. B., Hsiao, B. S., and Chu, B. (2014). “Thiol-modified cellulose nanofibrous composite membranes for chromium (VI) and lead (II) adsorption,” *Polymer (United Kingdom)*, 55(5), 1167–1176. DOI: 10.1016/j.polymer.2014.01.043
- Yang, R., Su, Y., Aubrecht, K. B., Wang, X., Ma, H., Grubbs, R. B., Hsiao, B. S., and Chu, B. (2015). “Thiol-functionalized chitin nanofibers for As (III) adsorption,” *Polymer (United Kingdom)*, 60, 9–17. DOI: 10.1016/j.polymer.2015.01.025
- Yilmaz, E., Memon, S., and Yilmaz, M. (2010). “Removal of direct azo dyes and aromatic amines from aqueous solutions using two  $\beta$ -cyclodextrin-based polymers,” *Journal of Hazardous Materials*, 174(1–3), 592–597. DOI: 10.1016/j.jhazmat.2009.09.093
- You, L., Lu, F., Li, D., Qiao, Z., and Yin, Y. (2009). “Preparation and flocculation properties of cationic starch/chitosan crosslinking-copolymer,” *Journal of Hazardous*

- Materials*, 172(1), 38–45. DOI: 10.1016/j.jhazmat.2009.06.120
- Yu, X., Tong, S., Ge, M., and Zuo, J. (2013). “Removal of fluoride from drinking water by cellulose@hydroxyapatite nanocomposites,” *Carbohydrate Polymers*, Elsevier Ltd., 92(1), 269–275. DOI: 10.1016/j.carbpol.2012.09.045
- Yuan, G., Prabakaran, M., Qilong, S., Lee, J. S., Chung, I. M., Gopiraman, M., Song, K. H., and Kim, I. S. (2017). “Cyclodextrin functionalized cellulose nanofiber composites for the faster adsorption of toluene from aqueous solution,” *Journal of the Taiwan Institute of Chemical Engineers* 70, 352–358. DOI: 10.1016/j.jtice.2016.10.028
- Yue, X., Li, J., Zhang, T., Qiu, F., Yang, D., and Xue, M. (2017). “In situ one-step fabrication of durable superhydrophobic- superoleophilic cellulose / LDH membrane with hierarchical structure for efficiency oil / water separation,” *Chemical Engineering Journal*, 328, 117–123. DOI: 10.1016/j.cej.2017.07.026
- Zhang, F., Wu, W., Sharma, S., Tong, G., and Deng, Y. (2015a). “Synthesis of cyclodextrin-functionalized cellulose nanofibril aerogel as a highly effective adsorbent for phenol pollutant removal,” *BioResources*, 10(4), 7555–7568.
- Zhang, J., Xiao, H., and Yang, Y. (2015b). “Preparation of hemicellulose-containing latex and its application as absorbent toward dyes,” *Journal of Materials Science*, 50(4), 1673–1678. DOI: 10.1007/s10853-014-8728-8
- Zhang, L., Liu, X., Xia, W., and Zhang, W. (2014a). “Preparation and characterization of chitosan-zirconium(IV) composite for adsorption of vanadium(V),” *International Journal of Biological Macromolecules* 64, 155–161. DOI: 10.1016/j.ijbiomac.2013.11.040
- Zhang, L., Xia, W., Teng, B., Liu, X., and Zhang, W. (2013a). “Zirconium cross-linked chitosan composite: Preparation, characterization and application in adsorption of Cr(VI),” *Chemical Engineering Journal* 229, 1–8. DOI: 10.1016/j.cej.2013.05.102
- Zhang, L., Zhou, J., and Zhang, L. (2013b). “Structure and properties of  $\beta$ -cyclodextrin/cellulose hydrogels prepared in NaOH/urea aqueous solution,” *Carbohydrate Polymers* 94(1), 386–393. DOI: 10.1016/j.carbpol.2012.12.077
- Zhang, T., and Marchant, R. E. (1996). “Novel polysaccharide surfactants: The effect of hydrophobic and hydrophilic chain length on surface active properties,” *Journal of Colloid and Interface Science*, 177(2), 419–426. DOI: 10.1006/jcis.1996.0054
- Zhang, T., Mei, Z., Zhou, Y., Bu, X., Wang, Y., Li, Q., and Yang, X. (2014b). “Template-controlled fabrication of hierarchical porous Zn-Al composites with tunable micro/nanostructures and chemical compositions,” *CrystEngComm*, 16(9), 1793–1801. DOI: 10.1039/c3ce41839a
- Zhang, X., Wang, Y., and Yang, S. (2014c). “Simultaneous removal of Co(II) and 1-naphthol by core-shell structured Fe<sub>3</sub>O<sub>4</sub>@cyclodextrin magnetic nanoparticles,” *Carbohydrate Polymers* 114, 521–529. DOI: 10.1016/j.carbpol.2014.08.072
- Zhang, Y., Xu, Y., Cui, H., Liu, B., Gao, X., Wang, D., and Liang, P. (2014d). “La(III)-loaded bentonite/chitosan beads for defluoridation from aqueous solution,” *Journal of Rare Earths* 32(5), 458–466. DOI: 10.1016/S1002-0721(14)60094-6
- Zhao, F., Repo, E., Sillanpää, M., Meng, Y., Yin, D., and Tang, W. Z. (2015a). “Green synthesis of magnetic EDTA- And/or DTPA-cross-linked chitosan adsorbents for highly efficient removal of metals,” *Industrial and Engineering Chemistry Research*, 54(4), 1271–1281. DOI: 10.1021/ie503874x
- Zhao, Y., Zhang, Y., Lindström, M. E., and Li, J. (2015b). “Tunicate cellulose nanocrystals: Preparation, neat films and nanocomposite films with glucomannans,”

- Carbohydrate Polymers* 117, 286–296. DOI: 10.1016/j.carbpol.2014.09.020
- Zheng, Y., Hua, S., and Wang, A. (2010). “Adsorption behavior of Cu<sup>2+</sup> from aqueous solutions onto starch-g-poly (acrylic acid)/sodium humate hydrogels,” *Desalination*, Elsevier B.V., 263(1–3), 170–175. DOI: 10.1016/j.desal.2010.06.054
- Zhou, Y., Jin, Q., Zhu, T., and Akama, Y. (2011a). “Adsorption of chromium (VI) from aqueous solutions by cellulose modified with  $\beta$ -CD and quaternary ammonium groups,” *Journal of Hazardous Materials* 87(1–3), 303–310. DOI: 10.1016/j.jhazmat.2011.01.025
- Zhou, Z.-Y., Tian, N., Li, J.-T., Broadwell, I., and Sun, S.-G. (2011b). “Nanomaterials of high surface energy with exceptional properties in catalysis and energy storage,” *Chem. Soc. Rev.* 40(7), 4167–4185. DOI: 10.1039/C0CS00176G
- Zubair, M., Daud, M., McKay, G., Shehzad, F., and Al-Harhi, M. A. (2017). “Recent progress in layered double hydroxides (LDH)-containing hybrids as adsorbents for water remediation,” *Applied Clay Science* 143(March), 279–292. DOI: 10.1016/j.clay.2017.04.002
- Zubair, M., Jarrah, N., Ihsanullah, Khalid, A., Manzar, M. S., Kazeem, T. S., and Al-Harhi, M. A. (2018). “Starch-NiFe-layered double hydroxide composites: Efficient removal of methyl orange from aqueous phase,” *Journal of Molecular Liquids* 249, 254–264. DOI: 10.1016/j.molliq.2017.11.022

Article submitted: July 9, 2019; Peer review completed: August 26, 2019; Revised version received and accepted: September 9, 2019; Published: October 10, 2019.  
DOI: 10.15376/biores.14.4.Gomez-Maldonado